

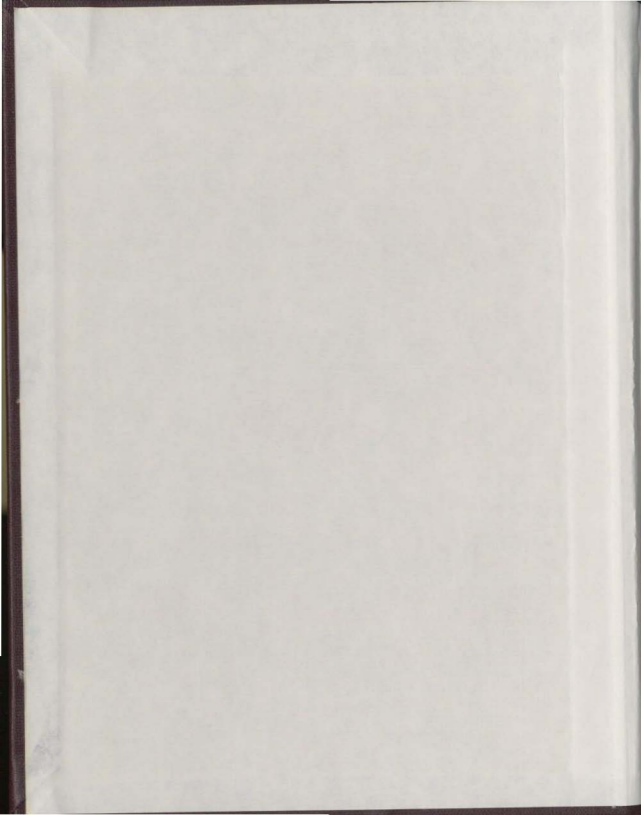
SYNOPTIC CONTROLS ON KATABATIC LAYER  
CHARACTERISTICS ABOVE A TEMPERATE  
ALPINE-TYPE GLACIER-PEYTO GLACIER, ALBERTA

CENTRE FOR NEWFOUNDLAND STUDIES

**TOTAL OF 10 PAGES ONLY  
MAY BE XEROXED**

(Without Author's Permission)

ALISON J. STENNING



000183







National Library of Canada  
Collections Development Branch

Canadian Theses on  
Microfiche Service

Bibliothèque nationale du Canada  
Direction du développement des collections

Service des thèses canadiennes  
sur microfiche

## NOTICE

The quality of this microfiche is heavily dependent upon the quality of the original thesis submitted for microfilming. Every effort has been made to ensure the highest quality of reproduction possible.

If pages are missing, contact the university which granted the degree.

Some pages may have indistinct print especially if the original pages were typed with a poor typewriter ribbon or if the university sent us a poor photocopy.

Previously copyrighted materials (journal articles, published tests, etc.) are not filmed.

Reproduction in full or in part of this film is governed by the Canadian Copyright Act, R.S.C. 1970, c. C-30. Please read the authorization forms which accompany this thesis.

**THIS DISSERTATION  
HAS BEEN MICROFILMED  
EXACTLY AS RECEIVED**

## AVIS

La qualité de cette microfiche dépend grandement de la qualité de la thèse soumise au microfilmage. Nous avons tout fait pour assurer une qualité supérieure de reproduction.

S'il manque des pages, veuillez communiquer avec l'université qui a conféré le grade.

La qualité d'impression de certaines pages peut laisser à désirer, surtout si les pages originales ont été dactylographiées à l'aide d'un ruban usé ou si l'université nous a fait parvenir une photocopie de mauvaise qualité.

Les documents qui font déjà l'objet d'un droit d'auteur (articles de revue, examens publiés, etc.) ne sont pas microfilmés.

La reproduction, même partielle, de ce microfilm est soumise à la Loi canadienne sur le droit d'auteur, SRC 1970, c. C-30. Veuillez prendre connaissance des formules d'autorisation qui accompagnent cette thèse.

**LA THÈSE A ÉTÉ  
MICROFILMÉE TELLE QUE  
NOUS L'AVONS REÇUE**

SYNOPTIC CONTROLS ON KATABATIC LAYER  
CHARACTERISTICS ABOVE A TEMPERATE ALPINE-  
TYPE GLACIER-PEYTO GLACIER, ALBERTA

by



Alison J. Stenning  
B.Sc., University of East Anglia, 1978.

A Thesis submitted in partial fulfillment  
of the requirements for the degree of  
Master of Science

Department of Geography  
Memorial University of Newfoundland

August 1980

St. John's

Newfoundland

## ABSTRACT

Previous glacier microclimatological research has emphasized the need for further study of synoptic scale controls on boundary and katabatic layer development. A better understanding of the influence of changing synoptic conditions on the characteristics of the near-glacier air layer should lead to more accurate prediction of the surface energy balance.

A subjective 'features of circulation' type synoptic classification is proposed which is used to physically explain variations in wind, temperature and stability conditions in the near-surface layer. Wind and temperature profiles were obtained during the summer of 1979 at a site on the tongue of Peyto Glacier, Alberta.

The katabatic layer was found to be most strongly developed under anticyclonic conditions, with frequent occurrence of a low level wind velocity maximum and associated thermocline. These conditions favoured steady down-glacier flow, strong surface-based temperature inversions and high stability. A weak positive correlation was found between the katabatic wind velocity and surface inversion strength. Diurnal variation in surface inversion strength was most pronounced under anticyclonic influence.

Cyclonic synoptic conditions were found to result in considerable disturbance of the near-surface air layer, resulting in weaker inversions, lower stability and more variable low-level wind direction. Deviations in the direction of the surface wind were strongly influenced by the direction of 700 mb flow. The geostrophic wind direction also affected near-surface temperature and stability conditions. A down-glacier flow, reinforcing the katabatic wind was associated with greater stability and inversion strength. A geostrophic wind directed perpendicular to the glacier fall-line caused considerable disturbance of wind and temperature conditions in the near-glacier air layer. The katabatic force was found to exceed the synoptic scale pressure gradient force under all synoptic conditions encountered, and to be greatest under anticyclonic conditions.

Local microclimatological studies emphasized the importance of differences in elevation, slope, aspect and proximity to ice-free areas. Greatest contrasts in temperature and wind conditions occurred under anticyclonic conditions. Turbulence in marginal ice areas may prevent the formation of a recognizable katabatic layer. Significant changes in radiation receipt around sunrise and sunset were found to result in modification of near-surface conditions.



#### ACKNOWLEDGEMENTS-

I am indebted to Dr. Gordon Young (National Hydrology Research Institute, Snow and Ice Division, Environment Canada) for his generous support of this thesis, by providing the wind profiling instrumentation and use of facilities at Peyto base camp during the summer of 1979.

Special thanks are due to Dr. Colin Banfield (Geography Department, Memorial University of Newfoundland) for his advice, enthusiastic assistance in the field and continued unfailing support as thesis supervisor. I am very grateful to Jason Edworthy for his help and advice with the profiling instrumentation, and would like to thank other members of the 1979 Peyto base camp party for a very enjoyable and rewarding field season. I am indebted to Dr. D.S. Munro for his advice during initial planning of the thesis.

I would like to thank Mr. J.T. Kotylak (Scientific Services, Western Region Atmospheric Environment Service) for providing synoptic charts and radiosonde data free of charge, and Mr. Hann (Atmospheric Environment Service, Upper Air Station, St. John's) for his help with interpretation of the radiosonde data.

Thanks are also due to the Geography Department, Memorial University, who purchased skidoo batteries for the profiling instrumentation. Sincere thanks to James Everard (Geography Department, Memorial University of Newfoundland) who constructed the portable anemometer mast used in local climatological studies, to Charles Conway for cartographic advice and to Sue Sharpe who typed the thesis.

## TABLE OF CONTENTS

	PAGE NUMBERS
Abstract	ii
Acknowledgements	iv
List of Tables	x
List of Figures	xi
CHAPTER ONE INTRODUCTION	
1.1 Research aims	1
1.2 Introduction to the study area	3
1.3 Climatological research on Peyto Glacier	5
1.4 Previous work on glacier katabatic flow	7
1.5 Inclusion of katabatic influence when considering heat transfer over glaciers: boundary and katabatic layer theory	12
1.6 Profile characteristics over glaciers	14
1.7 Synoptic aspect	17
CHAPTER TWO METHODOLOGY AND FIELD SAMPLING DESIGN	
2.1 Site	19
2.2 Profile instrumentation	20
2.2.1 The mast	

	PAGE NUMBERS
2.22 Anemometers	
2.23 Temperature difference measurements	
2.3 Wind direction	26
2.4 Recorders and printer	26
2.5 Base camp meteorology	26
2.6 Sampling design	28
 CHAPTER THREE SYNOPTIC PATTERN CLASSIFICATION	
3.1 Introduction	30
3.2 Summer weather conditions in the Peyto Glacier region	32
3.3 Synoptic classification system	35
3.4 Frequency of types	46
 CHAPTER FOUR ANALYSIS OF PROFILE DATA	
4.1 The influence of the 700 mb geostrophic wind on the glacier katabatic wind	50
4.2 Depth of the katabatic layer and wind velocity profile shape under different synoptic influences	63
4.3 Stability of the katabatic layer	71
4.4 The influence of the 700 mb wind direction on local stability	77
4.5 Variations in stability between synoptic types	80

4.6	Variations in surface inversion strength	83
4.61	Variations in strength of the temperature inversion with cloud cover	
4.62	Temperature fluctuations and stability	
4.7	Further evidence for a thermocline associated with a low level velocity maximum	90
4.8	Relationship between upper air temperature lapse (700 mb to 500 mb) and near-ice inversion strength	91
4.9	Diurnal variations	93
4.10	Relationship between katabatic wind velocity and inversion strength	99
4.11	Frequency of near-surface mean and maximum wind velocities according to synoptic category	104
4.12	Estimates of relative magnitudes of katabatic and pressure gradient forces	107

CHAPTER FIVE LOCALIZED MICRO-CLIMATOLOGICAL  
SURVEYS ON THE GLACIER TONGUE

5.1	The western ice-fall depression	110
5.11	Methodology	
5.12	Discussion of results	

	PAGE NUMBERS
5.2 The eastern side of the glacier snout	126
5.21 Methodology	
5.22 Discussion of results	
5.3 Conclusions to be drawn from local studies	131
CHAPTER SIX CONCLUSIONS AND SUGGESTIONS FOR FURTHER RESEARCH	133
REFERENCES	139
APPENDIX A SYMBOLS AND NOTATION USED	144
APPENDIX B STATISTICAL PROCEDURES	146
APPENDIX C 700 mb CHART CLASSIFICATION	152
APPENDIX D BASE CAMP METEOROLOGICAL DATA FOR PROFILE TIMES	157
APPENDIX E PROFILE DATA	171
APPENDIX F SIGNIFICANCE OF DIFFERENCES BETWEEN SYNOPTIC TYPES (10 PAIRINGS)	191

## LIST OF TABLES

		PAGE NUMBERS
TABLE 2.1	Anemometer field test	25
TABLE 3.1	Mean characteristics of synoptic types	38
TABLE 4.1	Frequency of low level wind velocity gradient ( $\frac{\Delta u}{\Delta z}$ ) reversals (within 6 m of the ice surface) according to synoptic category	67
TABLE 4.2	Mean local stability values ( $R_{11}$ )	82
TABLE 4.3	Mean bulk stability values ( $R_{1B}$ )	83
TABLE 4.4	Mean surface inversion strength	83
TABLE 4.5	Mean hourly standard deviation of the 1 to 4 m temperature difference	84
TABLE 4.6	Variation of inversion strength with cloud cover according to synoptic category	86
TABLE 4.7	Variation of inversion strength with cloud cover	87
TABLE 4.8	Correlation coefficients: correlation between wind velocity and inversion strength	100

## LIST OF FIGURES

		PAGE NUMBERS
Figure 1.1	Location of mast site and local study areas	4
Figure 1.2	Evolution of wind speed and temperature profiles over a melting glacier	8
Figure 1.3	Example of boundary and katabatic layers (with associated thermocline)	13
Figure 2.1	The instrumentation mast	21
Figure 2.2	Wind velocity and temperature sensors near the ice surface	24
Figure 2.3	Instrumentation mast and shelter	27
Figure 3.1	Mean frontal positions: summer	34
Figure 3.2	Synoptic type (1) Cyclonic Pacific	39
Figure 3.3	Synoptic type (2) 'Dodal' Cyclonic	40
Figure 3.4	Synoptic type (3) Pronounced Anticyclonic	41
Figure 3.5	Synoptic type (4) Weak Anticyclonic	42
Figure 3.6	Synoptic type (5) Westerly Zonal	43
Figure 3.7	Frequency of occurrence of synoptic types (number of charts in each category)	47
Figure 3.8	Distribution of profile observations between synoptic types	48



Figure 4.1	700 mb and surface wind roses: 6th July to 7th August 1979	51
Figure 4.2	Surface wind roses: Synoptic types (1) and (2)	53
Figure 4.3	Surface wind roses: Synoptic types (3) and (4)	54
Figure 4.4	Surface wind rose: Synoptic type (5)	55
Figure 4.5	Hodograms: Synoptic type (1)	56
Figure 4.6	Hodograms: Synoptic type (2)	57
Figure 4.7	Hodograms: Synoptic type (3)	58
Figure 4.8	Hodograms: Synoptic type (4)	59
Figure 4.9	Hodograms: Synoptic type (5)	60
Figure 4.10	700 mb wind roses for cyclonic and anticyclonic types	62
Figure 4.11	The correlation between 700 mb wind direction and maximum profile velocity	64
Figure 4.12	Depth of katabatic layer according to synoptic type	66
Figure 4.13	Wind profile shape according to synoptic type	69
Figure 4.14	Profile change due to frontal passage, 21st July 1979	72
Figure 4.15	Correlation between stability ( $R_{1B}$ ) and the 3m profile velocity: $0 < R_{1B} < 1$	75

Figure 4.16	Correlation between stability ( $R_{1B}$ ) and the 3m profile velocity.	76
	$R_{1B} > 1$	
Figure 4.17	Correlation between stability ( $R_{1B}$ ) and the 700 mb geostrophic wind direction	78
Figure 4.18	Correlation between stability ( $R_{1B}$ ) and the 700 mb geostrophic wind direction	79
Figure 4.19	Correlation between 1 to 4 m inversion strength and the 700 mb geostrophic wind direction	81
Figure 4.20	Relationship between stability ( $R_{1B}$ ) and the hourly standard deviation of 1 to 4 m temperature difference	89
Figure 4.21	Relationship between upper air lapse rate (700 mb - 500 mb) and the near-ice inversion strength (1 to 4 m)	92
Figure 4.22	Lull in wind velocity before sunrise, 30th July 1979	96
Figure 4.23	Frequency distribution of inversion strengths according to synoptic influence	98
Figure 4.24	Relationship between the 4 m wind speed and the 1 to 4 m temperature difference	101
Figure 4.25	Frequency of mean low level velocities according to synoptic type	105

Figure 4.26	Frequency of maximum low level velocities according to synoptic type	106
Figure 5.1	The western ice-fall depression	111
Figure 5.2	Post-sunrise warming rates: western ice-fall depression ( $^{\circ}\text{C hr}^{-1}$ )	111
Figure 5.3	Wind velocity and temperature profiles: sunrise, 15.7.1979. Western ice-fall depression	115
Figure 5.4	Conditions at profile mast: before and after sunrise. 15.7.1979	118
Figure 5.5	Wind velocity and temperature profiles: sunset, 20.7.1979. Western ice-fall depression	121
Figure 5.6	Post-sunset cooling rates: western ice-fall depression ( $^{\circ}\text{C hr}^{-1}$ )	122
Figure 5.7	Local survey sites: eastern glacier snout	122
Figure 5.8	Wind velocity and temperature profiles: early afternoon. 2.8.1979. Western ice-fall depression.	125
Figure 5.9	Wind velocity and temperature profiles: early afternoon. 18.7.1979. Eastern glacier snout	128

## CHAPTER ONE

## INTRODUCTION

1.1 Research aims

Previous studies of climate and energy exchange over glaciers have indicated the need for further research into the effects of synoptic scale changes on the near-surface air layer. For example, the geostrophic wind may exert substantial control over near-surface air flow (Streten and Wendler, 1968; Holmgren, 1971; Munro, 1975; Manins and Sawford, 1979). In such cases the glacier katabatic wind may not be sufficiently strong to dominate airflow immediately above the glacier. Manins and Sawford (1979) emphasize the importance of cross-slope ambient winds which may disrupt katabatic flow. There is a need for additional microclimatology research into katabatic flow and the incorporation of katabatic influences in flux estimation procedures (Munro, 1975). A better understanding of the influence of changing weather characteristics on the near-glacier air layer should lead to more accurate prediction of the surface energy balance.

This thesis aims to determine the influence of varying synoptic-scale weather conditions on katabatic layer formation

and micro-climatic parameters over a temperate alpine-type glacier surface during the ablation season. A synoptic classification system is proposed for the summer ablation season of 1979, on Peyto Glacier, Alberta, which will be used to physically explain:

1. Variation in the strength and direction of the katabatic wind.
2. Variation in the depth of the katabatic layer.
3. Variation in stability conditions of the near-surface air layer.
4. Variation in the strength of the surface-based temperature inversion.
5. Diurnal variation in the above parameters.
6. Localized spatial and temporal variation of temperature and wind characteristics on the glacier tongue.

Prediction of the synoptic weather characteristics most favourable for the development of strong temperature inversions and katabatic flow should be useful when assessing yearly differences in the seasonal energy and mass budget of a glacier. Variation in frequency of synoptic types encountered during the ablation season from year to year is an important factor in determining differences in ablation. A relatively simple system of synoptic classification is developed for maximum potential use.

## 1.2 Introduction to the study area

Peyto Glacier ( $50^{\circ}40' N$ ,  $116^{\circ}34' W$ ) is situated 37 km north-west of Lake Louise, Alberta, in the north-eastern portion of the Waputik Mountains section of the Rocky Mountains divide. It is one of many glaciers adjoining the Wapta Icefield. Peyto was one of five glacial basins selected for long term detailed studies during the International Hydrological Decade (I.H.D.) 1965-1974, by the Glaciology Division of the Inland Waters Directorate (Fisheries and Environment Canada). Research was directed at assessing the role of glaciers in the hydrological cycle (Young and Stanley, 1976).

Peyto Glacier is of the temperate alpine type, with an area of  $13.4 \text{ km}^2$  (60% of the total area of the drainage basin) and a mean surface slope of  $12.9^{\circ}$  (Young and Stanley, 1976). The accumulation and ablation areas are separated by an icefall. The accumulation area (elevation range 2,400 m to 3,200 m) is composed of three basins in the south, south-west and north-west, converging just above the icefalls (Fig. 1.1). The ablation area (elevation range 2,100 m to 2,400 m) is a small valley glacier ( $3.51 \text{ km}^2$ ) with a north-easterly aspect. The glacier tongue lies in a huge depression formed by Mt. Thompson to the south-east, Peyto Peak to the west, icefalls to the south-west and a ridge from Peyto Peak to Mt. Thompson in the north. Lateral ice-cored moraines rise

\* Now the Snow and Ice Division; National Hydrology Research Institute, Environment Canada.

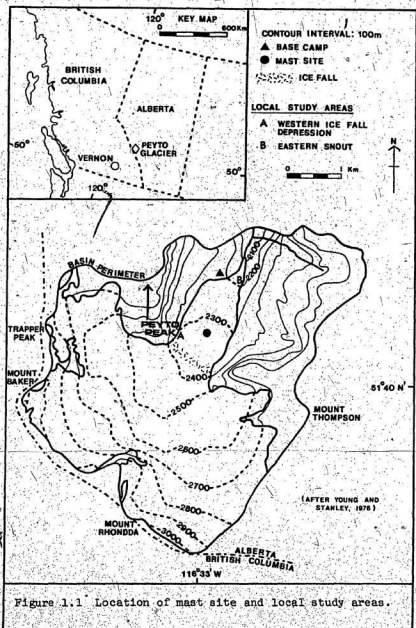


Figure 1.1 Location of mast site and local study areas.

to 100 m above the ice surface, with a slope of  $30^{\circ}$  to  $35^{\circ}$  near the terminus, and comprise  $1.16 \text{ km}^2$  of the basin area (Foessel, 1974). There are several small glaciers and perennial snow patches high on the eastern side of the basin. Two narrow medial moraine bands (from Mt. Baker and Trapper Peak) extend down the tongue and terminate at the snout and on the north side of the tongue.

A deep, narrow gorge occupied by Peyto Creek runs from the glacier terminus to Peyto Lake at the head of Mistaya Valley (3.2 km from the glacier snout). The gorge is carved in limestone, interlayered with softer shale, harder dolomite and sandstone (Sedgewick, 1966). Differential erosion of the softer beds has produced ledges or terraces, the more resistant beds forming vertical cliffs. The glacier terminus has been retreating at about 10 metres per year (mean value for the period 1967-1974, as given by Young, 1977).

### 1.3 Climatological research on Peyto Glacier

A number of studies concerning various aspects of the local climate of Peyto Glacier were carried out during the International Hydrological Decade. Young (1977) examined the relationship between glacier mass balance and meteorological variables using data from the base camp meteorological station, where detailed records of summer climate have been kept since 1967. Goodison (1969, 1970, 1972) studied the



distribution of global radiation over Peyto Glacier, with particular interest in the shading effect caused by the surrounding mountain ridges. He notes that the glacier tongue experienced a significant reduction in daily radiation, a small region on the eastern side receiving 16% less than the maximum possible value in August. The shadow effect predominated during hours of low solar altitude and as the ablation season progressed.

Foessel (1974) analysed the air temperature distribution over Peyto Glacier. Lapse rates over the glacier tongue were shown to be normal (mean value of  $+4^{\circ}\text{C}$  per 100 m) during the passage of unstable cyclonic systems, but decreased during anticyclonic conditions, favouring inversions. On the glacier tongue, pooling of cold air against the bedrock ridge produced a temperature inversion which increased in intensity as the ablation season progressed. Foessel suggests the need for detailed investigation of vertical wind and temperature profiles to characterize air drainage in and around the cold pools.

Munro (1975) undertook a detailed experimental investigation of flux-profile relationships near the glacier surface. His work provided new information about the glacier boundary layer, and suggests that previous experiments may have overestimated boundary layer depth when applying turbulent transfer theory. A log-linear relationship was found satisfactory to describe stability influences within the boundary layer.

#### 1.4 Previous work on glacier katabatic flow

The katabatic glacier wind owes its origin to a temperature contrast between glacier ice and surrounding, largely ice-free areas. It was first described by Tollner in 1931. A semi-permanent temperature inversion is formed over a cold ice surface, resulting in a stable boundary layer. A density contrast is produced as cold surface air is denser than that at the same altitude, but further down-glacier, and gravitational acceleration produces a thermally controlled glacier-wind (Mahrt and Schwerdtfeger, 1970). Katabatic flow is characterized by a low level wind velocity maximum and associated steep temperature gradient or thermocline (Holmgren, 1971; Munro, 1975; Munro and Davies, 1977), (Fig 1.2). The wind is directed down-gradient in the near surface katabatic layer.

Katabatic flow has been studied in a sub-polar ice-cap environment (Holmgren, 1971; Alt, 1978), on inland ice sheets (Whillans, 1975), snow domes (Businger and Ramano Rao, 1965), alpine-type glaciers (Ekhart, 1934; Hoinkes, 1954; Martin, 1975; Munro 1975), sub-arctic glaciers (Streten and Wendler, 1968; Streten, Ishikawa and Wendler, 1974; Rannie, 1977) and over the Antarctic ice shelf (Sverdrup, 1936; Lettau, 1966; Mather and Miller, 1966).

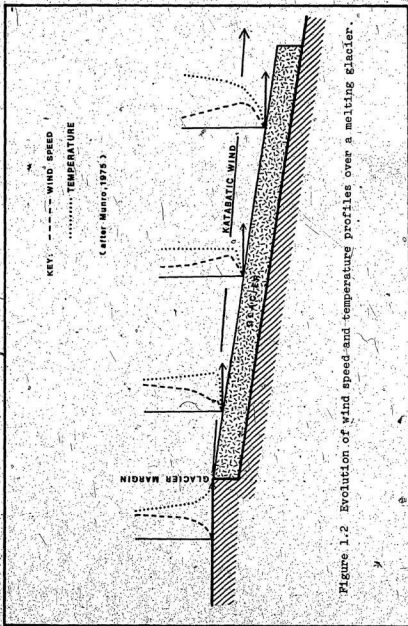


Figure 1.2 Evolution of wind speed and temperature profiles over a melting glacier.

Characteristics of the katabatic wind vary considerably according to the glacial environment. Holmgren (1971), working on a sub-polar ice cap, identified a single maximum in katabatic wind velocity, occurring in the middle of the night, with a minimum in the early afternoon. Streten, Ishikawa and Wendler (1974) describe a similar night time maximum in katabatic wind velocity on McCall glacier in northern Alaska.

In Antarctica a single diurnal variation is also characteristic (Sverdrup, 1936; Mather and Miller, 1966) and is most pronounced during the summer months. However, observations on sub-arctic glaciers in southern Alaska indicate a double maximum in velocity, one slightly before sunrise and the other in mid-afternoon (Streten and Wendler, 1968). Here the winds are lightest just before noon and in the early evening. Hoinkes (1954) also describes a double maximum at a number of glacier sites in the European Alps.

At high latitudes and altitudes the occurrence of a single velocity maximum at night may be the result of insufficient temperature contrast during the day, between the ice surface and the surrounding area, to produce a maximum inversion strength. During the night, surface radiative cooling produces a maximum contrast (Streten, Ishikawa and Wendler, 1974). Martin (1975) attributes the nocturnal velocity maximum which occurs on the Glacier de Saint-Sorlin to the development of a mountain wind blowing in the same direction as the glacier wind, causing an augmentation of

velocities. At lower latitudes, maximum temperature contrast in late afternoon often produces a second maximum before sunset. Velocities in such situations tend to be higher during the day due to the setting up of a local valley circulation (Munro, 1975). Air in the valley below the glacier is warmed by day, while air over the glacier is cooled. This cooled air flows into the valley beyond the glacier in response to density and altitudinal differences, resulting in relatively strong winds at the glacier terminus. At night, the air in the entire valley is cooled and the density differences and resulting down-valley wind reduced.

Several studies have attempted to correlate the strength of the glacier katabatic wind with the intensity of the associated surface-based temperature inversion (Streten, Ishikawa and Wendler, 1974; Martin, 1975; Munro and Davies, 1977). Since the glacier wind is a flow resulting from horizontal density difference induced by surface cooling over the glacier, significant positive correlations have been found between the positive temperature gradient and glacier wind velocity (Martin, 1975). When the temperature difference approaches zero, the down-glacier wind velocity also approaches zero (Streten, Ishikawa and Wendler, 1974). High velocity glacier winds would only occur in the presence of a strong temperature inversion.

In Antarctica, katabatic flow is rare on the central plateau (Lettau, 1966), but occurs through most of the year on the ice slopes (Mather and Miller, 1966). Katabatic winds in this environment were observed to begin suddenly, surge and remain gusty, varying over a period of a few hours, especially at night. Breakdown of katabatic flow also occurred abruptly, with a general lowering of temperature and reduction in vertical temperature gradients. Lettau (1966) attributed the observed general cooling to uplift of ice-cooled air with convergence of its horizontal flow.

The sudden onset of katabatic flow has been noted in several other studies. Martin (1975) observed that on the Glacier de Saint-Sorlin a 'classical' logarithmic profile regime can change within an hour to a katabatic wind regime with a low level wind maximum and associated thermocline. On Castner Glacier in Alaska, katabatic flow in the absence of strong synoptic pressure gradients was seen to begin within 15 minutes of sunset and end 2 to 2 1/2 hours after sunrise (Streten and Wendler, 1968). Katabatic winds on small, steep glaciers are typically gusty; however those on larger ice caps, where there is a long, relatively smooth fetch over an ice surface are generally quite steady (Holmgren, 1971).

1.5 Inclusion of katabatic influence when considering heat transfer over glaciers: boundary and katabatic layer theory

As warm air is advected over a glacier, turbulent cooling is confined to a shallow layer near the surface (Munro, 1975). Continuing down-glacier this cool air becomes increasingly colder than the original invading air and becomes separated from it by a distinct boundary, marked by a thermocline, across which only molecular transfer may occur. Stable gravity waves may travel along the interface of cold and warm air (Holmgren, 1971). Defant (1951) suggests that there may be a critical value of glacier surface slope above which katabatic flow becomes unstable.

Katabatic influence on the near surface wind profile causes a recurving from the log-linear relationship observed in the boundary layer (approximately the first metre above the ice surface). Within the boundary layer fluxes are constant with height (Holmgren, 1971; Munro and Davies, 1977), but above this fluxes decrease towards the top of the katabatic layer (Fig. 1.3).

The height of maximum katabatic wind velocity defines the upper limit of the katabatic layer and should be related to the depth of the boundary layer (Munro, 1975). At this level, transfers of sensible heat and momentum are close to zero, due to the near-zero vertical wind velocity gradient.

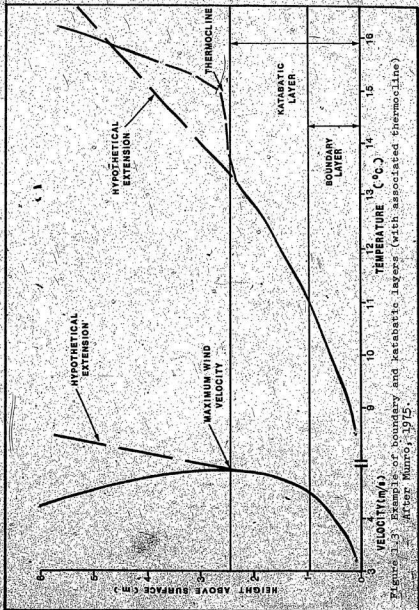


Figure 1.3. Example of boundary and katabatic layers (with associated thermocline) after Munro, 1975.



The maintenance of a thermocline is favoured by turbulence within the lowest, ice-coolest, layer of the glacier wind (Defant, 1951; Holmgren, 1971). Since the amount of heat transferred to the ice surface is directly proportional to the vertical temperature gradient in the near-surface air layer, the glacier wind is associated with large values of heat transfer (Hoinkes, 1953; Lettau, 1966). The katabatic wind does not therefore preserve the ice surface, but may lead to increased ablation (Geiger, 1965). However, the presence of a thermocline may substantially reduce the vertical turbulent exchange and heat transport across the zone of strong temperature gradient (Holmgren, 1971). Large temperature inversions may be destroyed by wind velocities of greater than 8 to 9  $\text{ms}^{-1}$  at the 10 m level (Liljequist, 1957; Holmgren, 1971).

#### 1.6 Profile characteristics over glaciers (see Appendix A, p.144, for notation)

The form of temperature and wind profiles in the near-surface layer is dependent on stability conditions and the nature of the surface. Early studies of heat transfer over glaciers made use of the power law (Sverdrup, 1936; Wallen, 1948; Orvig, 1954). However, the power index is dependent on surface roughness and stability and is subject to large variations which are not easily explained in terms of a physical process (Grainger and Lister, 1966; Alt, 1978).

Deacon (1949) modified the power law for use in all stabilities (Eq. 1):

$$U_z = \frac{U^*}{\kappa(1-\beta)} \left[ \left( \frac{z}{z_0} \right)^{1-\beta} - 1 \right] \quad (\text{Eq. 1})$$

The exponential law (Eq. 2) finds good agreement with observed profiles in lapse conditions, but not in neutral or stable conditions since greater deviations occur as stability increases (Grainger and Lister, 1966):

$$U_z = \frac{U^*}{\kappa L} \left[ 1 - \exp\left(-\frac{z}{L}\right) \right]^{-1} \quad (\text{Eq. 2})$$

Frandl (1952) used an exponential profile description predicting that the downslope velocity vanishes at four times the height of maximum velocity in katabatic flow (Eq. 3):

$$U_z = C \sin\left(\frac{z}{L}\right) \exp\left(-\frac{z}{L}\right) \quad (\text{Eq. 3})$$

However, Martin (1975) notes that this is not the case for profiles examined on the Glacier de Saint-Sorlin, and uses a more suitable law that combines both logarithmic and exponential functions (Eq. 4):

$$U_z = A \ln\left(\frac{z}{a}\right) \exp\left(-\frac{z}{b}\right) \quad (\text{Eq. 4})$$

Given the strong inversion conditions common over ice, the logarithmic law (Eq. 5) is generally unsuitable (Liljequist, 1957; Holmgren, 1971):

$$U_z = \frac{U^*}{K} \ln\left(\frac{z}{z_0}\right) \quad (\text{Eq. 5})$$

However, Alt (1978) used the logarithmic law to describe observed profiles on the Meighen Ice Cap, where stable stratification is uncommon. The power law was found to be more representative under stable conditions. Grainger and Lister (1966) found that the logarithmic law was most representative within the boundary layer, but at very great stabilities ( $Ri > 0.5$ ) fit was poor. Sverdrup (1936) found a tendency towards increased linearity within the profile as stability increased and turbulence was suppressed. Munro and Davies (1978) conclude that a log-linear model may be used to describe profiles in the near-ice layer, but should be restricted to within 1.5 m of the ice surface (Eq. 6):

$$U - U_0 = \frac{U^*}{K} \left[ \ln\left(\frac{z}{z_0}\right) + \alpha \frac{(z - z_0)}{L} \right] \quad (\text{Eq. 6})$$

Holmgren (1971) describes a logarithmic profile close to the ice surface during katabatic flow, but with increasing height there is greater departure from the logarithmic variation until recurving starts. Recurving of the wind profile tends to start closer to the ice surface than that of the temperature profile.

When stability (as indicated by the local Richardson number  $Ri_L$ ) exceeds a certain value, some authors say there is no predictable form for the wind profile (Oke, 1970; Businger, 1973). Businger suggests that the critical value of  $Ri_L$  is 0.2. Okamoto and Webb (1970) indicate that  $Ri_L = 0.2$  marks the separation between a turbulent regime ( $Ri_L < 0.2$ ) and a quiet regime ( $Ri_L > 0.2$ ). They observed that temperature fluctuations were greater in the 'turbulent' regime than in the 'quiet'. Webb (1970) suggests that when  $Ri_L$  exceeds the critical value, the profile may be described by a simple logarithmic function. At these values, flow is governed by processes other than turbulence, such as katabatic drift or gravity waves (Winn-Nielsen, 1965).

#### 1.7 Synoptic aspect

Initial development of the katabatic wind is favoured by calm, clear weather conditions (Businger and Ramano Rao, 1965; Lettau, 1966; Streten, Ishikawa and Wendler, 1974; Martin, 1975; Munro and Davies, 1977). Such conditions lead to weak overall control by synoptic pressure gradients and most pronounced temperature contrasts between an ice surface and the surrounding terrain (Streten, Ishikawa and Wendler, 1974). With weak synoptic pressure gradients, the katabatic wind dominates (Streten and Wendler, 1968). Its diurnal variation is also most pronounced on clear days.

Observations indicate that the velocity and diurnal variation of katabatic flow are closely related to the strength of the near-ice inversion, the free air lapse rate and the net radiation (Stréten, Ishikawa and Wendler, 1974; Martin, 1975; Munro, 1975). Stréten, Ishikawa and Wendler (1974) found a variable time lag of 3 to 5 hours between the peaks and troughs of net radiation and katabatic wind velocity on McCall Glacier. A broad similarity was noted in the diurnal variations of free air lapse rate and katabatic wind velocity. Sverdrup (1936) emphasizes the close interplay between radiation, wind and wind gradient, temperature and temperature gradient. With dense overcast the surface inversion is usually small, but decreasing wind velocity will allow increased inversion strength. The nature of the wind profile is determined by the temperature profile and vice versa, both being dependent on variations in radiation receipt. Turbulent transfer of heat to the glacier surface is determined by the form of wind and temperature profiles in the near-surface air layer and by the surface temperature (Sverdrup, 1936).

Under disturbed weather conditions, synoptic scale winds channelled through mountainous terrain may disturb local glacier wind patterns (Munro and Davies, 1977). Upper winds blowing perpendicular to the glacier fall-line enhance interfacial shear and may play a dominant role in determining whether an observable katabatic wind is present on a slope (Manins and Sawford, 1979).

## CHAPTER TWO

## METHODOLOGY AND FIELD SAMPLING DESIGN

2.1 Site

The profile mast was situated at an elevation of 2310 m, in a position central to and about 800 m from the icefall (Fig. 1.1 p. 4). The overlying air may be assumed representative of the surface up to a maximum height of 1/100 the fetch (Bradley, 1968) i.e. 8 m in 800 m. Measurements were made in the first 7 m above the ice surface. At the beginning of the ablation season the surface was relatively smooth and free of crevasses and moulins. As the season progressed, differential ablation resulted in considerable roughness, with a local relief of about 0.5 m. The glacier surface slope was 3.8° in the vicinity of the profile mast. The central glacier site was chosen as representative of wind and temperature conditions on the tongue, and to avoid excessive shading. It was within 1 km of base camp, allowing easy access for maintenance of the instrumentation.

## 2.2 Profile instrumentation

### 2.21 The Mast

The profiling instrumentation was supported by an 8-m aluminium mast (5 cm in diameter), with cross-arms secured at one metre intervals above the base (Fig. 2.1). The base was fastened to a flat rock using strong wire, enabling the mast to move down as the ice ablated and maintaining each sensor at a constant height above the surface. As the ablation season progressed there may have been some slight deviations from the 1 m interval above mean zero height. Six guy wires supported the mast in a vertical position, with four wires angled up-glacier and two down-glacier. The guy wires were secured with turnbuckles to large boulders on the ice surface which could easily be adjusted to maintain the mast upright. The mast could be lowered when necessary to remove the sensors.

### 2.22 Anemometers

Light-weight 3-cup anemometers (manufactured by C.W. Thornthwaite Associates) were used in this study. The conical cups, each 5 cm in diameter, were reinforced with aluminium rings. The whole cup assembly weighed less than 7 gm, had fast response to wind speed variations, and a low stall speed of  $0.1 \text{ ms}^{-1}$ .



Figure 2.1 The instrumentation mast



The anemometer shafts were made of stainless steel with miniature bearings. A pivot on the shaft end rides on a polished steel plate. A shutter on the shaft interrupts a light beam from a 3 volt 'grain-of-wheat' lamp housed in the base of the anemometer tee. Light is focused on a photo cell and converted to a charge of current which is transmitted by signal cable to a transistor amplifier, operating an electromechanical counter on a register cabinet.

All connections, anemometers and mountings were kept clean and dust free during operation, a silicone rubber sealant being used to repel moisture. The anemometer assemblage was fragile, which allows for sensitivity at low wind speeds, but necessitates protection from damage in heavy rain and hail.

#### Field Test

Since it was possible for a change of calibration to occur during transport of the anemometer system (Munro, 1975), a field test was carried out before sampling began. The six anemometers to be used were mounted at a height of 0.5 m above the ice surface, on a length of dexion, and directed into the wind. The test was carried out under anticyclonic conditions with cloud cover of 3/10 (Cu, Ci) and the near-surface wind blowing from 190° (directly over the eastern ice-fall). Readings were taken over a half-hour period and converted from counts per minute to metres per second.

(Table 2.1). A difference of 6% was noted between the highest and lowest values recorded. This field test suggests that some caution should be exercised in interpretation of profiles where there is little difference in velocity between sample levels.

Wucknitz (1977) warns that profile errors may result from disturbance of the wind field by the mast itself. However, since the glacier wind seldom varied by more than  $\pm 25^\circ$  from the down-glacier direction, and the anemometers protruded approximately 0.5 m up glacier from each cross-arm, the error was probably minimal in this situation. Error due to interference with the mast may also be minimized by ensuring that cup rotation, at the nearest point to the mast, is in the same direction as the wind (Munro, 1975). This procedure was followed before profile sampling began.

### 2.23 Temperature difference measurements

Double-shielded copper-constantan thermocouples (C.W. Thornthwaite Associates) were attached to the mast cross-arms at 1 and 4 metres above the ice surface (Fig. 2.2). Artificial ventilation of the sensors was not considered necessary, owing to the design of the radiation shields (Pers. comm. D.S. Munro). Parallel metal plates above and below the thermocouples allow free ventilation of the sensors. Signal cables from the thermocouples led to a Rustrak recorder.



Figure 2.2 Wind velocity and temperature sensors near the ice surface

TABLE 2.1 ANEMOMETER FIELD TEST

ANEMOMETER NUMBER	HEIGHT ABOVE ICE SURFACE (m)*	REGISTER NUMBER	1/2 HOUR PRINT	COUNTS min <sup>-1</sup>	ms <sup>-1</sup>
1639	1	4	3015	101	2.67
	2	-	-	-	-
1324	3	C3	3229	108	2.85
1450	4	C1	3184	106	2.80
1668	5	C2	3103	103	2.72
1473	6	2	3022	101	2.67
1668	7	3	3196	107	2.82

\* The anemometers were placed at these heights on the mast during the subsequent field experiments.

Anemometer number 1326 was not used for the profile measurement system as only five pairs of printer channels and registers were functional.

The seventh anemometer could not be used due to malfunction of its transmitter.

After 2nd August 1979 anemometer number 1473 was moved to the 2 m level and anemometer 1668 to the 5 m level prior to 24 hour sampling.

The heights of the temperature difference sensors were selected to provide a record of inversion strength within the katabatic layer, which could be correlated with the glacier wind velocity. The upper sensor height was chosen to coincide with the approximate mean level of wind velocity maximum in katabatic flow encountered by Munro (1975), at a point about 200 m further down-glacier.

The temperature difference system was capable of measuring differences of up to 12.5°C between the two levels, with a readout resolution of 0.05°C on the most sensitive

range. Laboratory calibration of the temperature difference system was carried out at Memorial University before its use in this study.

### 2.3 Wind direction

Wind direction was recorded continuously at a level of 2 m above the ice surface, by an anemograph. The anemograph was positioned 0.5 m above the instrument shelter on its up-glacier side, reducing possible turbulence effects.

### 2.4 Recorders and Printer

Hourly anemometer counts were registered by digital recorders with electromechanical counters (maximum counting speed of  $10 \text{ sec}^{-1}$ , i.e. an upper wind velocity limit of  $14.5 \text{ ms}^{-1}$ ). The recorder channels fed into a Moduprint count recorder, adjusted to print once an hour. The wind recorders, temperature difference recorder, printer and skidoo batteries used to power the systems were housed in a covered sled raised above the ice to keep the instruments dry. The sled was situated 10 m to one side of and slightly down-glacier from the profile mast, to minimize possible interference (Fig. 2.3).

### 2.5 Base camp meteorology

The Payto base camp meteorological station is situated at an altitude of 2220 m on moraine close to bedrock on the north side of the glacier terminus, about 100 m from the ice

\* Compilation of Base camp meteorological information is included in Appendix D.



Figure 2.3 Instrumentation mast and shelter

and 15 m above the ice surface (Fig. 1.1 p. 4). A Stevenson screen contained maximum and minimum thermometers (read at 09.00 M.D.S.T. and 21.00 M.D.S.T. daily) and a Casella thermohygrograph. During profile runs, air temperature, relative humidity, barometric pressure tendency, cloud cover and type, duration and type of precipitation were recorded hourly. This information was used with synoptic charts and radiosonde data (from nearby stations) to define synoptic categories in later analysis (Chapter 3). Local radio weather forecasts and personal observations were used for prior warning of hail storms which could damage the profile instrumentation and as an indication of the prevailing and anticipated synoptic patterns.

## 2.6 Sampling design

The duration and timing of profile sampling was directed toward:

1. A representative value of wind velocity at all sample heights - mean hourly velocity was recorded.
2. A representative mean value of temperature difference between 1 and 4 m - mean hourly values were calculated to correspond with wind velocity data.
3. An even distribution of hourly samples over a 24 hour period (with some bias towards sampling around sunrise and sunset periods, in order to study the effect of a drastic change in radiation regime).

4. An even distribution of hourly samples within synoptic types (in practice conditioned by type frequencies). The length of continuous sampling period was limited by the need to recharge the skidoo batteries available for powering the systems. Sampling was generally carried out over a 6 hour period, though several longer periods of up to 24 hours were also observed.

Sampling was carried out between 6th July and 7th August, 1979. The beginning of the field season was delayed due to slow retreat of the transient snow line. The mast could not be erected until the site chosen was clear of snow.



## CHAPTER THREE

## SYNOPTIC PATTERN CLASSIFICATION

3.1 Introduction

A synoptic climatology regards patterns of weather (clouds, rain, wind etc.) as an implicit function of the surface pressure distribution (Barry and Perry, 1973). A static approach is most appropriate in regions where a large proportion of features form and/or decay 'in situ' or are persistent. Over the Peyto Glacier area, an extensive ridge of high pressure extending from the north-western United States was a common and persistent feature during the summer of 1979.

Synoptic climatologies have been used to stratify sub-synoptic scale spatial variations in parameters such as rainfall, local winds and surface temperatures by establishing correlations with large scale patterns (e.g. Alt, 1978; Singh, Mooley and Kripalani, 1978; Suckling and Hay, 1978; Crane, 1979; Overland and Hiestler, 1980).

Alt (1978), used a summer period synoptic classification system of three main types to explain variations in mass balance of the Meighen Ice Cap in terms of physical processes related to the general circulation. Overland and Hiestler

(1980) established six subjective weather types for the north-east Gulf of Alaska, which they used to stratify coastal winds under strong orographic influence. Subjective synoptic analysis involves assigning daily weather maps to different categories, with recognition of the underlying meteorological processes. The variation of micro-scale climatic parameters may then be examined within the framework of a macro-scale synoptic classification. An alternative approach is to examine associated groups of local climatic data and relate different groups to distinct synoptic categories (e.g. Crane, 1979). Crane used cluster analysis to group days of similar turbulent flux characteristics, in a study of the synoptic controls of the energy budget over an ablating fast ice surface. Days within a particular group were characterized by broadly similar pressure patterns and directions of air flow.

In this study, a subjective 'features of circulation' approach is used to produce a synoptic classification system for the study period, during the ablation season of 1979, on Peyto Glacier. Sands (1966) defines a 'feature of circulation' as a 'recurring, dynamically or thermodynamically caused; pattern of flow over a limited portion (or specific adjacent portion) of a study area. It may be a surface feature, or an upper air feature, but not both.'

This particular study produces a classification system based on the position of major features at the 700 mb level, direction of air flow over the Peyto Glacier area and the associated upper air characteristics of dry-bulb temperature, relative humidity, temperature lapse and wind velocity.

It is suggested that significant differences in micro-scale climatic parameters of the katabatic layer may be physically explained by variations in synoptic scale weather conditions. It is important to be able to predict the nature of profiles of wind and temperature within the boundary and katabatic layers (and their implications for heat flux magnitude) from large-scale, more readily available synoptic information.

### 3.2. Summer weather conditions in the Peyto Glacier region

During the summer, zonal flow and cyclonic activity reach a minimum over western Canada (Bryson and Hare, 1974). Pacific cyclones are most active over the Gulf of Alaska, the Aleutians and inland Alaska. Southern British Columbia and Alberta lie south of the main disturbance zone in most summers.

In spring and summer, strong warm-cored ridges or blocking anticyclones commonly form over the Gulf of Alaska, the Pacific west of British Columbia or over the northern interior. These blocking anticyclones screen western mainland areas from Pacific storms and if persistent, may result in considerable anomalies in precipitation and temperature (Bryson and Hare, 1974). Commonly, persistent warm-cored ridges or highs over the north-western United States cause mild Pacific air to flow onshore. The low level Pacific regime is dominated by the sub-tropical high pressure centre 1,500 km off the Oregon coast.

The origins of the major air masses influencing southern British Columbia and Alberta during the summer are (Fig. 3.1):

1. Maritime Arctic: Westerly winds moving over the cool north-eastern portions of the Pacific ocean arrive on the west coast with a near-moist adiabatic lapse rate, and with high humidity to a considerable depth (Bryson and Hare, 1974).

2. Maritime Polar: Westerly winds from warmer, more southern portions of the north Pacific subside from a sub-tropical anticyclone and move directly eastward to the coast. Maritime polar air will dominate over the study area whenever the sub-tropical high is well established off or over western British Columbia.

3. Continental/Maritime Tropical: With the sub-tropical anticyclone positioned further south, maritime tropical air may be drawn in from the warmer sub-tropical portion of the eastern Pacific ocean. Alternately (and more commonly in the summer of 1979) continental tropical air, conditioned over the hot, dry areas of the south-western United States, arrives over southern British Columbia and Alberta from the south or south-west.

However, the predominantly westerly upper airstream over British Columbia and Alberta carries maritime Arctic or maritime polar air into the Peyto Glacier region (Fig. 4.1, p. 51). Both air masses are considerably modified by passage over the Rocky Mountains. Maritime polar air is warmer and more moist than maritime Arctic air, but loses much

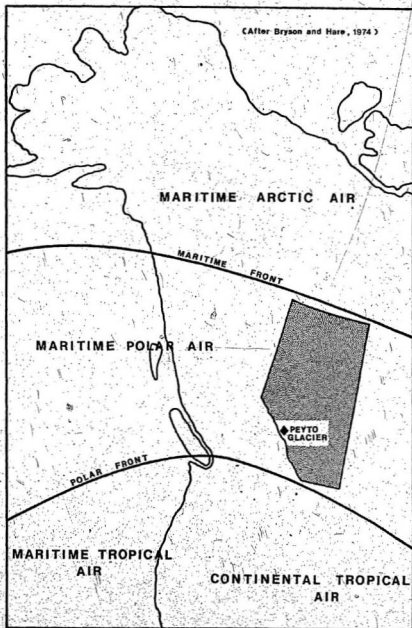


Figure 3.1 Mean frontal positions: summer

of its moisture on the windward slopes of the Coastal Range of British Columbia, and ranges further east. Adiabatic warming occurs during descent on the eastern side of the mountains (occasionally causing chinooks on western sections of the prairies). Intervening spells of continental tropical air are characterized by high temperatures and low relative humidity, and are responsible for the hottest summer weather in the Peyto area (Poessel, 1974).

Cyclonic depressions influencing the area begin as waves on the polar front between tropical and maritime polar air, developing rapidly into closed depressions which move north-eastwards towards British Columbia. Some may terminate off the coast, others follow the coast northwards, and some continue east over southern British Columbia and cross the Rocky Mountains into Alberta, bringing frontal systems with accompanying cloud and precipitation to Peyto Glacier. Orographic depressions or 'Alberta Lows' may form over the mountains as a result of turbulence and unstable conditions. Cyclonic disturbance may also arrive as cold frontal extensions from sub-polar lows over the North-West Territories and Yukon.

### 3.3 Synoptic classification system

A classification system consisting of five different synoptic types for the summer ablation season of 1979 is proposed, based on:

1. The pressure patterns as observed on twice daily synoptic charts (0000Z, 1200Z) at the 700 mb level.\* 700 mb charts were used in preference to 850 mb charts, as the 700 mb level (approximate altitude: 3000 m a.m.s.l.) is the lowest level in which smooth flow may be assumed (Walker, 1961). The 700 mb level was considered most representative of 'free-air' conditions above the purely localized disturbing influence of most mountain ridges.

2. Twice-daily (0000Z, 1200Z) dry-bulb temperature readings at the 700mb (approx. 3000 m) and 500 mb (approx. 5550 m) levels from Vernon radiosonde station (240 km southwest of Peyto Glacier. Fig. 1.1. p. 4 ).

3. Twice-daily (0000Z, 1200Z) relative humidity at the 700 mb and 500 mb levels, obtained from dry-bulb and dew-point depression data from Vernon radiosonde station.

4. The upper air temperature lapse rate between 700 mb and 500 mb (from Vernon data).

5. Cloud cover and type (from observations at Peyto Glacier).

6. 700 mb geostrophic wind direction for Peyto Glacier, computed from the twice-daily synoptic charts (0000Z, 1200Z).

\*Synoptic charts and radiosonde data were provided by the Atmospheric Environment Service (A.E.S), Fisheries and Environment Canada (Edmonton Regional Office).

7. Base camp barometric pressure, maximum and minimum daily temperatures and observed weather conditions.

Five synoptic categories are defined, at the 700 mb level, as follows (Table 3.1):

- TYPE (1) CYCLONIC PACIFIC: Influence from a 700 mb low pressure system, centred to the west of the study area over the Pacific Ocean. This category is normally associated with a well developed surface 'low', (Fig. 3.2).
- TYPE (2) 'LOCAL' CYCLONIC: Influence from a 700 mb centre of low pressure over the Rocky Mountains of Alberta/ British Columbia. (Fig. 3.3).
- TYPE (3) PRONOUNCED ANTICYCLONIC: Influence from a pronounced broad 700 mb ridge of high pressure extending from the western United States, through Alberta, British Columbia and into Yukon and Alaska. (Fig. 3.4).
- TYPE (4) WEAK ANTICYCLONIC: Influence from a weaker amplitude 700 mb ridge of high pressure extending from the western United States into British Columbia and Alberta. (Fig. 3.5).
- TYPE (5) WESTERLY ZONAL: Flow at the 700 mb level westerly zonal - not classifiable as cyclonic or anti-cyclonic (Fig. 3.6).



TABLE 3.1 MEAN CHARACTERISTICS OF SYNOPTIC TYPES

	TYPE 1 CYCLONIC PACIFIC	TYPE 2 'LOCAL' CYCLONIC	TYPE 3 PRONOUNCED ANTICYCLONIC	TYPE 4 WEAK ANTICYCLONIC	TYPE 5 WESTERLY ZONAL	'P' RATIO	LEVEL OF SIGNIFICANCE
700 mb dry bulb temperature (°C)	2.2	-1.5	8.3	5.9	4.2	26.9	0.01
700 mb relative humidity (%)	66	80	42	45	61	13.8	0.01
500 mb dry bulb temperature (°C)	-15.3	-16.7	-10.5	-13.2	-12.9	10.4	0.01
500 mb relative humidity (%)	45	44	26	42	32	1.7	N.S.
700 mb wind direction	260°	280°	250°	250°	275°	W > B	N.S.
700 mb wind velocity (m/s)	6.2	8.5	6.0	6.4	7.8	2.6	0.05
Upper air temperature lapse (°C per 100 m)	0.68	0.59	0.73	0.72	0.64	3.7	0.01
Cloud cover and type	7/10 Cu, Sc	9/10 <sup>As, St</sup> Ac, Sc Low Cu	2/10- <sup>Cb, Ci</sup> Ac, Cb	3/10 Ac, Sc Ci, Cu	5/10 Cu, Ci Ac, Sc	64.8	0.01
Base camp pressure (mb)	797	799	804	803	798	21.7	0.01
Base camp max. temperature (°C)	11.5	8.7	15.8	13.7	12.6	7.0	0.01
Base camp min. temperature (°C)	2.7	2.0	5.4	5.0	3.5	2.0	0.05

N.S. Difference between mean values is not significant.

W > B Variance within samples is greater than between.

\* Specific values of variables for each chart time are included in Appendix C.

Further details of significant differences between synoptic types are contained in Appendix F.

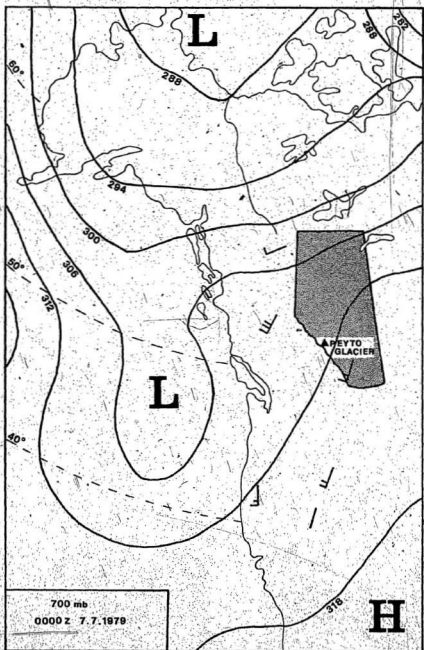


Figure 3.2 Synoptic type (1) Cyclonic Pacific

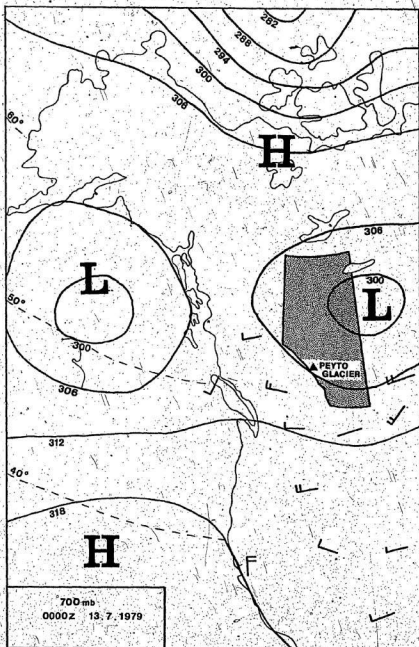


Figure 3.3: Synoptic type (2) 'Local' Cyclonic

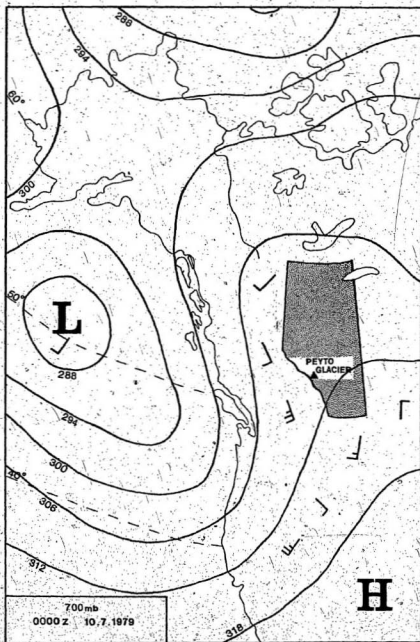


Figure 3.4 Synoptic type (3) Pronounced Anticyclonic

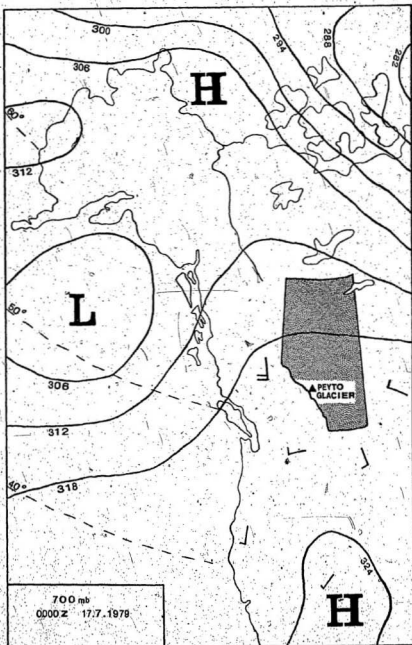


Figure 3.5 Synoptic type (4) Weak Anticyclonic

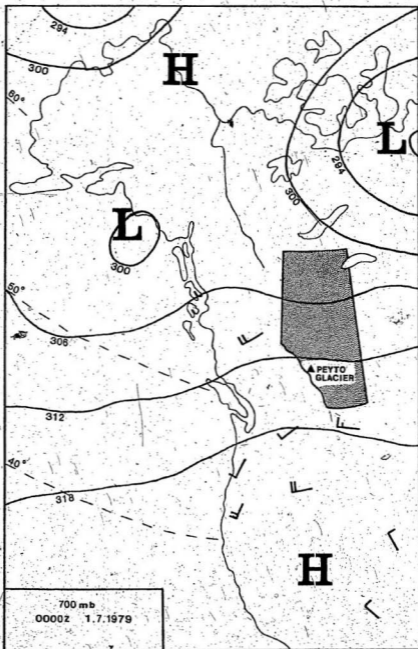


Figure 3.6 Synoptic type (5) Westerly Zonal

Snedecor's F test of Variance<sup>\*</sup> revealed that, using a random sample selected from the study period, differences between the five categories were significant at the 0.01 level (1%) in the following (Table 3.1):

1. 700 mb dry-bulb temperature.
2. 700 mb relative humidity.
3. 700 mb wind velocity (only significant at the 0.05 level).
4. 500 mb dry-bulb temperature.
5. Upper air temperature lapse-rate (700 mb to 500 mb).
6. Mean cloud cover.
7. Base camp mean daily maximum temperature.
8. Base camp mean daily minimum temperature, (only significant at the 0.05 level).
9. Mean base camp pressure.

The 500 mb relative humidity did not show significant variation (at the 0.01 level) between synoptic categories, nor did the 700 mb geostrophic wind direction. All but two of the twice-daily calculated values of the 700 mb geostrophic wind direction lay between 180° and 360°, producing insufficient variation for use as a distinguishing inter-group characteristic.

---

\* Statistical procedures are outlined in Appendix B. A random sample size of one third the total number of hourly observations was used for the variance test.

Synoptic types 2 and 3 show most contrast in characteristics (Table 3.1). The 'Local' Cyclonic category (Type 2) has lowest mean temperatures at both 700 mb and 500 mb levels ( $-1.5^{\circ}\text{C}$  and  $-16.7^{\circ}\text{C}$  respectively), and the smallest upper air temperature lapse rate ( $0.59^{\circ}\text{C}$  per 100 m). This type is characterized by high mean relative humidity (80% at 700 mb) and high mean cloud cover (9/10). Thick stratus and stratocumulus cloud, often with a base as low as 2000 m to 3000 m brings precipitation as heavy rain, soft hail or snow, accompanied by gusty winds.

In contrast, synoptic type 3 (Pronounced Anticyclonic) has highest mean temperatures at both 700 mb and 500 mb ( $8.3^{\circ}\text{C}$  and  $-10.5^{\circ}\text{C}$  respectively) and the greatest mean upper air temperature lapse rate ( $0.73^{\circ}\text{C}$  per 100 m). The high value of upper air temperature lapse is due primarily to intensive surface heating by day under anticyclonic conditions, causing heating of the lower atmosphere and a greater temperature difference between the 700 mb and 500 mb levels. Synoptic category 3 has the lowest mean relative humidity (42% at 700 mb) and lowest mean cloud cover (2/10). No precipitation was recorded while this synoptic type was dominant. Cloud types observed were mainly cirrus and altocumulus.

Synoptic type 4 (Weak Anticyclonic) is also accompanied by warm mean upper air temperatures ( $5.9^{\circ}\text{C}$  at 700 mb and  $-13.2^{\circ}\text{C}$  at 500 mb) with a relatively large mean temperature



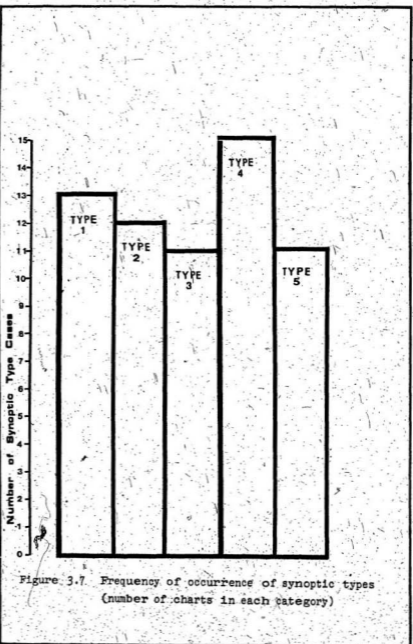
lapse-rate ( $0.72^{\circ}\text{C}$  per 100 m) and low relative humidity (45% at 700 mb). Mean cloud cover was 3/10 (Haze, Ac, Sc, Ci, Cu) with no precipitation recorded.

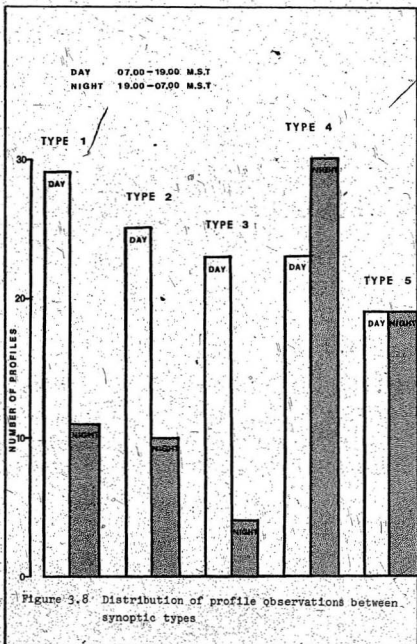
Synoptic type 1 (Cyclonic Pacific) is accompanied by slightly warmer air temperatures than type 2 ('Local' Cyclonic), the 700 mb and 500 mb mean dry bulb temperatures being  $2.2^{\circ}\text{C}$  and  $-15.3^{\circ}\text{C}$  respectively, with a temperature lapse-rate of  $0.68^{\circ}\text{C}$  per 100 m. The air is quite moist (mean relative humidity of 66% at the 700 mb level) with a mean cloud cover of 7/10 (Cu and Sc predominate). Precipitation with this type occurred as rain, hail or sleet with occasional thunder showers.

Synoptic type 5 (Westerly Zonal) has upper air temperatures intermediate between anticyclonic (types 3 and 4) and cyclonic (types 1 and 2), with 700 mb and 500 mb mean dry bulb temperatures of  $4.2^{\circ}\text{C}$  and  $-12.9^{\circ}\text{C}$  respectively (upper air temperature lapse rate of  $0.64^{\circ}\text{C}$  per 100 m). The zonal flow is quite moist (mean relative humidity of 61% at 700 mb) with a mean cloud cover of 5/10 (Cu, Ci, Ac, Sc). Precipitation occurred as rain or hail in thunderstorms.

### 3.4 Frequency of types

Figure 3.7 shows the number of charts (twice daily at 0000Z and 1200Z) classified in each synoptic category over the period 6th July to 7th August 1979. Anticyclonic conditions (synoptic types 3 and 4) account for 41% of the





charts classified. Figure 3.8 shows the number of wind and temperature profiles recorded in each category and also subdivides the observations into day (0700 to 1900 M.D.S.T.) and night (1900 to 0700 M.D.S.T.) periods.

## CHAPTER FOUR

## ANALYSIS OF PROFILE DATA

4.1 The influence of the 700 mb geostrophic wind on the glacier katabatic wind.

During the summer field season of 1979, westerly upper air winds (as computed from twice-daily 700 mb synoptic charts) prevailed at Peyto Glacier. More than 20% of winds at the 700 mb level were from  $275^{\circ}$ . There were relatively few cases in which the upper wind was in a down-glacier direction (i.e. from  $207^{\circ}$ ) (Fig. 4.1). The upper air wind rose shows a pronounced clockwise deviation from the glacier fall-line.

In contrast, the wind at 2-m above the ice surface, as observed at the glacier meteorological site, demonstrates a predominantly down-glacier direction (Fig. 4.1). There is a definite clockwise deviation of the mean surface wind direction from the glacier fall-line, which coincides with the 700 mb frequency distribution. Only 3% of the recorded hourly mean wind directions fall outside the quadrant  $180^{\circ}$  to  $270^{\circ}$ , with over 20% of observed winds being from  $205^{\circ}$  and over 20% from  $225^{\circ}$ .

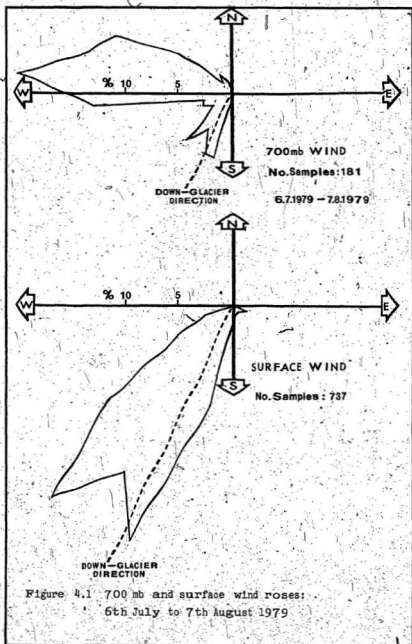
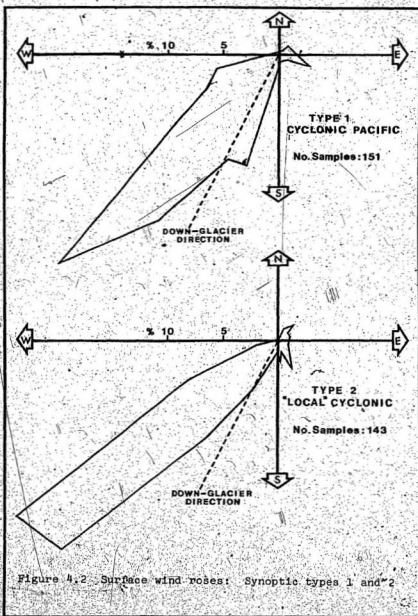


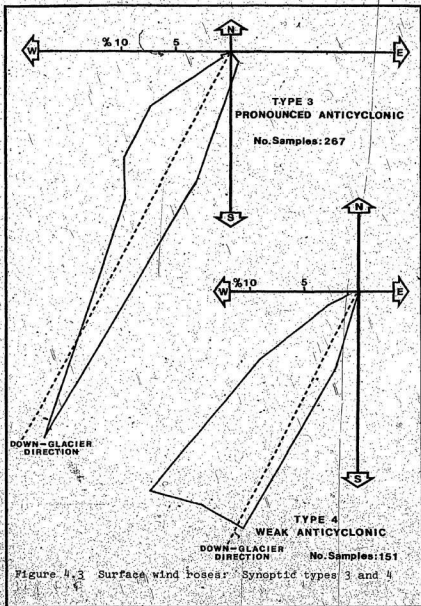
Figure 4.1 700 mb and surface wind roses:  
 6th July to 7th August 1979

However there is considerable variation in surface wind direction within this quadrant, under different synoptic categories (Figs. 4.2 to 4.4 and 4.5 to 4.9). Under cyclonic conditions the surface wind direction shows a greater tendency to deviate more from the glacier fall-line. Under Cyclonic Pacific influence (Synoptic category 1) 30% of the surface winds observed were from  $225^{\circ}$ , and a small number of hourly observations (7%) were of winds directed either up-glacier or roughly perpendicular to the fall-line (Fig 4.2). Greatest disturbance of the surface wind direction occurred under 'Local' Cyclonic conditions (Synoptic category 2). Observations in this category include an up-glacier low level wind associated with roughly up-glacier flow at the 700 mb level (Fig. 4.6), whilst 13% of the hourly mean surface winds were directed either up-glacier or perpendicular to the fall-line (Fig. 4.2). The predominant surface wind direction was from  $235^{\circ}$ . Under Westerly Zonal flow (Synoptic category 5), 40% of the surface winds were from  $225^{\circ}$ . Despite a fairly consistent upper wind direction under these conditions (clockwise of the glacier fall-line by  $45^{\circ}$  to  $75^{\circ}$ ), there were substantial deviations observed in the direction of the glacier wind as compared to anticyclonic conditions (Figs. 4.4 and 4.9).

Thus, during cyclonic and zonal conditions, there appears to be relatively strong geostrophic control of the surface wind. Clockwise deviation of the upper wind from







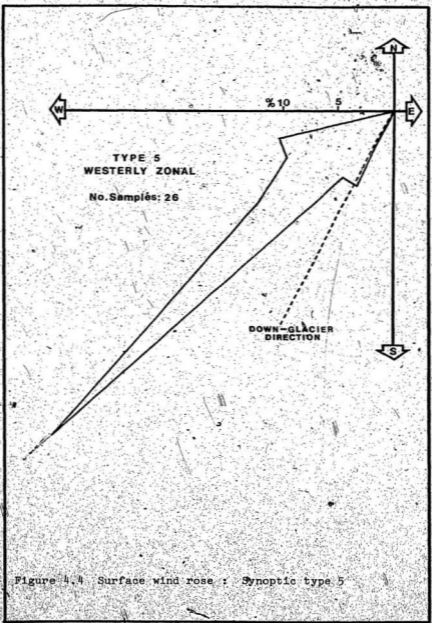


Figure 4.4 Surface wind rose : Synoptic type 5

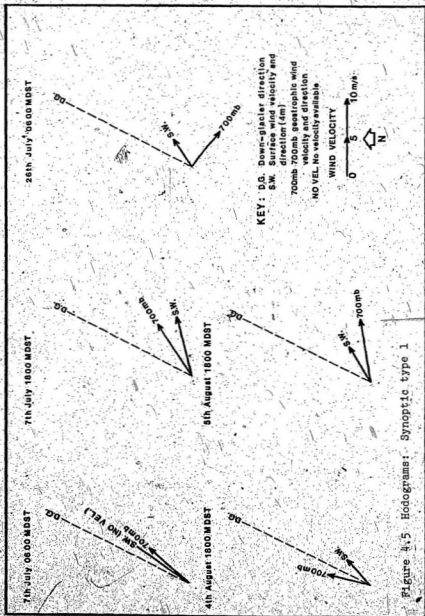


Figure 4.5 Hodograms: Synoptic type 1

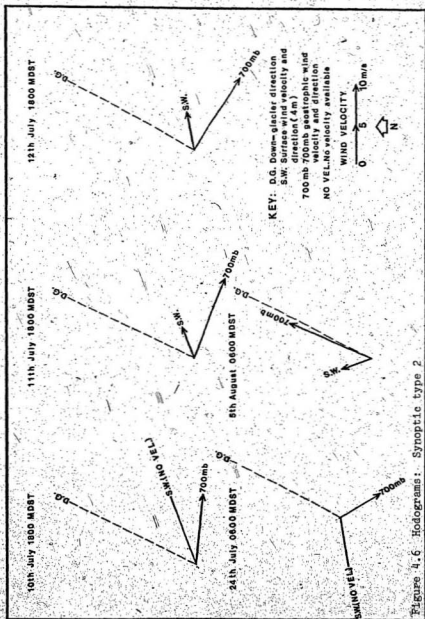


Figure 4.6. Hodograms: Synoptic type 2

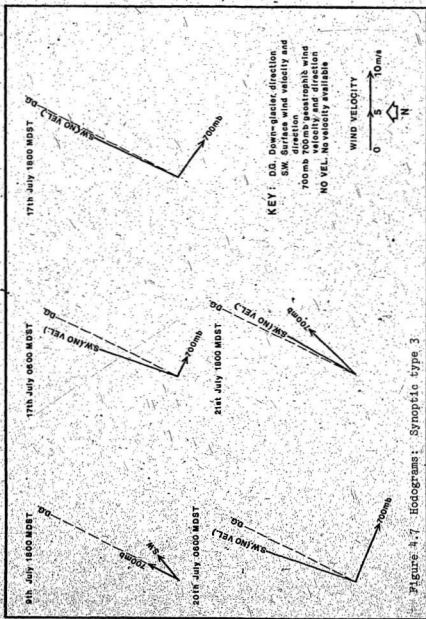


Figure 4.7. Hodograms: Synoptic type 3

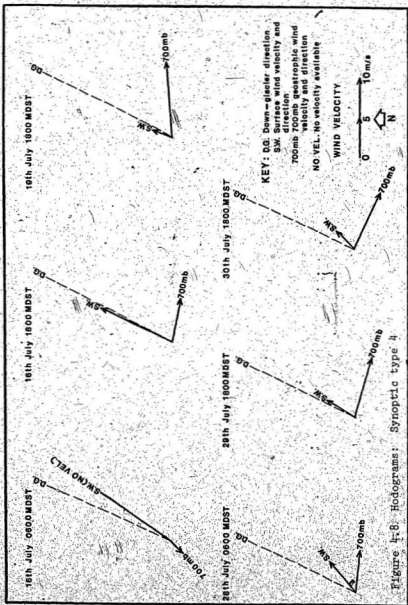


Figure 4-8. Hodograms: Synoptic type 4

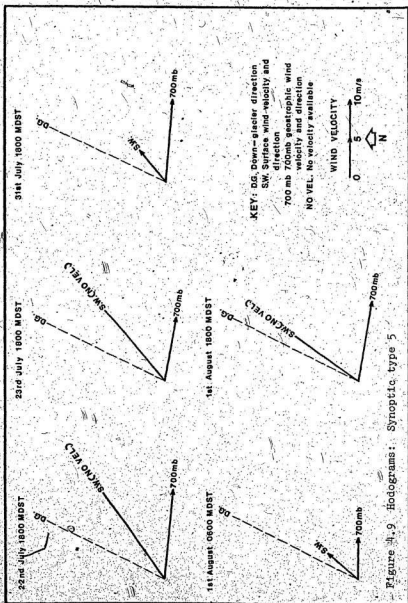
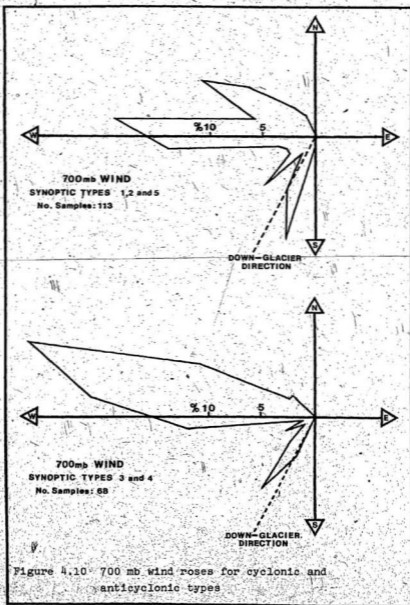


Figure 4.9 Hodograms: Synoptic type 5

the glacier fall-line (Fig. 4.10) causes the low level wind to be similarly deflected under synoptic categories 1, 2 and 5 (Figs. 4.2 and 4.4). Most pronounced geostrophic control occurs under 'Local' Cyclonic influence (Synoptic category 2). Fig. 4.6 shows that under such strong control, the surface wind may be characterized by an up-glacier flow (observed only infrequently), or more commonly modified to flow roughly perpendicular to the fall-line. Figures 4.5 and 4.9 demonstrate that under both synoptic categories 1 and 5 there is a similar geostrophic control of the glacier wind direction, which is deflected in a clockwise direction from the fall-line.

Under anticyclonic influence, with weak synoptic pressure gradients, the surface wind direction is little affected by the 700 mb direction (Figs 4.3 and 4.10), and flows consistently down the glacier fall-line, with deviations of less than  $\pm 25^\circ$ . With a dominant high pressure ridge over the Peyto Glacier area (Synoptic category 3), 40% of the observed surface winds were from  $205^\circ$ , i.e. directly down-glacier (Fig. 4.3). Figure 4.7 further emphasizes the weakness of control by upper winds under anticyclonic conditions, when a slightly anticlockwise deviation of the surface wind occurs on several occasions. With a weak high pressure ridge over Peyto Glacier (Synoptic category 4), more than 20% of observed surface winds blew directly down-glacier, more than 20% were from  $215^\circ$  and a further 20% from  $225^\circ$  (Fig. 4.3). This category shows slight





clockwise deviation of mean low level wind direction from the fall-line. Comparison of 700 mb and surface wind direction for individual hours (Fig. 4.8) shows that even with the 700 mb wind directed up-glacier, there is little deviation of the surface katabatic wind from the fall-line.

The relationship between 700 mb wind direction and surface wind velocity was also considered. Several previous studies have noted the apparent augmentation of surface wind velocities by synoptic scale winds blowing in the same direction (Businger and Ramano Rao, 1965; Holmgren, 1971; Streten, Ishikawa and Wendler, 1974; Martin, 1975). The 700 mb wind directions were computed from synoptic charts to correspond with all daytime surface wind profile observations. Fig. 4.11 shows a negative correlation between maximum surface profile wind velocity and the direction of the 700 mb wind i.e. greatest surface velocities occur with a reinforcing wind at upper levels (for all synoptic categories). This correlation was found to be significant at the 0.05 level.

#### 4.2 Depth of the katabatic layer and wind velocity profile shape under different synoptic influences.

Since initial development of katabatic flow has been shown elsewhere to be favoured by calm, clear conditions (Businger and Ramano Rao, 1965; Lettau, 1966; Streten,

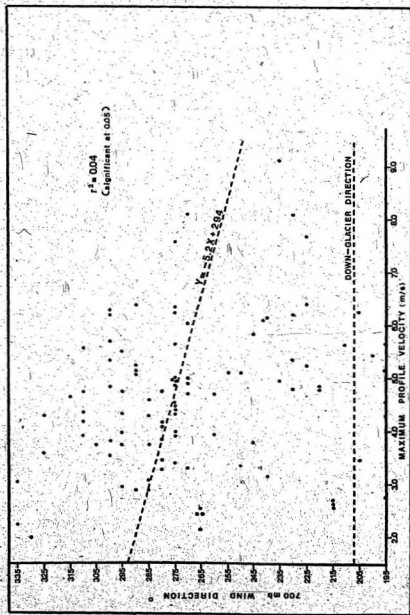


Figure 4.11. The correlation between 700 mb wind direction and maximum profile velocity

Ishikawa and Wendler, 1974; Martin, 1975; Munro and Davies, 1977), wind and temperature profiles obtained at Peyto Glacier were examined for katabatic characteristics under the different synoptic categories.

In theory, anticyclonic conditions in summer should favour a strong near-surface temperature inversion above the glacier, with a low level wind velocity maximum and thermocline which typify katabatic flow. During the day, with high incoming radiation and only scattered clouds, the temperature contrast between the ice surface and surrounding ice-free areas is at a maximum, and air advected over the glacier has a relatively high ambient temperature. At night, strong near-surface inversions may be maintained due to significantly warmer air temperatures associated with anticyclonic conditions and strong surface cooling (Table 3.1 p. 38). Anticyclonic synoptic conditions, which favour well-developed katabatic flow (Fig. 4.12 and Table 4.1), thus result in a higher frequency of low level wind velocity gradient reversals. Under cyclonic and zonal conditions however, small strength inversions and turbulent wind conditions lead to infrequent low level wind velocity gradient reversals and poorly developed katabatic flow.

A  $\chi^2$  test (see Appendix B) showed a very significant difference (at the 0.001 level) in the number of low level wind velocity maxima observed under each synoptic type, as compared to the expected frequency (Table 4.1).

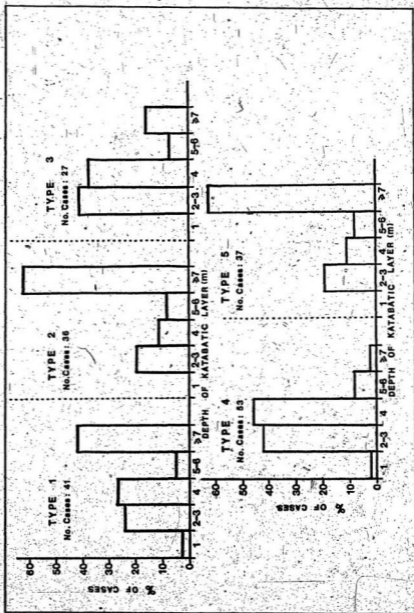


Figure 4.12 Depth of katabatic layer according to synoptic type

TABLE 4.1 FREQUENCY OF LOW LEVEL WIND VELOCITY GRADIENT ( $\frac{\Delta u}{\Delta z}$ ) REVERSALS (WITHIN 6 m OF THE ICE SURFACE) ACCORDING TO SYNOPTIC CATEGORY.

SYNOPTIC CATEGORY	CYCLONIC	'LOCAL'	PRONOUNCED	WEAK	WESTERLY	TOTAL
	PACIFIC	CYCLONIC	ANTI-	ANTI-	ZONAL	
	1	2	3	4	5	
No. of hourly profiles observed	41	36	27	53	37	194
No. of profiles with low level $\Delta u/\Delta z$ reversal	24	14	23	52	14	127
Expected frequency (E)	27	24	18	34	24	127
% profiles with low level velocity reversal (i.e. demonstrating katabatic flow).	59%	39%	85%	98%	38%	

The depth of the katabatic layer (as defined by the height above the ice surface of the wind velocity maximum), thus varies significantly according to prevailing synoptic weather conditions (Fig. 4.12). Synoptic categories 2 and 5 show identical features. Sixty percent of the profiles do not have a velocity maximum within the first 7 m. Strong katabatic flow rarely develops, which results from weak stability and inversion strength, with disruption of the surface layer by

gusty, storm-associated winds (particularly under 'Local' Cyclonic influence: synoptic type 2). Under 'Local' Cyclonic influence profiles show little variation in wind velocity with height (Fig. 4.13b). Similarly, under Westerly Zonal flow (synoptic type 5) profiles tended towards a regular logarithmic variation (Fig. 4.13c). A steady wind velocity of 4 to 6  $\text{m s}^{-1}$  was maintained over long periods.

Synoptic type (1) (Cyclonic Pacific) also includes a large number of profiles which do not exhibit a low level wind velocity maximum (42%). These profiles typically demonstrate a large variation in velocity between height intervals (Fig. 4.13a). Upper levels often experienced considerably higher velocities than levels nearer the ice surface, which may have been a result of the reinforcing effect of synoptic scale winds. Profile shape varied considerably between hourly samples, with turbulence in the near-surface air layer due to synoptic scale cyclonic disturbance.

However, with average or below average cloud cover for this type, a low level velocity maximum characterizing katabatic flow was developed more frequently than under synoptic types 2 and 5. Near-surface mean inversion strength, local and bulk stability values were also found to be greater under synoptic type 1 (sections 4.3 and 4.6).

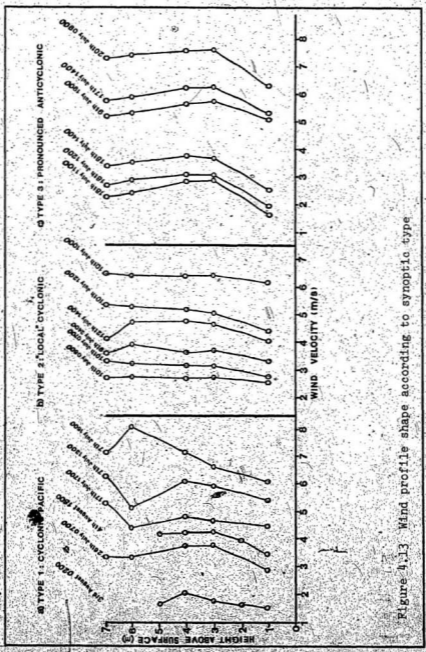


Figure 4.13 Wind profile shape according to synoptic type



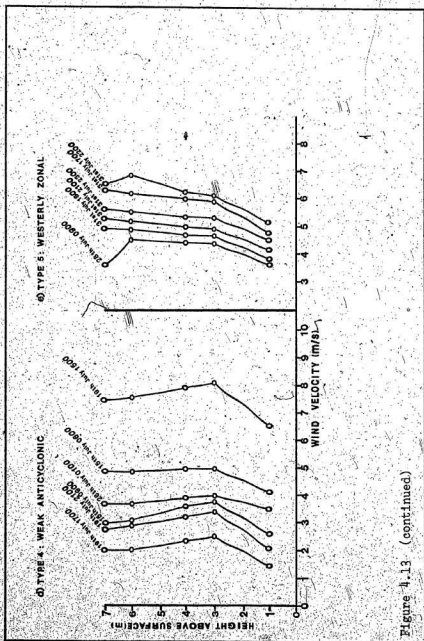


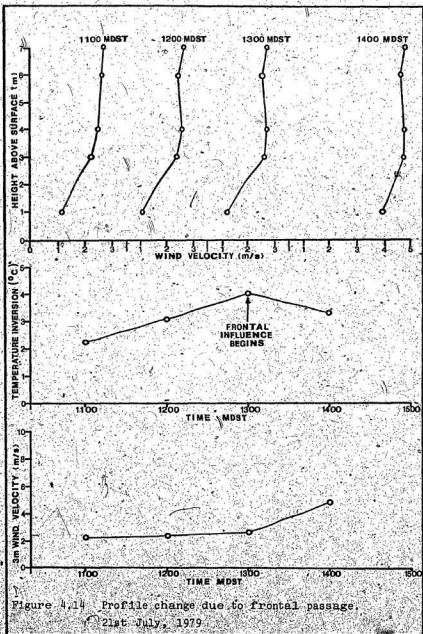
Figure 4.13 (continued)

Both anticyclonic types (synoptic types 3 and 4) favour the development of a shallow katabatic layer with a wind velocity maximum between 2 and 4 m above the ice surface. However, occasionally the profiles may be modified by the passage of weak frontal systems (not associated with strong cyclonic flow at the 700 mb level). Fig. 4.14 shows the modification of profiles on 21st July with the passage of a weak warm front through the area (overall strong anticyclonic influence). With the passage of the front, the strength of the near-surface temperature inversion decreased, low level wind velocities increased and the profiles became more linear, showing less katabatic curvature.

Only a small number of profiles in each category demonstrate a velocity maximum at 5 or 6 m, suggesting that the synoptic types encountered are mostly associated with either a low level wind velocity maximum (anticyclonic types) or only rarely show a maximum velocity within the first 6 m (cyclonic and zonal types).

#### 4.3 Stability of the katabatic layer

Stability in the near-surface air layer was described by both a local and a bulk Richardson number. The Richardson number is defined as, "the ratio of the rate at which mechanical energy for the turbulent motion is being dissipated (or produced) by buoyancy forces (free or natural convection) to the rate at which mechanical energy is being produced or dissipated by inertial forces (forced or mechanical convection)". (Richardson, 1920). The Richardson number is less than zero in unstable conditions and greater than zero in stable conditions.



The local Richardson number ( $Ri_L$ ) is given by:

$$Ri_L = \frac{g}{T} \frac{\frac{\Delta T}{\Delta Z}}{\left(\frac{\Delta U}{\Delta Z}\right)^2}$$

$g$  = acceleration due to gravity ( $ms^{-2}$ ).

$T$  = mean temperature of the air layer (K).

$\frac{\Delta T}{\Delta Z}$  = temperature difference over the height interval  
 $\Delta Z$  ( $Km^{-1}$ ).

$\frac{\Delta U}{\Delta Z}$  = difference in wind velocity over the height interval  
 $\Delta Z$  ( $s^{-1}$ ).

The local Richardson number is valid at a specific reference level  $Z$ , and is best used when the purpose of the analysis is to detect a possible functional relationship between the relative curvature of the wind profile and convective stability (Lettau, 1957).

The bulk Richardson number ( $Ri_B$ ) defines the stability of a finite air layer and may be used to group wind profiles at a certain site into classes according to the degree of convective stability (Holmgren, 1971).

$$Ri_B = \frac{g \Delta T l_c}{T U_c^2}$$

$g$  = acceleration due to gravity ( $ms^{-2}$ ).

$T$  = mean temperature of the air layer ( $^{\circ}C$ ).

$\Delta T$  = temperature difference between two standard levels  
 (in this case 1 and 4 m)  $^{\circ}C$ .

$l_c$  a critical distance above the surface at which the wind velocity is  $U_c \text{ ms}^{-1}$ . This distance was taken to be the height above the ice surface of maximum wind velocity (following Holmgren, 1971).

The stability of the near-ice air layer, as described by the bulk Richardson number, is thus dependent on the temperature stratification (free or natural convection forces) and on the low level wind velocity (forced or mechanical convection forces).

The data obtained for Peyto Glacier show a strong negative correlation between stability (as defined by  $Ri_B$ ) and the 3m profile velocity (Fig. 4.15). The correlation coefficient of -0.63 is significant at the 0.001 level. The regression equation calculated for this relationship is

$$Ri_B = -0.15 V_{3m} + 11.14$$

(for  $0 < Ri_B \leq 1$ )

$$\text{and } Ri_B = -0.94 V_{3m} + 4.60$$

(for  $Ri_B > 1$ ) Fig. 4.16

Thus increasing low level wind velocity leads to increasing turbulence and decreased stability of the near-surface air layer. Wind velocity plays a slightly more important role in determining stability in this case than does the ambient temperature stratification. A partial correlation between  $Ri_B$  and the 3m wind velocity carried out to

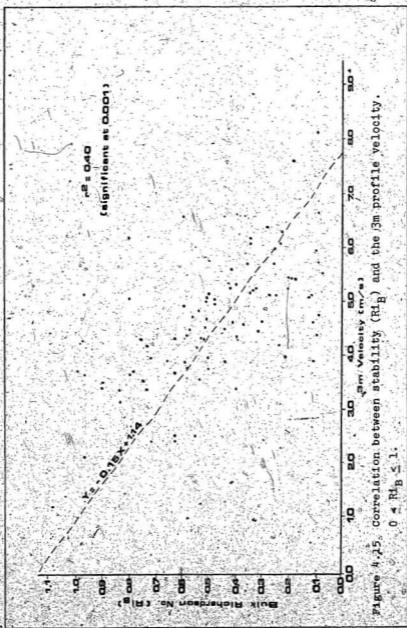


Figure 4.15. Correlation between stability ( $Ri_B$ ) and the 3m profile velocity.

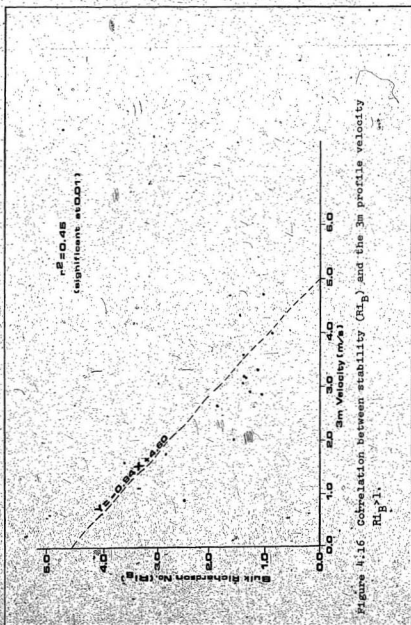


Figure 4.16 Correlation between stability ( $Ri_B$ ) and the 3m profile velocity  
Fig. 1.

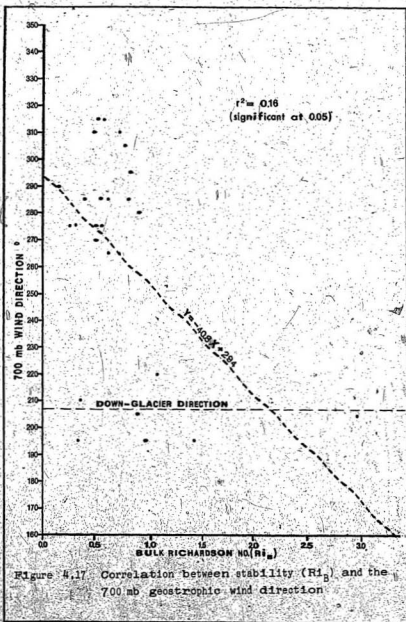
exclude the effect of inversion strength, yields a negative partial correlation coefficient significant at 0.001. The positive partial correlation coefficient between  $R_{1B}$  and inversion strength (excluding the effects of wind velocity) is also significant at 0.001.

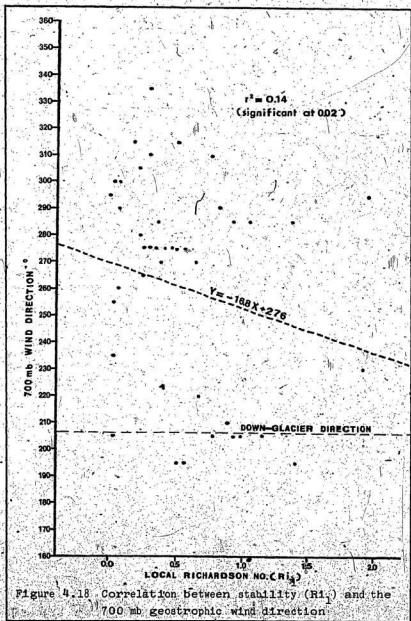
#### 4.4 The influence of the 700 mb wind direction on local stability

The direction of the 700 mb wind (above the influence of the glacier) has important implications for the stability of the near-glacier air layer. Under cyclonic conditions, upper winds blowing across an ice slope enhance interfacial shear and may play a dominant role in determining whether or not a true katabatic flow is present (Manins and Sawford, 1979). At Peyto, upper winds blowing perpendicular to the glacier fall-line cause considerable turbulence in the glacier basin, resulting in distortion of the temperature and wind fields in the near-surface layer. Under these conditions a considerable decrease in the stability of the katabatic layer is to be expected.

The Peyto Glacier results show that when the 700 mb geostrophic wind is oriented down-glacier, reinforcing the glacier katabatic wind, near-ice stability is greater than when the 700 mb wind is directed across or up-glacier (Figs. 4.17 and 4.18). Both local ( $R_1$ ) and bulk ( $R_{1B}$ )







measures of stability show a decrease as the upper wind direction deviates from the fall-line. The strength of the near-ice inversion also tends to decrease as the upper wind deviates from down-glacier and increased turbulence disturbs the near-surface temperature stratification (Fig 4.19). Augmentation of surface wind velocities by an upper wind in the same direction is noted in section 4.1.

Holmgren (1971) found that on the Devon Island Ice-Cap, upper winds directed down-glacier resulted in lower stability of the near-ice air layer, than upper winds directed up-glacier. These contrasting observations are a result of the difference in glacial environment. In the Devon Island situation upper winds directed up-glacier result in advection of warmer air from the surrounding oceanic areas, with a corresponding increase in near-ice inversion strength and stability.

#### 4.5 Variations in stability between synoptic types.

A mean value of stability in the near-surface air layer was calculated for each synoptic type. The local Richardson number demonstrated a significant difference in stability between types (Table 4.2). The near surface air layer was stable under all the synoptic types encountered, but greatest values of stability occurred under anticyclonic influence (specifically synoptic category 4). Synoptic category (1) (Pacific Cyclonic) also shows a surprisingly high mean stability. Synoptic category (2) is associated with least stability in the near-ice layer.

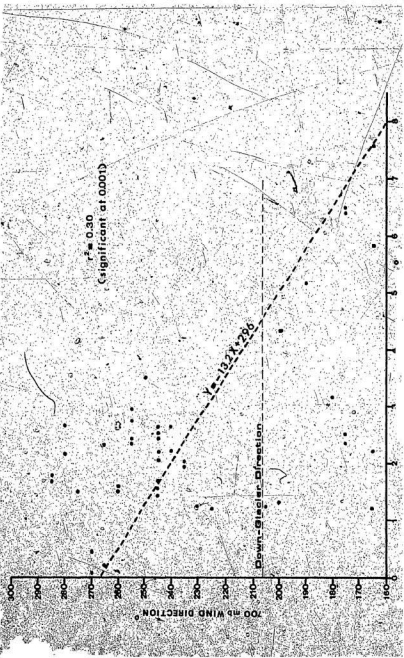


Figure 4.19 Correlation between 1 to 4m inversion strength and the 700 mb geostrophic wind direction.

TABLE 4.2 MEAN LOCAL STABILITY VALUES ( $R_1$ )

SYNOPTIC CATEGORY	1 CYCLONIC PACIFIC	2 'LOCAL' CYCLONIC	3 PRONOUNCED ANTICYCLONIC	4 WEAK ANTICYCLONIC	5 WESTERLY ZONAL
MEAN $R_1$	0.35	0.18	0.36	0.50	0.29

(A square root transformation was used to normalize the data. The difference between means is significant at the 0.01 level (F ratio: 4.4); Snedecor's F-test for variance. APPENDIX B).

Mean values of the bulk Richardson number calculated for observations under each synoptic type also show a significant difference between types (at the 0.05 level). The stability values demonstrate similar variation between types to those calculated using a local Richardson number (Table 4.3). In order to calculate a measure of bulk stability, the level of maximum wind velocity had to lie within the 7 m sampled. Under cyclonic conditions, many profiles did not show such a low level velocity maximum (section 4.2) which may have led to a less significant variation between categories.

The differences in stability observed between synoptic categories are due to variations in wind and temperature characteristics of the near-surface layer. Variations in these parameters according to prevailing synoptic conditions are discussed in the following sections.

TABLE 4.3 MEAN BULK STABILITY VALUES ( $R_1$ )

SYNOPTIC CATEGORY	1 CYCLONIC -PACIFIC	2 'LOCAL' CYCLONIC	3 PRONOUNCED ANTICYCLONIC	4 WEAK ANTICYCLONIC	5 WESTERLY ZONAL
MEAN $R_1$ B	0.64	0.25	0.56	0.62	0.46

(A square-root transformation was used to normalize the data. The difference between means is significant at the 0.05 level (F ratio: 2.5): Snedecor's F-test for variance. APPENDIX B).

#### 4.6. Variations in surface inversion strength

The strength of the near-surface inversion was found to be significantly greater under anticyclonic conditions (synoptic categories 3 and 4) than under cyclonic and zonal influence (synoptic categories 1, 2 and 5), (Table 4.4).

TABLE 4.4 MEAN SURFACE INVERSION STRENGTH

SYNOPTIC CATEGORY	1 CYCLONIC PACIFIC	2 'LOCAL' CYCLONIC	3 PRONOUNCED ANTICYCLONIC	4 WEAK ANTICYCLONIC	5 WESTERLY ZONAL
INVERSION STRENGTH (1 to 4 m) <sup>o</sup> C	2.12	1.07	3.27	2.33	1.84

(The difference between means is significant at the 0.01 level (F ratio: 13.3): Snedecor's F-test for variance. APPENDIX B).

Synoptic type 2 ('Local' Cyclonic) was associated with the weakest strength inversions. This category is typified by unstable, stormy conditions which influence the entire basin. However, even under these unfavourable conditions a small strength inversion was maintained near the ice surface in all but three hourly observations when a very small lapse was recorded between 1 and 4 m.

Variability of the strength of the surface inversion (shown by a mean hourly standard deviation of temperature difference) also demonstrates significant differences under different synoptic conditions (Table 4.5).

TABLE 4.5 MEAN HOURLY STANDARD DEVIATION OF THE  
1 to 4 m TEMPERATURE DIFFERENCE

SYNOPTIC CATEGORY	1 CYCLONIC PACIFIC	2 'LOCAL' CYCLONIC	3 PRONOUNCED ANTICYCLONIC	4 WEAK ANTICYCLONIC	5 WESTERLY ZONAL
STANDARD DEVIATION °C	0.78	0.29	1.66	0.81	1.00

(A logarithmic transformation was used to normalize the data. The difference between means is significant at the 0.01 level (F ratio: 16.9): Snedecor's F-test for variance. APPENDIX B).

There is greater variation under anticyclonic conditions (synoptic categories 3 and 4) than under cyclonic and zonal conditions (synoptic categories 1, 2 and 5). This may be partly due to rapid fluctuations in temperature which occur

with occasional cloud passage across otherwise clear anti-cyclonic skies. Under anticyclonic conditions a thermocline develops associated with the low level wind velocity maximum (Munro, 1975). The observed large variation in temperature difference within each hourly observation may thus be partially due to the passage of 'thermal' waves travelling along the interface between air above and within the katabatic layer (Holmgren, 1971). With the upper temperature sensor positioned at a level often coinciding with the height of the low level wind maximum, temperature fluctuations along the interface would be recorded as a highly variable temperature difference.

Under cyclonic conditions (particularly synoptic type 2) there is relatively little fluctuation in temperature difference and the small inversion strength appears to be maintained quite steadily. Under these conditions cloud cover is considerable, with little variability in insolation. The height of maximum velocity is usually not within the lowest few metres, so that any fluctuations along the interface will not be recorded by the temperature difference system.

#### 4.61 Variations in strength of the temperature inversion with cloud cover

Cloud cover, through influencing radiation receipt in the near-ice air layer, influences the intensity of the surface based inversion. Greater cloud cover associated



with cyclonic and zonal conditions (synoptic categories 1, 2 and 5) causes a decrease in radiation received at and near the surface. This results in a smaller contrast in air/surface temperatures and a lower value of inversion strength than with anticyclonic conditions (Table 4.6).

TABLE 4.6 VARIATION OF INVERSION STRENGTH WITH CLOUD COVER ACCORDING TO SYNOPTIC CATEGORY

SYNOPTIC CATEGORY	1 CYCLONIC PACIFIC	2 'LOCAL' CYCLONIC	3 PRONOUNCED ANTICYCLONIC	4 WEAK ANTICYCLONIC	5 WESTERLY ZONAL
MEAN CLOUD COVER	7/10	9/10	2/10	3/10	5/10
MEAN INVERSION STRENGTH (OC) 1 to 4 m	2.12	1.07	3.27	2.33	1.84

(The differences between categories in mean cloud cover and inversion strength are both significant at the 0.01 level (F ratios: 64.8 and 13.3 respectively): Snedecor's F-test for variance. APPENDIX B).

Greatest cloud cover occurs with intense local cyclonic disturbances (synoptic category 2). Under these conditions the cloud base is usually very low (2,000 to 3,000 m), with thick stratus and stratocumulus, heavy rain, soft hail or snow, and gusty winds. Least cloud cover occurs under

anticyclonic conditions (synoptic categories 3 and 4) and is generally high cloud (cirrus and altocumulus).

Observations of surface inversion strength were subdivided according to four cloud cover categories (Table 4.7). Significant differences between categories were obtained which conform with the results obtained under different synoptic types.

TABLE 4.7 VARIATION OF INVERSION STRENGTH WITH CLOUD COVER

CLOUD COVER	NO. OF CASES	MEAN INVERSION STRENGTH (1. to 4m) OC
< 2/10	34	2.86
3/10 - 5/10	23	3.05
6/10 - 8/10	49	2.12
9/10 -10/10	24	0.72

(The difference between means is significant at the 0.01 level (F ratio: 18.4): Snedecor's F-test for variance. APPENDIX B).

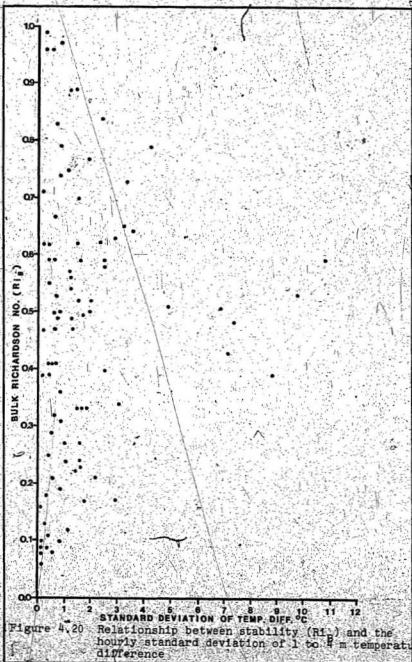
#### 4.62 Temperature fluctuations and stability

The temperature difference as measured between 1 and 4 m above the ice surface showed considerable variation about the mean value within each hourly sample, particularly under anticyclonic influence. The relationship between stability of the near ice air layer (as defined by the bulk Richardson

number  $Ri_B$ ) and the hourly standard deviation of temperature difference was examined (Fig. 4.20). There appears to be greater variation of temperature difference about the mean value with increasing stability of the near-surface air layer (i.e. as  $Ri_B$  increases from 0 to 1).

Under the least stable conditions encountered ( $Ri_B < 0.35$ ) the near surface layer was well mixed by strong, gusty low level winds. Maximum velocity within the first 7 m was generally greater than  $4.0 \text{ ms}^{-1}$ . This results in weak inversion strength and little variation of the temperature difference within an hourly sample. Such conditions are commonly encountered under cyclonic and zonal synoptic influence (synoptic categories 1, 2 and 5), with storm passage and associated instability within the basin.

5. With greater stability ( $Ri_B > 0.35$ ) and strong temperature inversions associated with anticyclonic conditions there was greater variability of inversion strength within an hourly sample. This may be due to a combination of cloud passage and the effect of 'thermal' waves travelling along the thermocline (section 4.6). Hoinkes (1954) describes a linear relationship between the near-surface temperature inversion and amplitudes of temperature variation which reach a maximum in the glacier wind. He attributes this principally to the turbulent mixing process of air near the ice surface.



4.7 Further evidence for a thermocline associated with a low level velocity maximum

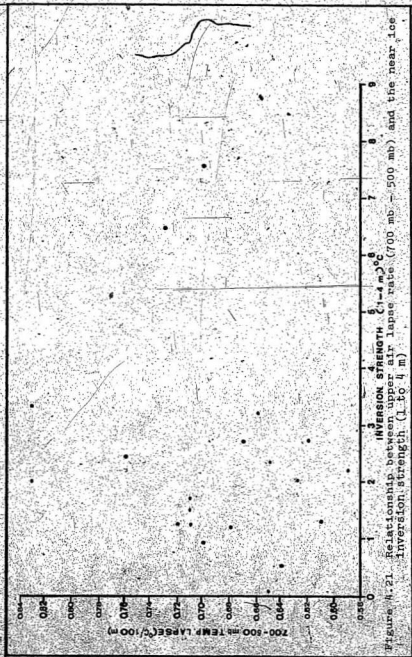
The presence of a thermocline at approximately the same level as the wind velocity maximum, during katabatic flow, was referred to in the previous section. Further evidence for the presence of a thermocline is given by the fact that under the same synoptic conditions, the mean strength of the temperature inversion (between 1 and 4 m above the surface) is greater for wind velocity maxima at or below 4 m, than for wind velocity maxima at or higher than 5 m above the surface. This is to be expected if the thermocline occurs at approximately the same level as the wind velocity maximum. The thermocline will often be included in the 1 to 4 m temperature difference for wind velocity maxima at or below 4 m, resulting in a higher value of inversion strength.

Inversion strengths under synoptic categories 1, 3 and 5 all demonstrate a significantly greater value for wind velocity maxima at or below 4 m above the surface. Synoptic category 2 ('Local' Cyclonic) shows no significant difference in inversion strength with a low level wind velocity maximum, due to the infrequent occurrence of such profiles. Under synoptic category 4 (Weak Anticyclonic) no significant difference was noted, but there are few profile observations in this category which do not have a wind velocity maximum at or below 4 m.

#### 4.8. Relationship between upper air temperature lapse (700 mb to 500 mb) and near-surface inversion strength

A mean upper air dry bulb temperature lapse rate characterizing each synoptic type was calculated using radiosonde data from Vernon, British Columbia, for the air layer between 700 mb and 500 mb. Charts with frontal disturbance between Vernon and Peyto were not included in the analysis. The upper air temperature lapse was found to be significantly greater under anticyclonic conditions (mean values were significantly different at the 0.01 level; Snedecor's F-test for variance. APPENDIX B) (Table 3.1 p. 38). Strong daytime surface heating under anticyclonic conditions, due to scattered cloud cover, causes considerable warming of the lower atmosphere and thus contributes to a greater temperature lapse than under cyclonic conditions. With considerable cloud cover, associated with cyclonic weather types, intensive surface heating does not occur, and the upper air temperature lapse is correspondingly less.

Values of the surface inversion strength (1 to 4 m), calculated for times coinciding with those of the available upper air data, show a consistent, though not powerful, relationship with the upper air temperature lapse (Fig. 4.21). Anticyclonic conditions favour both high values of upper air temperature lapse and strong near-surface inversions, so that a positive correlation may be seen between upper air



temperature lapse and surface inversion strength for the times considered. A better correlation may have been obtained if there had been more upper air observations available at corresponding times.

#### 4.9 Diurnal variations

Wind velocity and dry bulb temperature difference data obtained during the observation period (6.7.1979 to 7.8.1979) were examined, according to synoptic category, for possible diurnal variations in the following:

1. Low level wind velocity.
2. Near-ice inversion strength.
3. Near-ice stability as described by bulk and local Richardson numbers.

#### Synoptic Category (1): Cyclonic Pacific

The maximum wind velocity in the first 7 m above the ice surface and mean wind velocity (1 to 4 m) show no evidence of diurnal variation without differentiation between synoptic categories. Munro (1975) found a tendency for higher wind velocities to occur during the day, due to the setting up of a local valley circulation which reinforced the glacier katabatic wind. A difference in sampling procedure is probably responsible for these conflicting results. Munro's study involved specific 24 hour periods under favourable, anticyclonic conditions (particularly



suited to the study of diurnal variation), whereas this particular study used shorter sampling periods, under a variety of synoptic types.

However, under synoptic category 1 (Cyclonic Pacific), there was evidence of higher day-time velocities. This may have been due to a greater controlling intensity of the synoptic pressure gradient during the day, as mean wind velocity at the 700 mb level was found to be slightly greater than during the night, under these synoptic conditions.

Under cyclonic influence, when near-ice inversion strengths are considerably reduced (most commonly 1 to 2°C over the 1 to 4 m interval), there is little evidence of diurnal variation in temperature difference. Under Cyclonic Pacific influence there is a slight tendency for inversion strengths to be greater during the night. This may be due to less frequent katabatic flow, and significantly greater daytime wind velocities, which break down strong surface-based temperature inversions. With low incoming radiation associated with extensive cloud cover, and lower air mass temperatures, daytime temperature contrasts will not be as pronounced as under anticyclonic conditions. An extreme hourly value of inversion strength was obtained under the influence of Synoptic Category (1). A value of > 7°C was obtained at 1800 M.D.S.T. on 4.8.1979 when the low level wind deviated by 23° from the fall line, causing warmer air to eddy from Peyto Peak. Cloud cover was below average for this category, at < 5/10.

In this synoptic category, stability of the near-ice air layer (as defined by both the bulk Richardson number,  $R_{ib}$ , and the local Richardson number,  $R_{iL}$ ) was greater during the night. Since there is a very close relationship between stability and wind velocity in the near surface layer (section 4.3), lower stabilities during the day are probably due to the greater mean low level wind velocities experienced under these conditions.

Synoptic Category (2): 'Local' Cyclonic

Under 'Local' Cyclonic influence, extremely disturbed conditions prevail within the glacier basin. As a result, low level wind velocity is gusty and shows no evidence of diurnal variation. Similarly, disruption of the near-surface air layer results in only very small temperature inversions, and high cloud cover with resulting reduced insolation does not produce a noticeable diurnal variation in inversion strength or stability.

Synoptic Categories (3) and (4): Pronounced and Weak Anticyclonic

Diurnal variation of the low level wind velocity was not apparent during the observation period. However, a lull in wind velocity just before sunrise was a common occurrence, and was most pronounced under anticyclonic conditions. Figure 4.22 shows an example of this phenomenon

## SYNOPTIC TYPE 4: WEAK ANTICYCLONIC

Cloud Cover:  $\frac{1}{10}$  Cu

29th July to 30th July 1979

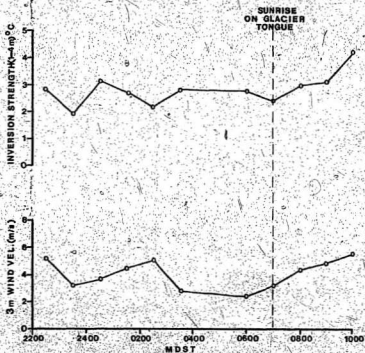


Figure 4.22 Lull in wind velocity before sunrise,  
30th July, 1979

occurring under weak anticyclonic conditions. Increasing low level wind velocities following the pre-sunrise lull appear to be associated with increasing strength of the near surface inversion as the air temperature rises. A similar lull was noted during local observations in the ice-fall depression area (Chapter 5.12).

Under anticyclonic conditions the near-ice inversion (1 to 4 m) was significantly stronger during the day (Snedecor's F-test for variance: Significant at 0.01. APPENDIX B). With clear skies there is a maximum day-time temperature contrast between the near-ice air layer and that over surrounding, warmer ice-free areas. Temperature inversions of 3 to 4°C (over the height range 1 to 4 m) are most common during the day (41% of observations), whereas during the night 60% of observed inversions were between 2 and 3°C (1 to 4 m), with no cases of very strong inversions (> 4°C between 1 and 4 m) recorded (Fig. 4.23).

Despite a distinct diurnal variation in inversion strength under anticyclonic conditions, the data obtained showed little evidence of higher daytime stabilities. This may be due to the limited number of hourly stability values available for night-time periods under these conditions.

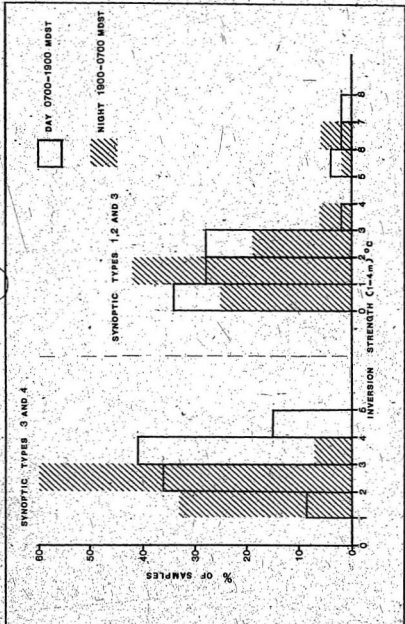


Figure 4.23 - Frequency distribution of inversion strengths according to synoptic influence.

Synoptic Category (5): Westerly Zonal

Synoptic category 5 showed remarkably little variation in low level wind velocity, a steady wind of 4 to 6 ms<sup>-1</sup> being characteristic. This may be due to the fact that under Westerly Zonal flow the 700 mb wind showed little variation in direction from 275°, cross-slope flow neither reinforcing or opposing the low level wind.

The mean near-ice inversion of 1.8°C (1 to 4 m) was also maintained quite steadily, although there was evidence of slightly stronger daytime inversions. A mean cloud cover of 5/10 under this synoptic category allowed sufficient diurnal variation of incoming radiation to produce a similar diurnal variation in inversion strength to that which occurred under anticyclonic conditions. The mean inversion strength (1 to 4 m) during the daytime under synoptic category 5 was 2.1°C, decreasing to a mean value of 1.5°C during the night. A diurnal variation in stability of the near-surface air layer was not apparent while Westerly Zonal flow influenced the region.

4.10 Relationship between katabatic wind velocity and inversion strength

The mean hourly wind velocity as measured at 4 m above the ice surface was correlated with the mean hourly 1 to 4 m temperature difference, using all the available data regardless

of synoptic influence or presence/absence of a low level velocity maximum. A weak positive correlation coefficient of + 0.05 (only significant at the 0.6 level) was obtained (Fig. 4.24). Since the katabatic wind is a flow resulting from horizontal density difference due to the degree of surface cooling by the glacier, a positive correlation between katabatic wind velocity and inversion strength in the katabatic layer would be expected (Streten, Ishikawa and Wendler, 1974; Martin, 1975; Muhro and Davies, 1977).

The relationship between mean hourly wind velocity and inversion strength was then examined according to synoptic category. The correlation coefficients obtained are shown in Table 4.8

TABLE 4.8 CORRELATION COEFFICIENTS: CORRELATION BETWEEN WIND VELOCITY AND INVERSION STRENGTH

SYNOPTIC CATEGORY	1 CYCLONIC PACIFIC	2 'LOCAL' CYCLONIC	3 PRONOUNCED ANTICYCLONIC	4 WEAK ANTICYCLONIC	5 WEL... ZONAL
MEAN 4m VEL. v. IN- VERSION STRENGTH	0.20	-0.05	-0.19	-0.06	0.35
MEAN 4m VEL. v. IN- VERSION STRENGTH (for U <sub>max</sub> at or > 4 m)	0.36	-0.09		-0.18A	0.47
U <sub>max</sub> v. IN- VERSION STRENGTH	0.11	0.07	-0.16	-0.05	0.28

\* Correlation coefficient is significant at the 0.05 level.  
 A Correlation coefficient combines categories 3 and 4 (due to small number of profiles in synoptic category 3 with a velocity maximum above 4 m).

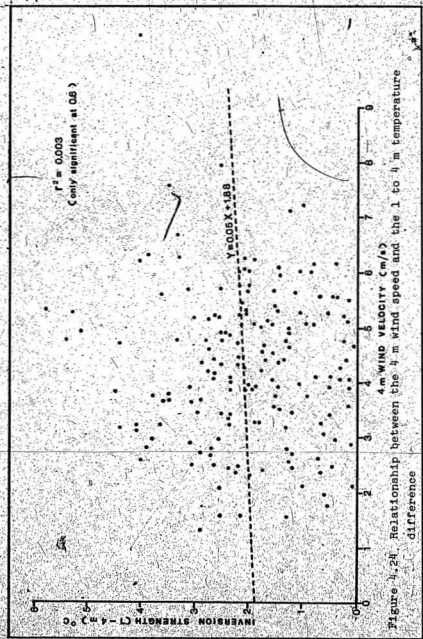


Figure 4.24. Relationship between the 4 m wind speed and the 1 to 4 m temperature difference



The only category to show a significant positive correlation between glacier wind velocity and inversion strength was synoptic category 5 (Westerly Zonal flow). The steady wind and temperature conditions experienced with this synoptic category have been previously noted (section 4.10). This may account for the stronger relationship obtained between low level wind velocity and inversion strength under synoptic category 5. The gusty nature of the glacier katabatic wind under anticyclonic conditions means that, on a short time scale, increasing wind velocity causes decreased temperatures near the top of the katabatic layer, and thus an inverse relationship between wind velocity and inversion strength. Similarly, under strong cyclonic influence (synoptic category 2, 'Local' Cyclonic), gusty winds and weak inversions result in a poor correlation.

With a low level velocity maximum, the temperature sensor at 4 m above the ice surface may frequently have recorded rapid temperature fluctuations associated with the presence of a thermocline (section 4.6). In order to exclude this effect a second correlation was carried out between mean low level velocity and inversion strength (1 to 4 m temperature difference) within synoptic categories, for cases where the wind velocity maximum (and associated thermocline) was above the 4 m level. The correlations obtained are shown in Table 4.8. Improved positive correlations were obtained under synoptic categories 1 and 5.

but only the correlation coefficient under Westerly Zonal flow (synoptic category 5) was significant.

The relationship between the maximum wind velocity within 7 m of the surface and the inversion strength was also examined. When all values were considered, a very small negative correlation coefficient of  $-0.004$  (not significant) was obtained. When observations were subdivided according to synoptic category, small negative values of the correlation coefficient were obtained under anticyclonic conditions (synoptic categories 3 and 4) and small positive values under cyclonic and zonal conditions (synoptic categories, 1, 2 and 5) (Table 4.8). The largest positive correlation was obtained under synoptic category 5 (Westerly Zonal).

In this particular study, a strong correlation between low level (4m) wind velocity and the strength of the surface based inversion (1 to 4 m) was not obtained. This is probably due to the strong control imposed by the low level wind on near-ice stability conditions (section 4.3). On a short time scale, increased wind velocity in the katabatic layer causes decreased temperatures and inversion strength. Turbulence increases with wind speed, causing increased cooling from below (Munro, 1975). Lulls in the wind velocity produce relatively warm temperatures.

Martin (1975) obtained a strong positive correlation between katabatic wind velocity (0.5m) and the 0.5 m to 9.5m temperature difference at a site on the Glacier de St. Sorlin. All the wind velocity profiles were characterized by a maximum between one and five metres above the ice surface. Thus, the temperature difference values used in the correlation would include the thermocline, and lead to a stronger correlation than that obtained in this study.

#### 4.11 Frequency of near-surface mean and maximum wind velocities according to synoptic category

The frequency of mean and maximum velocities within katabatic flow (i.e. cases where a maximum wind velocity occurred within 7 m of the surface) was examined according to synoptic category (Figures 4.25 and 4.26). No significant difference was found in either mean or maximum velocities between synoptic categories (Snedecor's F-test for variance: APPENDIX B), but the results emphasize the conclusions drawn in sections 4.1 and 4.9.

Firstly, under the influence of synoptic category 5 (Westerly Zonal flow) mean velocity within the katabatic layer is very steady (4 to 6  $\text{ms}^{-1}$ ), with little variation between hourly mean values. A maximum low level velocity of 4 to 6  $\text{ms}^{-1}$  occurred in 70% of the profiles examined. A close relationship between the direction of the 700 mb geostrophic wind and the velocity of the glacier katabatic

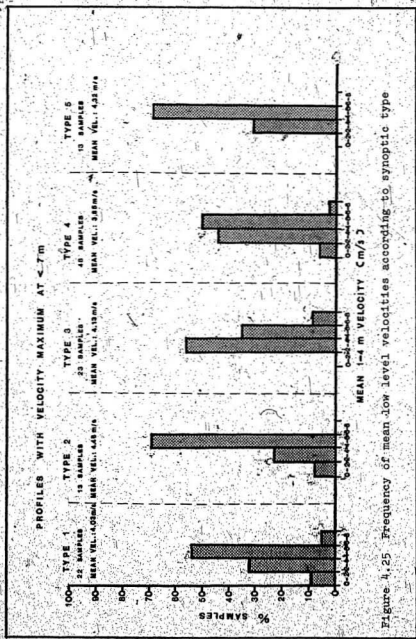


Figure 4.25 Frequency of mean low level velocities according to synoptic type



wind was noted in section 4.1. However, since the direction of the 700-mb wind does not vary significantly according to synoptic category (Table 3.1 p. 38), it follows that the mean and maximum wind velocities do not show a significant difference according to synoptic type.

4.12 Estimates of relative magnitudes of katabatic and pressure gradient forces

The horizontal pressure gradient force above the local near-ice inversion is given as:

$$-\frac{1}{\rho} \frac{dp}{dn}$$

where  $\rho$  is the air density ( $\text{kg m}^{-3}$ )

$\frac{dp}{dn}$  is the pressure gradient over the horizontal distance  $dn$  ( $\text{mb m}^{-1}$ ).

Following Holmgren (1971) the katabatic force  $G_s$ , is given as:

$$G_s = \frac{\sigma_a - \sigma_b}{\sigma_a} g \sin \theta$$

where  $\sigma_a - \sigma_b$  is the difference between the temperature close above the thermocline and that below the thermocline (K) ( $\sigma_a - \sigma_b$  was taken to be the mean 1 to 4m temperature difference),  $\sigma_a$  is the base camp mean hourly temperature (K) (used as an approximation of the temperature close above the thermocline). This approximation is likely to make only a small difference in the calculation, which is solely illustrative.  $g$  is the acceleration due to gravity ( $\text{ms}^{-2}$ ),  $\theta$  is the angle of slope of the glacier ( $3.8^\circ$  at the mast site).

A representative value of the katabatic force was calculated for each synoptic category as follows:

Synoptic Category (1): Cyclonic Pacific

Mean value of  $\sigma_a - \sigma_l$       2.12°

Mean  $\sigma_k$       280.1 K

Thus  $G_s = 4.9 \times 10^{-3} \text{ ms}^{-2}$

Synoptic Category (2): 'Local' Cyclonic

Mean value of  $\sigma_a - \sigma_l$       1.07°

Mean  $\sigma_k$       278.4 K

Thus  $G_s = 2.5 \times 10^{-3} \text{ ms}^{-2}$

Synoptic Category (3): Pronounced Anticyclonic

Mean value of  $\sigma_a - \sigma_l$       3.27°

Mean  $\sigma_k$       283.6 K

Thus  $G_s = 7.5 \times 10^{-3} \text{ ms}^{-2}$

Synoptic Category (4): Weak Anticyclonic

Mean value of  $\sigma_a - \sigma_l$       2.33°

Mean  $\sigma_k$       282.4 K

Thus  $G_s = 5.4 \times 10^{-3} \text{ ms}^{-2}$

Synoptic Category (5): Westerly Zonal

Mean value of  $\sigma_a - \sigma_l$       1.84°

Mean  $\sigma_k$       281.0 K

Thus  $G_s = 4.3 \times 10^{-3} \text{ ms}^{-2}$

For a representative mean horizontal pressure gradient ( $\Delta p/\Delta n$ ) of  $6.2 \times 10^{-6}$  mb  $m^{-1}$  at 700 mb, the synoptic pressure gradient force above the local ice inversion is  $\sim 0.6 \times 10^{-3}$   $ms^{-2}$ .

Thus, under all the synoptic types encountered in this study the katabatic force was considerably greater than the large-scale pressure gradient force. The katabatic force under anticyclonic conditions is greater than under cyclonic influence.



## CHAPTER FIVE

LOCALIZED MICRO-CLIMATOLOGICAL SURVEYS ON THE  
GLACIER TONGUE5.1 The western ice-fall depression

In order to supplement information obtained from the central glacier site, concerning the nature of near-surface wind and temperature conditions, an area of special interest beneath the western ice-fall was chosen for detailed investigation. The western side of the tongue appears to be decaying more rapidly (Sedgewick, 1966), so that a shallow depression is formed beneath the ice-fall (Fig. 5.1). The depression is bounded to the north-west by ice-cored moraine at the base of the steep rock face of Peyto Peak, to the south-west by the ice-fall and rises towards the centre of the glacier in the east.

The ice-fall depression is an area of particular micro-climatological interest. Its proximity to a steep rock face and ice-cored moraine suggest possible modification of the near-ice air layer. Foessel (1974) also describes such depressions as areas of cold air pooling, and suggests that



Figure 5.1 The western ice-fall depression

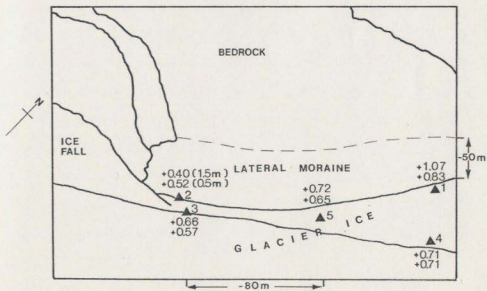


Figure 5.2 Post-sunrise warming rates: western ice-fall depression ( $^{\circ}\text{C hr}^{-1}$ )

near-ice wind and temperature profiles are affected. The presence of an ice-fall cliff creates the potential for turbulence near the ice surface.

Wind and temperature profile observations were concentrated around sunrise and sunset. Shading of parts of the glacier tongue after sunrise and before sunset is very significant when considering the radiation budget (Goodison, 1969, 1970, 1972). It is to be expected that, accompanying the dramatic change in radiation receipt at these times, there should be notable changes in the characteristics of the near-glacier air layer, specifically a variation in intensity of the temperature inversion and variations in low level wind velocity.

#### 5.11 Methodology

Five sites were selected within the ice-fall depression (Fig. 5.2). At each site, representative profiles of wind velocity and dry and wet bulb temperatures were obtained during periods before and after sunrise and before and after sunset. The number of sites chosen was limited by the time required for adequate observations at each site. Measurements were made under anticyclonic conditions when, with minimal cloud cover, changes due to shading and differential warming of air over ice and rock surfaces should be most pronounced.

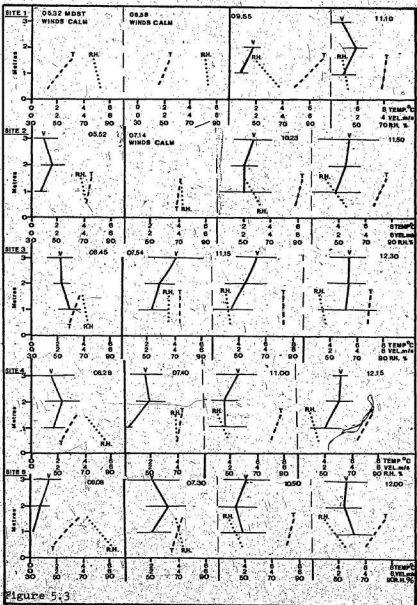
At each site, values of maximum and minimum wind velocity were obtained at 1 m, 2 m and 3 m above the ice surface (2 minute means) using a portable anemometer that could be attached to an extendable mast. The portable anemometer (Science Associates, Inc.) had an approximate starting speed of 2.2 mph (1m/sec) and an accuracy of  $\pm 3\%$ . The mast was held across wind from the body to avoid shielding. Simultaneous dry and wet bulb temperature readings were made at 0.5m and 1.5m above the ice surface using an Assmann aspiration psychrometer (Lambrecht Measuring Instruments). Radiation influence on the temperature measurement is eliminated by double radiation protection of the thermometer bulbs. Temperature readings were accurate to 0.1 K over a range of 10 K.

In order to obtain comparable readings, measurements at each site were obtained within ten minutes. A mean value of wind velocity at each height was interpolated from the maximum and minimum velocities recorded. Two pairs of profiles were obtained at each site before and after sunrise on 15th July and before and after sunset on 20th July (both under anticyclonic conditions). Profile measurements were also made at the same sites under Westerly Zonal influence (Synoptic category 5) during the early afternoon of 2nd August to provide a contrast to those made under anticyclonic conditions.

### 5.12 Discussion of results

a) BEFORE AND AFTER SUNRISE: 15.7.1979 (Anticyclonic synoptic conditions. Cloud cover  $\leq$  2/10 with haze. Glacier wind at mast site from  $210^\circ$ . Mean base camp temperature before sunrise:  $3.0^\circ\text{C}$ . Mean base camp temperature after sunrise:  $5.5^\circ\text{C}$ ) (Figs. 5.2 and 5.3).

Site 1 was the lowest site within the ice-fall depression (2348 m). It was close to the lateral ice-cored moraine and the ice surface at the site itself was strewn with small rocks. Strong temperature inversions were experienced both before and after sunrise. Before sunrise, the temperature at 0.5 m was considerably lower than at other sites. This may be due to drainage of coldest air to the lowest areas overnight. However, following sunrise the temperature at 0.5 m increased quite rapidly ( $1.07^\circ\text{C hr}^{-1}$ ), and remained higher than at any other site. This is a result of heating of the steep slopes of Peyto Peak following sunrise which caused greater warming of the near-ice air layer at this site. Temperature at 1.5 m above the ice surface was also affected at this site, and was more than  $0.6^\circ\text{C}$  higher than at the furthest sites from the rocky slopes (sites 3 and 4). Wind velocities at site 1 increased from calm (before sunrise), but remained low and steady ( $< 2 \text{ ms}^{-1}$ ) after sunrise, helping to maintain a strong temperature inversion.



At site 2 which was the highest site (2384 m), close to the ice-fall cliff, a weak inversion occurred before sunrise, strengthening by  $0.4^{\circ}\text{C}$  (0.5 m to 1.5 m) after sunrise. The rate of temperature increase at both 0.5 m and 1.5 m was considerably lower than at site 1 (Fig. 5.2). Site 2 was more exposed and less influenced by the warmth of rock areas. Winds increased and became gustier following sunrise.

Site 3 (2376 m), located on the rim of the depression, showed evidence of considerable turbulence as air flowing down the ice-fall 'step' from the accumulation basins was accelerated. This site experienced the highest wind velocities at all levels both before and after sunrise, and as a result of the enhanced mixing, the inversion strength was less than at other sites. The rate of temperature increase following sunrise was lower than at site 1, but slightly greater than at site 2 (Fig. 5.2).

Site 4 (2371 m) was furthest removed from the centre of the depression and the disturbing influence of the ice-fall and moraine ridges. The temperature inversion was weakest during the period just after sunrise (0740 M.D.S.T.). This is a result of significant warming at the lower level (0.5 m). Warming may be due to absorption of infra-red radiation by water vapour in the air nearest the ice surface (especially with low wind velocities), as suggested by La Casinière (1974). The heated layer increases in depth as time progresses

following sunrise, and eventually results in warming at the higher level (1.5 m). Wind velocities increased following sunrise and demonstrated a recurving profile suggestive of katabatic influence. During this period conditions at site 4 were similar to those at the central tongue site (Fig. 5.4). At the mast, a strengthening of the temperature inversion occurred following sunrise, with a low level velocity gradient reversal at 2 m. Windspeeds at the central tongue site were considerably greater (4 to 5  $\text{ms}^{-1}$ ), at 3 metres above the ice-surface, than at any of the ice-fall depression sites.

Site 5 (2368 m), at the centre of the ice-fall depression, experienced a decreasing inversion strength following sunrise. This was due to a slightly greater rate of warming at 0.5 m than at 1.5 m (Fig. 5.2), which may also be attributed to low level absorption of infra-red radiation. A further factor in decreasing inversion strength may have been inflow of cool air as the katabatic mechanisms intensified following sunrise. The upper accumulation basins are sunlit before the ice-fall area, so that stronger katabatic flow may be initiated before the tongue itself is sunlit. Wind profiles at site 5 showed gusty, turbulent conditions as air flowed into the depression.

All sites demonstrated slight decreases in stability (as defined by the local Richardson number,  $Ri_1$ ) immediately following sunrise, with a subsequent increase as the upper



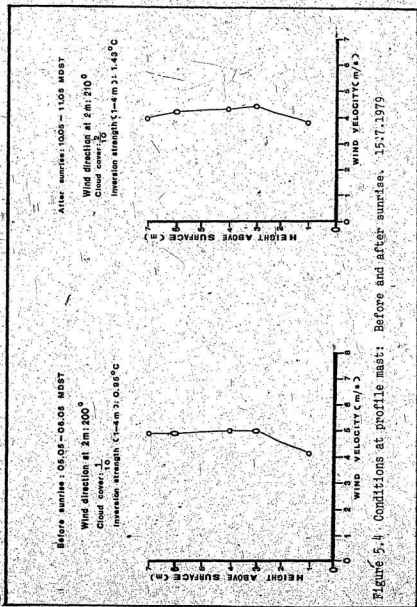


Figure 5.4. Conditions at profile mast: Before and after sunrise. 15.7.1979

level (1.5 m) was also warmed. Martin (1975) suggests that modification of near-ice temperature profiles following sunrise occurs as the ice surface temperature (below freezing during the night due to long-wave re-radiation) returns to  $0^{\circ}\text{C}$ . At equal ambient temperatures there is then reheating of the surface air. Thus the lowest level (0.5 m) will be warmed first, resulting in a slight decrease in inversion strength until the upper level (1.5 m) is also affected. At site 3, greater turbulence after sunrise caused a decreased inversion strength.

Relative humidity of the near surface air layer decreased rapidly at all sites following sunrise (a mean decrease of 28%). Lowest post-sunrise humidities were experienced at site 1, associated with substantially greater temperatures at both 0.5 m and 1.5 m.

At all five sites sampled, an increase in wind velocity was experienced following sunrise. There was also greater gustiness (apart from at site 1, where winds remained steady). As a greater area of the glacier basin became sunlit, so the temperature contrast between ice and rock increased, resulting in increased strength of flow in the katabatic layer (over a major part of the glacier tongue) and greater turbulence (gustiness) in marginal ice areas such as the ice-fall depression.

b) BEFORE AND AFTER SUNSET: 20.7.1979 (Anticyclonic Synoptic conditions. Cloud cover  $\leq 3/10$ . Glacier wind at mast site from  $210^\circ$ ). Figs. 5.5 and 5.6.

Observations before and after sunset were made at the same sites under similar synoptic conditions. Before sunset site 1 showed great stability in the near-ice air layer. The inversion strength was the greatest recorded during the study (mean value of  $3.3^\circ\text{C}$  between 0.5 m and 1.5 m), and winds were light and steady (Fig. 5.5). This site was strongly influenced, under these conditions, by the adjacent warmer rocky slopes of Peyto Peak. The 1.5 m level was  $7^\circ\text{C}$  warmer than at site 4, at comparable times before sunset, and the 0.5 m level was  $4.8^\circ\text{C}$  warmer. Following sunset the temperature at both levels decreased quite rapidly (Fig. 5.6) and a substantial decrease in inversion strength was recorded (mean inversion strength of  $1.0^\circ\text{C}$  between 0.5 m and 1.5 m) due to a greater decrease at the 1.5 m level. Winds remained fairly light, but were more gusty than before sunset, especially at the 1 m level. The resulting turbulence in the near surface layer contributed to break up of inversion strength by mixing cool air upwards into the profile.

Site 2 also experienced a substantial decrease in inversion strength after sunset (from  $1.6^\circ\text{C}$  to  $0.4^\circ\text{C}$  over 0.5 m to 1.5 m). The rate of cooling at 1.5 m was less than at site 1 (Fig. 5.6). Winds increased, and became gustier, with little variation in velocity with height (Fig. 5.5).

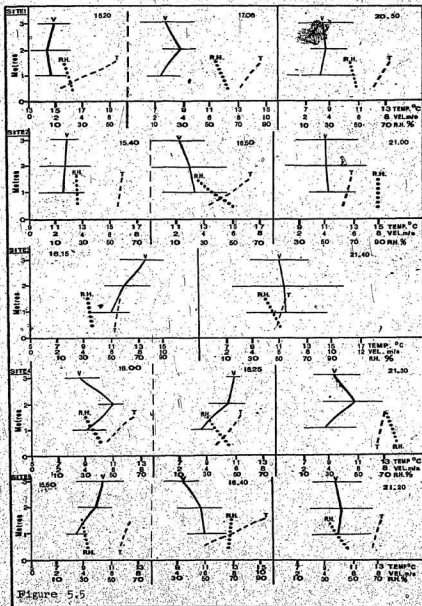


Figure 5.5

Wind velocity and temperature profiles: Sunset, 20.7.1979.

Western ice-fall depression (R.H. = relative humidity).

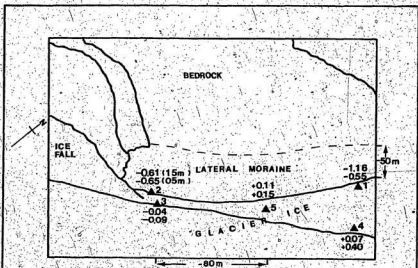


Figure 5.6. Post-sunset cooling rates: western ice-fall depression ( $^{\circ}\text{C hr}^{-1}$ ).

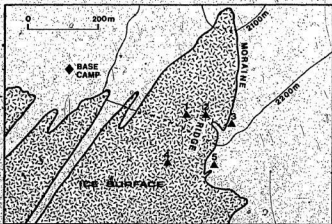


Figure 5.7. Local survey sites: eastern glacier about.

Site 3 showed only a small strength inversion both before and after sunset. Wind velocities were high and gusty, turbulent conditions preventing a stronger temperature inversion (as occurred at sunrise). The rate of cooling following sunset at this site was very low (Fig. 5.6).

Site 4, nearest to the centre of the glacier, also experienced a decrease in inversion strength following sunset (from 1.8°C to 0.4°C between 0.5 m and 1.5 m). However, temperatures at both levels continued to increase following sunset (Fig. 5.6). Winds were strong before sunset, becoming gustier following sunset. The wind profiles indicate a wind velocity reversal at 2 m above the surface, indicative of katabatic influence at this particular site (Fig. 5.5).

At site 5, in the centre of the depression, the inversion strength decreased following sunset (from 2.4°C to 0.6°C between 0.5 m and 1.5 m), although slight warming continued at both levels (Fig. 5.6). Winds at all levels sampled tended to become gustier following sunset (Fig. 5.5).

Under anticyclonic conditions there appeared to be a substantial decrease in the near-surface temperature inversion following sunset (except at site 3), with increasing gustiness of low level winds. All sites apart from the centre of the depression (Site 5) showed increased relative humidity following sunset (mean increase of 28%) with a mean decrease of 9% at site 5. Sites 1 and 2 (close to the rock face)

showed considerably lower relative humidity than other sites before sunset. A slight increase in stability following sunset was experienced at sites 2, 3 and 5.

c) EARLY AFTERNOON: 2.8.1979 (Westerly Zonal flow conditions. Cloud cover 8/10. Glacier wind at mast site fluctuating between  $195^{\circ}$  and  $225^{\circ}$ ). Fig. 5.8.

Profiles were taken at the same five sites during the early afternoon under contrasting synoptic conditions of Westerly Zonal flow, with substantial cloud cover (8/10 Cu, Ac).

At site 1, the mean inversion strength of  $1^{\circ}\text{C}$  (between 0.5 m and 1.5 m) was considerably less than under clear sky conditions. Winds during the second profile observation were extremely gusty, in contrast to the calm conditions observed under anticyclonic conditions both before and after sunrise/sunset (Fig. 5.8). Wind direction at the main glacier site was observed to fluctuate between  $195^{\circ}$  and  $225^{\circ}$  during the observation period with a mean hourly standard deviation of  $16^{\circ}$ . These fluctuations could account for the gustiness observed in the ice-fall depression area, with eddying from the ice-fall and Peyto Peak. With considerable cloud cover, the daytime temperature contrast between the near ice layer and the surrounding rocky slopes is considerably less than with clear skies, leading to a smaller inversion strength.

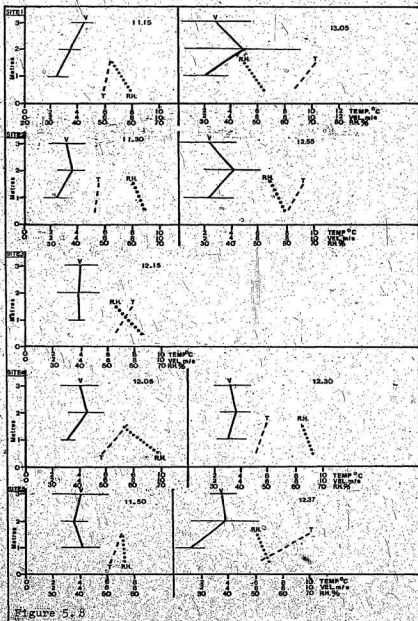


Figure 5.8

Wind velocity and temperature profiles: Early afternoon, 2.8.1979. Western ice-fall depression (R.H. - relative humidity)



At site 2, a small mean inversion ( $0.7^{\circ}\text{C}$  between 0.5 m and 1.5 m) and gusty winds were experienced, with considerable eddying from the ice-fall and turbulence in the near glacier air layer (Fig. 5.8).

At site 3 there was very little variation in wind velocity with height, and the inversion strength ( $1.3^{\circ}\text{C}$  between 0.5 m and 1.5 m) was the greatest measured at this site (greater than under anticyclonic conditions).

Site 4 (nearest the centre of the tongue) showed slight recurving of the wind profile at 2 m above the surface, demonstrating possible katabatic influence. The mean inversion strength of  $1.2^{\circ}\text{C}$  was considerably less than that at the same site under anticyclonic conditions before sunset.

Site 5 showed an anomalously high mean inversion strength of  $2.1^{\circ}\text{C}$  (between 0.5 m and 1.5 m). A temperature of  $10.1^{\circ}\text{C}$  was recorded at 1.5 m during the second set of profile observations (Fig. 5.8). Wind was gusty at this time and appeared to be eddying from the warmer slopes of Peyto Peak to the west.

## 5.2 The eastern side of the glacier snout

Observations of local wind and temperature conditions were also made in an area on the eastern side of the glacier snout (Fig. 5.7). Access to this area became increasingly difficult as the ablation season progressed, with the

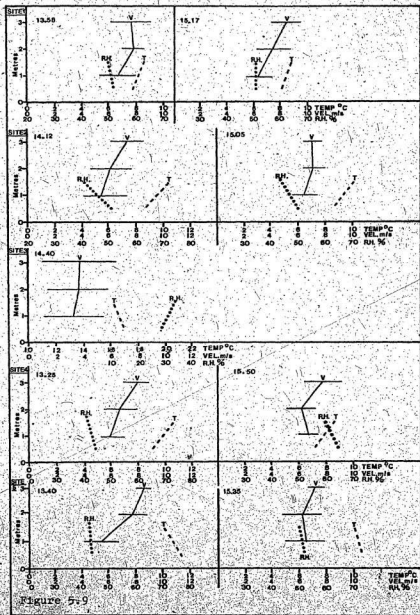
opening of numerous moulins and the undermining of the glacier margin by meltwater streams. However, profile measurements were obtained at five sites within the area under anticyclonic conditions (Synoptic category 3: Pronounced Anticyclonic), aimed specifically at assessing differences in temperature conditions between marginal ice areas and surrounding ice-free areas. This temperature contrast is the major driving mechanism of the glacier katabatic wind.

#### 5.21 Methodology

Two sites were selected on the lateral ice-cored moraine (Fig. 5.7) and three sites at differing elevations on the eastern side of the snout. Wind velocity was recorded at 1 m, 2 m and 3 m above the surface at each site, with simultaneous wet and dry bulb temperature readings at 0.5 m and 1.5 m, using the same instrumentation as in 5.11. Observations were made in the early afternoon when, with clear skies, maximum contrasts would be expected between ice and moraine sites.

#### 5.22 Discussion of results

(18.7.1979: Anticyclonic synoptic conditions.  
Cloud cover  $\leq$  1/10. Glacier wind at mast from 205°. Mean base camp temperature: 15.4°C) (Fig. 5.9).



Wind velocity and temperature profiles: Early afternoon.  
18.7.1979. Eastern glacier snout (R.H. = relative humidity)

Site 1 (2202 m) was the lowest ice-surface site, and had a mean inversion strength of  $0.7^{\circ}\text{C}$  (between 0.5 m and 1.5 m). One of the wind profiles taken at this site showed evidence of low level recurving (at 2 m), with high wind velocities of 7 to  $8 \text{ m s}^{-1}$  (Fig. 5.9).

Site 2 (2207 m) was situated at the crest of a small ice ridge about 60 m from the glacier margin. The mean inversion strength of  $1.6^{\circ}\text{C}$  (between 0.5 m and 1.5 m) was the highest recorded in the area. There was little variation of wind velocity with height at this site.

At site 3 (2195 m) on the lateral moraine, a lapse of  $0.7^{\circ}\text{C}$  (0.5 m to 1.5 m) was recorded. Temperatures were considerably higher at this site ( $6^{\circ}\text{C}$  higher at 1.5 m than at site 2 at comparable times), due to its position low on the far side of a trough formed between the proximal glacier ice and the lateral moraine. Relative humidity at this site was on average 20% lower than over the ice. Winds at all levels were very gusty as a result of turbulent eddies in the trough.

Site 4 was the highest ice site (2237 m), and was exposed to the dominant down-glacier flow occurring on the glacier tongue (the central tongue site was experiencing a low level wind from  $205^{\circ}$  to  $210^{\circ}$  during the sample period). The mean inversion strength of  $1.4^{\circ}\text{C}$  (between 0.5 m and 1.5 m) was similar to that at the mast ( $1.2^{\circ}\text{C m}^{-1}$ ). This is despite

considerably higher wind velocities on the snout (7 to 8  $\text{ms}^{-1}$  at 3 m above the surface as compared to 3 to 4  $\text{ms}^{-1}$  at the central tongue site).

Site 5 (2248 m) was 50 m east of site 4 on the lateral moraine. Temperatures at this site indicated a lapse profile as would be expected over a rock surface ( $0.9^{\circ}\text{C m}^{-1}$  over 0.5 m to 1.5 m). This site experienced greatest wind velocities (7 to 9  $\text{ms}^{-1}$  at 3 m) due to its exposed position. Relative humidity at site 5 was similar to that over the ice. The site was exposed to flow directly from the glacier (Fig. 5.7) resulting in little modification of humidity conditions. The surface conditions also favoured fairly high humidity, with only a thin layer of debris covering the ice-core.

The eastern side of the snout experienced higher velocity, more gusty winds during the survey period than the main tongue site. Values of inversion strength were generally similar to or slightly greater than those recorded at the mast. Higher wind velocities on the snout are due to accelerated flow as the surface slope steepens from  $4^{\circ}$  at the central tongue site to  $15^{\circ}$  on the snout. In the snout area flow is also constricted by rock walls in a section of Peyto valley only 0.15 km wide, which may be a further factor in causing increased velocities.

### 5.3 Conclusions to be drawn from local studies

Although the mast site is representative of conditions over a large portion of the glacier tongue, it is clear from these studies that wind and temperature profiles will reflect local differences in slope, aspect and proximity to ice-free areas. Depressions in the glacier surface such as that beneath the western ice-fall, form localized areas of nocturnal cold air pooling with calm conditions and frequently strong temperature inversions near the ice margin. More steeply sloping areas of the snout experience accelerated flow.

Local differences are most pronounced under anticyclonic conditions, when the influence of surrounding, warmer ice-free areas is important. Proximity to steep mountain walls may result in turbulent eddies, particularly under cyclonic influence, when the low level wind is most variable in direction. Cyclonic conditions, with greater cloud cover and reduced insolation, lead to a lower strength local inversion and generally less stability. Relative humidity in the near surface air layer of the ice-fall depression was on average 15% higher under Westerly Zonal influence than under anticyclonic conditions (700 mb relative humidity under Westerly Zonal flow was on average 17% greater than under anticyclonic influence. Table 3.1 p.38 ).

Under anticyclonic conditions the ice-fall depression experienced lighter winds and stronger inversions than at the central tongue site. The importance of increased wind velocity in preventing the development of strong inversions was demonstrated on a short time scale. This is to be expected when air is cooled from below by turbulent mixing, as turbulence increases with wind velocity. As turbulence increases, so does the degree of cooling at a given height. Reduced wind speed produces relative warmth (Munro, 1975). However, over a longer period of time there appears to be a fairly rapid increase in near-surface temperature following sunrise associated with strengthening winds. Over a long time period, a positive correlation between inversion strength and katabatic wind velocity has been found elsewhere (Chapter 4.10).

A characteristic lull in wind velocities before sunrise was noted in the ice-fall depression area, and was also recorded at the central tongue site. This period of lower velocities occurs before the onset of strong katabatic flow, and was most pronounced under anticyclonic conditions.

## CHAPTER SIX

## CONCLUSIONS AND SUGGESTIONS FOR FURTHER RESEARCH

This study aimed to develop a simple synoptic classification scheme which would physically explain variations in the development of katabatic flow over a temperate alpine type glacier during the summer ablation season.

The katabatic layer, defined as a cooled air layer flowing down gradient in response to density and altitudinal differences and separated from air above by a thermocline and wind velocity maximum, was found to be most strongly developed under anticyclonic conditions. Under these conditions a low level wind velocity maximum occurs frequently, with evidence for an associated thermocline. With weak synoptic pressure gradients, the katabatic wind was directed down-glacier, with little deviation from the fall-line. Such conditions favoured the development of strong surface-based temperature inversions and high stability, with maximum temperature contrast between the near-glacier air layer and that over surrounding ice-free areas. Inversion strength showed great variability about an hourly mean value due to cloud passage, turbulent mixing and the movement of thermal 'waves' along the thermocline. On a short time



scale, increases in low level wind velocity resulted in decreased inversion strength and local stability, with turbulent mixing of cooled air from below. However, over the entire study period a weak positive correlation was found between the katabatic wind velocity and the strength of the surface-based inversion. This is to be expected since the major driving mechanism of the glacier katabatic wind is the temperature and density contrast between the air layer over ice and that over surrounding ice-free areas. A diurnal variation in inversion strength was found to be most pronounced under anticyclonic conditions, strongest inversions occurring during the day. Strong evidence of diurnal variation in low level wind velocity was not found during this study.

Cyclonic synoptic conditions were found to result in considerable disturbance of the katabatic layer. The near-surface inversion was much weaker than under anticyclonic influence, with less variability due to turbulent mixing of cooled air and infrequent presence of a low level wind velocity maximum and associated thermocline. Stability of the near-surface air layer was significantly less under cyclonic conditions than when anticyclonic influence prevailed. Under cyclonic influence, the direction of the low level wind was very variable and strongly influenced by the direction of the 700 mb geostrophic wind. On occasions, the down-glacier surface flow was replaced by an up-glacier wind, or more commonly modified to blow perpendicular to the glacier fall-line.

The direction of the 700 mb wind (above the influence of the glacier surface) has important implications for near-surface stability, wind velocity and direction. An upper wind directed down-glacier results in reinforcement of the surface wind under all synoptic conditions. Near-surface stability is greatest with reinforcing flow. With the upper wind directed across glacier, considerable turbulence within the glacier basin was noted under cyclonic influence. This resulted in decreased stability in the near-surface layer. Similarly, an upper wind blowing across glacier causes decreased low level inversion strength. A clockwise deviation of the 700 mb geostrophic wind direction from the glacier fall-line was found to result in a similar deviation of the surface wind under cyclonic conditions.

Considerable variation in the shape of the near surface wind profile was noted under different synoptic conditions. Low level katabatic curvature was common under anticyclonic influence, cyclonic conditions resulting in irregular shaped profiles with poorly developed katabatic flow. Synoptic category 5 (Westerly Zonal) was notable for the steady low level wind velocities and inversion conditions developed.

Synoptic scale variation was thus found to exert important control on the near-glacier air layer. In particular, variations in radiation receipt with changing cloud cover result in variable strength of the surface-based

inversion. Upper wind direction plays an important role in determining stability and wind conditions of the near-surface layer. However, the katabatic force was found to be far greater than the synoptic pressure gradient force (above the direct influence of the glacier), and to be greater under anticyclonic than cyclonic conditions.

Localized studies of temperature and wind conditions in the near-surface air layer emphasized the importance of differences in elevation, slope, aspect and proximity to ice-free areas. Marginal microclimates may differ considerably from those experienced on the central glacier tongue. Under anticyclonic synoptic conditions, greater heating of the near-surface air layer over rock surfaces may increase inversion strength over marginal ice areas. Depressions in the ice surface create localities for nocturnal cold air pooling, with stronger inversions and decreased velocity surface winds during the day. Turbulence created within these areas may prevent the formation of a recognizable katabatic flow regime. Constriction of surface flow, accompanied by an increase in surface gradient (as occurs at the glacier snout) may cause acceleration, with stronger winds than on the main glacier tongue.

Significant changes in radiation receipt occurring around sunrise and sunset were found to result in modification of wind and temperature conditions in the near-surface air

layer within a marginal ice depression. Under anticyclonic conditions, rapid warming and increased inversion strength occur following sunrise with associated strengthening of the low level wind. A pre-sunrise lull in wind velocity was found to occur at both the tongue and ice-fall depression sites. Cooling following sunset occurred less rapidly than warming after sunrise, with areas at some distance from the influencing rock areas experiencing continued warming of the surface air layer for some time after sunset.

Future research may be directed towards study of the development of katabatic flow from its origin in the upper accumulation basins and modification on the glacier tongue. Automatic continuous profiling instrumentation would be required in the upper basins. In this way, diurnal variations in near surface parameters could be better distinguished.

An extension of this thesis would incorporate the synoptic controlled differences established in katabatic layer development into a simple ablation model. A strong katabatic wind, with warm air and strong temperature inversions over the ice surface may lead to increased ablation. Such conditions are favoured by anticyclonic synoptic influence with warm air advection over the glacier. Reinforcement of the katabatic wind (by a 700 mb wind in the same direction) may lead to an increased ablation rate with more rapid removal of saturated near-surface air.

Local differences in temperature and wind conditions such as those occurring in marginal ice areas may lead to anomalies in ablation. Greater ablation is likely to occur in those areas near exposed rock outcrops. The different thermal characteristics of ice and rock surfaces lead to a complex heat flow from one to the other (Young, 1977). A thin layer of surface debris in marginal ice areas may emphasize the anomalous ablation.

Katabatic winds may play an important role in redistribution of the winter snow accumulation (Whillans, 1975). Over steeply sloping areas of the glacier, accelerated katabatic winds may remove snow, resulting in a local negative balance. In depressions, and flatter areas, deposition may be increased, resulting in a local positive balance.

The frequency of occurrence of different synoptic types within an ablation season may help to explain variations in mass balance from year to year. With a high frequency of anticyclonic types, favouring the development of katabatic flow and strong temperature inversions, ablation should be high and a negative mass balance result. An ablation season with high frequency of cyclonic types however, would favour a positive mass balance.

## REFERENCES

- Alt, B.T. 1978. Synoptic climate controls of mass balance variations on Devon Island ice-cap. Arctic and Alpine Research. 10: 61 - 80.
- Barry, R.G., and Perry, A.H. 1973. Synoptic Climatology, Methods and Applications. London: Methuen, 555 pp.
- Bradley, E.F. 1968. A micrometeorological study of velocity profiles and surface drag in the region modified by a change in surface roughness. Quarterly Journal of the Royal Meteorological Society. 94: 361 - 379.
- Brooks, C.E.P., and Carruthers, N. 1953. Handbook of Statistical Methods in Meteorology. London: Meteorological Office, Air Ministry. Pub. M.O. 538, 412 pp.
- Bryson, R.A., and Hare, F.K. (eds.) 1974. Climates of North America. Vol. II: World Survey of Climatology. Elsevier, 420 pp.
- Businger, J.A. 1973. Turbulent transfer in the atmospheric surface layer. Workshop on Micrometeorology. Edited by D.A. Haugen. Boston, Mass.: American Meteorological Society.
- Businger, J.A., and Ramano-Rao, K. 1965. The formation of a drainage wind on a snow-dome. Journal of Glaciology. 5: 833 - 841.
- Crane, R.G. 1979. Synoptic controls on the energy budget regime of an ablating fast ice surface. Archiv fur Meteorologie, Geophysik und Bioklimatologie. Ser. A. 28: 53 - 70.
- Deacon, E.L. 1949. Vertical diffusion in the lowest layers of the atmosphere. Quarterly Journal of the Royal Meteorological Society. 75: 89 - 103.
- Defant, F. 1951. Local winds. Compendium of Meteorology. Edited by T.F. Malone. Boston, Mass.: American Meteorological Society, 655 - 673.

- Ekhart, E. 1934. Neuere untersuchungen zur aerologie der talwinde. Beitr. Phys. d. fr. Atm. 21: 245 - 268.
- Fisher, R.A., and Yates, F. 1953. Statistical Tables for Biological, Agricultural and Medical Research. New York: Hafner, 126 pp.
- Foessel, D.G. 1974. Analysis of the Temperature Distribution Over the Peyto Glacier, Alberta. M.Sc. Thesis, Guelph University, Ontario, Canada, 137 pp.
- Geiger, R. 1965. The Climate Near the Ground. Harvard, Mass.: Harvard University Press, 611 pp.
- Goodison, B. 1969. A Preliminary Investigation of the Distribution of Global Radiation over Peyto Glacier, Alberta. M.A. Thesis, University of Toronto, Ontario, Canada.
- Goodison, B. 1970. The relation between ablation and global radiation over Peyto Glacier, Alberta. Glaciers. Proceedings of a workshop seminar, Canadian National Committee for I.H.D., 39 - 42.
- Goodison, B. 1972. The Distribution of Global Radiation over Peyto Glacier, Alberta. Inland Waters Directorate, Scientific Series No. 22, Environment Canada, Ottawa, Canada, 22 pp.
- Grainger, M.E., and Lister, H. 1966. Wind speed, stability and eddy viscosity over melting ice surfaces. Journal of Glaciology. 6: 101 - 127.
- Hoinkes, H. 1954. Beitrage zur kenntnis des gletscherwindes. Archiv fur Meteorologie, Geophysik und Bioklimatologie. Ser. B. 6: 36 - 53.
- Hoinkes, H. 1965. Glacial meteorology. Vol. II. Research in Geophysics. Solid Earth and Interface Phenomena. Edited by H. Odishaw. Cambridge, Mass., M.I.T. Press, 391 - 424.
- Holmgren, B. 1971. Climate and Energy Exchange on a Sub-Polar Ice-Cap in Summer. Arctic Institute of North America Devon Island Expedition 1961 - 1963. Meddelande Nr 107: Meteorologiska Institutionen Uppsala Universitet, 403 pp.
- La Casiniere, A.C. de. 1974. Heat exchange over a melting snow surface. Journal of Glaciology. 13: 55 - 72.
- Lettau, H.H. 1957. Summary of non-dimensional characteristics of boundary layer theory. Vol. I. Exploring the Atmosphere's First Mile. Edited by H.H. Lettau and B. Davidson. Pergamon Press, 376 pp.

- Lettau, H.H. 1966. A case study of katabatic flow on the south polar plateau. Studies in Antarctic Meteorology. Edited by M.J. Rubin. Antarctic research series Vol. 9, 231 pp.
- Liljequist, G.H. 1957. Wind structure in the low layer. Energy Exchange of an Antarctic Snow-Field (Maudheim 71° 03'S, 10° 56'W). Norwegian - British - Swedish Antarctic Expedition, 1949 - 52. Scientific Results, Vol. 2, Part 1D, p 235 - 298. Oslo: Norsk Polarinstitutt.
- Mahrt, L.J., and Schwerdtfeger, W. 1970. Ekman spirals for exponential thermal wind. Boundary Layer Meteorology. 1: 137 - 145.
- Mahins, P.C., and Sawford, B.L. 1979. A model of katabatic winds. Journal of Atmospheric Science. 36: 619 - 630.
- Martin, S. 1975. Wind régimes and heat exchange on Glacier de Saint-Sorlin. Journal of Glaciology. 14: 91 - 105.
- Mather, K.B., and Miller, G.S. 1966. Wind drainage off the high plateau of eastern Antarctica. Nature. 209: 281 - 284.
- Munro, D.S. 1975. Energy Exchange on a Melting Glacier. Ph.D. Thesis, McMaster University, Hamilton, Ontario, Canada, 182 pp.
- Munro, D.S., and Davies, J.A. 1977. An experimental study of the glacier boundary layer over melting ice. Journal of Glaciology. 18: 425 - 436.
- Munro, D.S., and Davies, J.A. 1978. On fitting the log-linear model to wind speed and temperature profiles over a melting glacier. Boundary Layer Meteorology. 15: 423 - 437.
- Okamoto, M., and Webb, E.K. 1970. The temperature fluctuations in stable stratification. Quarterly Journal of the Royal Meteorological Society. 96: 591 - 600.
- Oke, T.R. 1970. Turbulent transport near the ground in stable conditions. Journal of Applied Meteorology. 9: 778 - 786.
- Orvig, S. 1954. Glacial meteorological observations on ice caps in Baffin Island. Geografiska Annaler. Bd. 36: 197 - 311.
- Overland, J.E., and Hiestor, T.R. 1980. Development of a synoptic climatology for the north-east Gulf of Alaska. Journal of Applied Meteorology. 19: 1 - 14.



- Frandtl, L. 1952. Essentials of Fluid Dynamics. London and Glasgow: Blackie and Sons Limited.
- Rannie, W.F. 1977. A note on the effect of a glacier on the summer thermal climate of an ice-marginal area. Arctic and Alpine Research. 9: 301 - 304.
- Richardson, L.F. 1920. The supply of energy from and to atmospheric eddies. Proceedings of the Royal Society of London. A97: 354 - 373.
- Sands, R.D. 1966. A Feature of Circulation Approach to Synoptic Climatology Applied to Western United States. Tech. Paper 66 - 2. Geography Dept., Univ. of Denver. 332 pp.
- Sedgewick, J.K. 1966. Geomorphology and Mass Budget of Peyto Glacier, Alberta. M.A. Thesis, McMaster University, Hamilton, Ontario, Canada, 165 pp.
- Singh, S.V., Mooley, D.A., and Kripalani, R.H. 1978. Synoptic climatology of the daily 700 mb summer monsoon flow patterns over India. Monthly Weather Review. 106: 510 - 525.
- Streten, N.A., and Wendler, G. 1968. Some observations of Alaskan glacier winds in midsummer. Arctic. 21: 98 - 102.
- Streten, N.A., Ishikawa, N., and Wendler, G. 1974. Some observations of the local wind régime on an Alaskan arctic glacier. Archiv für Meteorologie, Geophysik und Bioklimatologie, Ser. B. 22: 337 - 350.
- Suckling, P.W., and Hay, J.E. 1978. On the use of synoptic weather map typing to define solar radiation regimes. Monthly Weather Review. 106: 1521 - 1531.
- Sverdrup, H.U. 1936. The eddy conductivity of the air over a smooth snowfield. Geofys. Publ. 11: 5 - 49.
- Tollner, H. 1931. Gletscherwinde in den Ostalpen. Met. Z. 48: 414 - 421.
- Walker, E.R. 1961. A Synoptic Climatology for Parts of the Western Cordillera. Pub. in Met. No. 35. Montreal: McGill Univ. 218 pp.
- Wallen, C.C. 1948. Glacial-meteorological investigations on the Karsa Glacier in Swedish Lapland 1942 - 1948. Geografiska Annaler. Arg. 30: 451 - 672.

- Webb, E.K. 1970. Profile relationships: the log-linear range, and extension to strong stability. Quarterly Journal of the Royal Meteorological Society. 96: 67 - 90.
- Whillans, I.M. 1975. Effect of inversion winds on topographic detail and mass balance on inland ice sheets. Journal of Glaciology. 14: 85 - 90.
- Winn-Nielsen, A. 1965. On the propagation of gravity waves in a hydrostatic, compressible fluid with vertical wind shear. Tellus. 17: 306 - 320.
- Wucknitz, J. 1977. Disturbance of wind profile measurements by a slim mast. Boundary Layer Meteorology. 11: 155 - 170.
- Young, G.J., and Stanley, A.D. 1976. Canadian Glaciers in the International Hydrological Decade Program, 1965 - 1974. No. 4. Peyto Glacier, Alberta - Summary of Measurements. Inland Waters Directorate, Scientific Series No. 71, Water Resources Branch, Ottawa, Canada, 59 pp.
- Young, G.J. 1977. Relations Between Mass Balance and Meteorological Variables on Peyto Glacier, Alberta, 1967 - 1974. Presented at Symposium on Dynamics of Temperate Glaciers and Related Problems. 4th European Geophysical Society Meeting, Munich, Germany, Sept. 6-9, 1977, 12 pp.

## APPENDIX A

## SYMBOLS AND NOTATION USED

The following symbols and abbreviations are used:

A } Empirical constants in Equation 4:

$$a \left. \begin{array}{l} \\ b \end{array} \right\} U_z = A \ln \left( \frac{z}{a} \right) \exp \left( -\frac{z}{b} \right)$$

C } Empirical constants in Equation 3:

$$c \left. \begin{array}{l} \\ l \end{array} \right\} U_z = C \sin \left( \frac{z}{l} \right) \exp \left( -\frac{z}{l} \right)$$

a } Empirical constant in Equation 6:

$$U - U_0 = \frac{U^*}{\kappa} \left[ \ln \left( \frac{z}{z_p} \right) + a \left( \frac{z - z_0}{L} \right) \right]$$

G<sub>s</sub> } The katabatic force (ms<sup>-2</sup>)

g } Acceleration due to gravity (ms<sup>-2</sup>)

κ } Von Karman constant = 0.4

l<sub>c</sub> } A critical distance above the ice surface at which the wind velocity is U<sub>c</sub> ms<sup>-1</sup> (This distance was taken to be the height above the ice surface of maximum wind velocity, following Holmgren, 1971).

L } Obukhov stability length (m)

$\frac{dp}{dn}$  } The pressure gradient over the horizontal distance dn (m<sup>-1</sup>)

Ri<sub>B</sub> } Bulk Richardson number

$$Ri_B = \frac{g \Delta T_c}{T U_c^2}$$

Ri<sub>L</sub> } Local Richardson number

$$Ri_L = \frac{g \Delta T}{T \Delta Z} \frac{1}{\left( \frac{\Delta U}{\Delta Z} \right)^2}$$

- T Mean temperature of air layer (K).
- $\Delta T$  Temperature difference between two standard levels  
(in this case 1 and 4m), °C.
- $\frac{\Delta T}{\Delta Z}$  Temperature difference over the height interval  $Z$ ,  $\text{km}^{-1}$
- $U_c$  Critical wind velocity ( $U_c = U_{\text{max}}$  in this study)  $\text{ms}^{-1}$ .
- $U_{\text{max}}$  Maximum profile velocity ( $\text{ms}^{-1}$ )
- $U_0$  Wind velocity at  $Z_p$  ( $\text{ms}^{-1}$ )
- $U_z$  Wind velocity ( $\text{ms}^{-1}$ ) at height  $Z$  (m)
- $U^*$  Friction velocity =  $\left(\frac{\tau_0}{\rho}\right)^{1/2}$   $\text{ms}^{-1}$
- $\frac{\Delta U}{\Delta Z}$  Difference in wind velocity over the height interval  
 $Z$  ( $\text{s}^{-1}$ )
- $Z$  Height above the surface (m)
- $Z_p$  The surface roughness length (cm)
- $\beta$  A stability index
- $\beta = 1$  neutral stability
- $\beta < 1$  stable conditions
- $\beta > 1$  unstable conditions
- $\theta$  Angle of slope of glacier ( $3.8^\circ$  at mast site)
- $\rho$  Air density ( $\text{kg m}^{-3}$ )
- $\theta_{a-s1}$  The difference between the temperature close above  
the thermocline and that below the thermocline (K).  
Taken to be the mean 1 to 4m temperature difference.
- $\tau_0$  Surface shear stress per unit area ( $\text{kg m}^{-1} \text{sec}^{-2}$ )

## APPENDIX B

## STATISTICAL PROCEDURES

Statistical testing for variance and correlation assumes that the populations consist of independent, normally distributed data. Meteorological data are generally non-independent (Brooks and Carruthers, 1953).

All data series used in statistical tests were checked for normality. Data that showed a distinct departure from a normal distribution were normalized using the necessary transformation, which is indicated in the text. To ensure that data used were independent, a random sample from each population used in Snedecor's F test for variance was re-tested for significance. A significant difference between samples is only quoted if a re-test using a random selection of data from within the sample also proved significant.

Snedecor's F-Test for variance

Snedecor's F-test provides a means of testing whether two or more observed variances differ significantly, or whether the difference between them is only such as might arise by chance between independent estimates of the same population variance.

If  $K$  samples are taken from a population and the  $i$ th sample has size  $n_i$  and mean  $m_i$  and the combination of all the samples together has size  $n$ , mean  $m$ , where  $x$  is the value of an individual, then two estimates may be made of the variance of the population as follows:

1. Variance between samples

$$\frac{\sum n_i (m_i - m)^2}{K - 1} \quad (K - 1 \text{ degrees of freedom})$$

2. Variance within samples

$$\frac{\sum f (x - m_i)^2}{n - K}$$

$F$  is the ratio of the variance between to the variance within,

$$\text{i.e. } F = \frac{s_1^2}{s_2^2} \quad \text{where } s_1 > s_2$$

The computed  $F$  value is compared with values, at the 0.05 and 0.01 levels of significance, of the ratio of independent estimates of the variance in a normal population when the two estimates are made from samples drawn from the same population.

The  $F$  ratio for a specified level of significance decreases as the number of degrees of freedom (of either variance estimate or both) is increased.  $F$  does not give

any indication of the amount by which one population variance exceeds the other, but only tests the significance of the difference (Brooks and Carruthers, 1953). A measure of the closeness of the relation between different sources of variation can be obtained by the coefficient of correlation.

#### The coefficient of correlation

A quantitative measure of the relationship between two variables is obtained by computing the 'coefficient of correlation'. This is a number independent of the dimensions of the observations correlated and of the number of pairs of such observations. In its simplest form it assumes the relationship between two variables to be linear i.e. if  $X$  and  $Y$  are the variables, the most probable value of  $Y$  corresponding to any given value of  $X$  is determined by the expression:

$$Y = aX + b$$

The constants  $a$  and  $b$  depend on the units of  $X$  and  $Y$  as well as the relationship between them. A measure of this relationship is given by the correlation coefficient  $r_{xy}$  between the two variables  $X$  and  $Y$ :

$$r_{xy} = \frac{\sum [(x-\bar{x})(y-\bar{y})]}{\sqrt{[\sum (x-\bar{x})^2 \sum (y-\bar{y})^2]}}$$

$X$  and  $Y$  are the paired values of 2 variables, and  $\bar{X}$ ,  $\bar{Y}$  their mean values.

The expression may be written:

$$r_{xy} = \frac{\sum xy}{N \sigma_x \sigma_y}$$

Where  $x$ ,  $y$  are the deviations of  $X$  and  $Y$  from their mean values,  $N$  is the number of pairs of observations, and  $\sigma_x$ ,  $\sigma_y$  are the standard deviations of the  $X$  and  $Y$  series.

#### Partial Correlation

Partial correlation is used to test the inter-relationships between more than two variables. The partial correlation coefficient between variables 1 and 2 when the effect due to variable 3 has been removed ( $r_{12.3}$ ) is given as follows:

$$r_{12.3} = \frac{r_{12} - r_{13} r_{23}}{\sqrt{(1-r_{13}^2)} \sqrt{(1-r_{23}^2)}}$$

Where  $r_{12}$  is the correlation coefficient between variables 1 and 2,  $r_{13}$  is the correlation coefficient between variables 1 and 3, and  $r_{23}$  is the correlation coefficient between variables 2 and 3.

#### Statistical significance of a correlation coefficient

In order to decide whether an observed correlation coefficient is significant, it is necessary to decide whether the odds against a coefficient of the same magnitude arising by chance between two unrelated series are large.



enough to justify the assumption that the two series correlated are probably related in the statistical sense (Brooks and Carruthers, 1953).

A  $t$ -test with  $(N-2)$  degrees of freedom ( $N$  is the number of pairs) may be used as follows:

$$t = \frac{r}{\sqrt{\frac{1-r^2}{N-2}}}$$

Where  $r$  is the correlation coefficient.

Calculated values of  $t$  are compared with tables of different significance levels of  $t$  (Fisher and Yates, 1953).

#### The Regression Equation

The regression of  $Y$  on  $X$  may be described by the following equation:

$$Y - \bar{Y} = r \frac{\sigma_y}{\sigma_x} (X - \bar{X})$$

Where  $\sigma_y$  and  $\sigma_x$  are the standard deviations of  $Y$  and  $X$  from their means  $\bar{Y}$  and  $\bar{X}$  respectively.

#### Chi-square ( $\chi^2$ ) test

The chi-square test is based on the comparison of the frequencies which are observed to fall into various classes with the frequencies which are expected on the hypothesis under examination.

If  $E$  is the number expected in any class and  $(E + d)$  is the number observed ( $d$  positive or negative), a value of  $d^2/E$  is formed for each class and the sum obtained, giving:

$$\chi^2 = \sum (d^2/E)$$

The  $\chi^2$  value obtained is compared with a table which gives, for different degrees of freedom, the values of  $\chi^2$  which have various probabilities ( $P$ ) of being exceeded by chance. A probability level of 0.05 is generally accepted as the critical level.

## APPENDIX C 700 mb CHART CLASSIFICATION

## TYPE (1) CYCLONIC PACIFIC

DATE	CHART TIME	700mb TEMP °C	700mb REL. HUM. %	500mb TEMP °C	500mb REL. HUM. %	LAPSE (700mb- 500mb) °C/100m	700mb WIND DIRM.	700mb WIND VEL. ms <sup>-1</sup>	PEYTO CLOUD COVER
7.7.1979	0000Z	3.6	70	-13.7	77	0.67	195°	7.2	
7.7.1979	1200Z	1.4	65	-16.3	92	0.68	220°	6.7	
8.7.1979	0000Z	-	-	-14.9	90	0.68	235°	7.2	8/10
8.7.1979	1200Z	-1.5	94	-17.1	46	0.60	225°	9.8	
25.7.1979	0000Z	2.6	65	-16.1	20	0.72	320°	5.2	
25.7.1979	1200Z	2.2	48	-16.1	22	0.70	310°	2.6	
26.7.1979	0000Z	4.4	49	-11.7	48	0.62	310°	5.2	
26.7.1979	1200Z	4.6	42	-13.9	30	0.71	305°	5.2	3/10
8.8.1979	1200Z	0.4	98	-17.9	60	0.70	310°	5.2	
4.8.1979	0000Z	0.4	69	-15.9	20	0.63	275°	7.7	7/10
4.8.1979	1200Z	1.8	75	-15.1	29	0.65	205°	5.2	
5.8.1979	0000Z	5.2	49	-13.1	21	0.70	195°	5.2	
6.8.1979	0000Z	1.4	55	-17.1	26	0.71	260°	7.7	8/10
MEAN		2.2	66	-15.3	45	0.68	260°	6.2	

\* Values from Vernon radioonde station. (240 km south-west of Peyto Glacier).

## TYPE (2) - 'LOCAL' CYCLONIC

DATE	CHART TIME	700 mb TEMPG	700 mb REL HUM.	500 mb TEMPG	500 mb REL HUM	LAPSE (700mb-500mb) °C/100m	700 mb WIND DIR.	700 mb WIND VEL. ms <sup>-1</sup>	PEYTO CLOUD COVER
10.7.1979	1200Z	0.4	97	-15.5	84	0.61	185°	7.7	10/10
11.7.1979	0000Z	-0.7	84	-16.3	24	0.65	275°	9.3	
11.7.1979	1200Z	-2.9	91	-17.7	82	0.57	270°	5.7	
12.7.1979	0000Z	-1.3	88	-17.9	65	0.64	290°	10.3	10/10
12.7.1979	1200Z	-4.3	63	-11.9	21	0.29	280°	7.7	
13.7.1979	0000Z	-3.5	88	-20.3	59	0.65	300°	10.3	10/10
13.7.1979	1200Z	-4.3	85	-18.7	31	0.55	310°	10.3	10/10
14.7.1979	0000Z	-1.5	68	-16.7	38	0.58	310°	9.3	
14.7.1979	1200Z	-1.7	95	-17.4	29	0.62	335°	7.7	9/10
24.7.1979	1200Z	1.0	64	-14.7	20	0.60	330°	5.2	
5.8.1979	1200Z	2.6	52	-16.5	35	0.73	205°	10.3	7/10
MEAN		-1.5	80	-16.7	44	0.59	280°	8.5	

## TYPE (3) PRONOUNCED ANFICYCLONIC

DATE	CHART TIME	700 mb TEMP°C	700 mb REL. HUM %	500 mb. TEMP°C	500 mb REL. HUM %	LAPSE (700mb- 500mb) °C/100m	700 mb WIND DIRN.	700 mb WIND VEL. ms <sup>-1</sup>	PEYTO CLOUD COVER
10.7.1979	0000Z	-	-	-	-	-	205°	5.2	2/10
16.7.1979	0000Z	4.0	38	-13.3	28	0.67	210°	2.6	
17.7.1979	1200Z	7.0	45	-10.1	20	0.66	295b	2.6	1/10
18.7.1979	0000Z	9.0	46	-9.1	24	0.70	305°	5.2	
18.7.1979	1200Z	9.2	37	-10.5	19	0.76	300°	2.6	1/10
19.7.1979	0000Z	10.4	40	-10.3	31	0.80	275°	5.2	
19.7.1979	1200Z	11.0	38	-10.5	28	0.83	290°	7.7	3/10
20.7.1979	0000Z	12.6	36	-9.1	22	0.84	200°	7.7	
21.7.1979	1200Z	7.4	49	-10.5	44	0.69	205°	11.8	5/10
22.7.1979	0000Z	6.0	57	-10.7	24	0.64	225°	7.7	
31.7.1979	0000Z	6.4	36	-10.7	24	0.66	280°	7.7	
MEAN		8.3	42	-10.5	26	0.73	250°	6.0	

## TYPE (4) WEAK ANTICYCLONIC

DATE	CHART-TIME	700 mb TEMP°C	700 mb REL. HUM	500 mb TEMP°C	500 mb REL. HUM	LAPSE (700mb- 500mb 50C/100m	700 mb WIND DIRN	700 mb WIND VEL. ms-1	PXTO CLOUD COVER
9.7.1979	0000Z	1.4	69	-15.3	42	0.64	250°	8.2	
9.7.1979	1200Z	2.4	44	-14.5	80	0.65	255°	6.7	
15.7.1979	0000Z	0.0	64	-17.7	34	0.68	-	-	
15.7.1979	1200Z	0.0	55	-15.9	38	0.61	-	-	
16.7.1979	1200Z	3.4	52	-10.1	34	0.52	045°	2.6	
17.7.1979	0000Z	7.4	22	-9.7	67	0.66	280°	5.2	2/10
19.7.1979	1200Z	10.4	32	-19.7	20	0.77	285°	5.2	1/10
20.7.1979	0000Z	12.0	38	-9.7	22	0.83	265°	9.3	2/10
27.7.1979	0000Z	7.0	46	-11.5	21	0.71	280°	7.7	
27.7.1979	1200Z	6.0	56	-14.1	25	0.71	315°	21.6	
28.7.1979	0000Z	8.0	49	-22.9	93	1.19	270°	7.7	2/10
28.7.1979	1200Z	5.8	42	-13.9	33	0.76	275°	5.2	5/10
29.7.1979	1200Z	4.2	48	-12.5	21	0.64	130°	7.7	7/10
30.7.1979	0000Z	5.4	21	-11.5	61	0.65	285°	7.7	8/10
30.7.1979	1200Z	3.8	48	-12.3	40	0.62	295°	7.7	1/10
MEAN		5.9	45	-13.2	42	0.72	250°	6.4	

## TYPE (5) WESTERLY ZONAL

DATE	CHART TIME	700 mb TEMP °C *	700 mb REL. HUM % *	500 mb TEMP °C *	500 mb REL. HUM % *	LAPSE (700mb- 500mb) °C/100m *	700 mb WIND DIRRN.	700 mb WIND VEL. ms <sup>-1</sup>	PEYTO CLOUD COVER
22.7.1979	1200Z	3.0	65	-11.1	23	0.54	265°	7.7	
23.7.1979	0000Z	5.4	56	-10.5	19	0.61	275°	11.3	
23.7.1979	1200Z	3.2	78	-12.9	39	0.62	275°	7.2	
29.7.1979	0000Z	5.0	38	-13.7	23	0.72	275°	2.6	
31.7.1979	1200Z	6.0	61	-11.9	43	0.69	255°	5.2	
1.8.1979	0000Z	4.2	79	-11.1	26	0.59	275°	10.3	3/10
1.8.1979	1200Z	-	-	-	-	-	270°	5.2	4/10
2.8.1979	0000Z	3.4	70	-11.9	22	0.59	280°	10.3	
2.8.1979	1200Z	2.4	58	-13.3	36	0.60	280°	8.2	
3.8.1979	0000Z	5.0	56	-14.1	47	0.73	285°	7.7	6/10
6.8.1979	1200Z	-	-	-	-	-	265°	10.3	6/10
MEAN		4.2	61	-12.9	32	0.64	275°	7.8	

## APPENDIX D BASE CAMP METEOROLOGICAL DATA FOR

## PROFILE TIMES

## TYPE (1) CYCLONIC PACIFIC

PROFILE NO.	DATE	TIME (M.I.D.S.T.)	CLOUD COVER	PRESS. mb	MEAN DRY BULB TEMP. °C	MEAN REL. HUM. %	DAILY MAX. TEMP. °C	DAILY MIN. TEMP. °C
1	7.7.1979	12.44-13.09	9/10 Cu, As	799	8.9	61		
2	7.7.1979	13.09-14.10	7/10 Cu	799	9.2	58		
3	7.7.1979	14.10-15.10	7/10 Cu	799	10.9	54	11.4	5.8
4	7.7.1979	15.10-16.10	7/10 Cu	799	10.4 0.4	47		
5	7.7.1979	16.10-17.10	7/10 Cu	799	-	-		
6	7.7.1979	17.10-18.10	As, St Cu	799	8.0	55		
81	26.7.1979	06.31-07.31	3/10 Cu	799	5.4	71		
83	26.7.1979	08.31-09.31	3/10 Cu	799	6.4	70	12.9	3.0
86	26.7.1979	11.31-12.31	8/10 Cu, Sc	799	8.9	58		



APPENDIX D (continued)  
 TYPE (1) CYCLONIC PACIFIC

PROFILE NO.	DATE	TIME (M.D.S.T)	CLOUD COVER	PRESS. mb	MEAN DRY BULB TEMP. °C	MEAN REL. HUM. %	DAILY MAX. TEMP. °C	DAILY MIN. TEMP. °C
153	3.8.1979	23.11-00.11	6/10 rain M11	797	3.0	92		
155	3.8.1979	01.11-02.11		797	3.6	86 <sup>b</sup>		
156	3.8.1979	02.11-03.11		796	3.1	86		
157	3.8.1979	14.47-15.47	10/10 rain sleet	795	8.2	57	10.8	1.6
158	3.8.1979	15.47-16.47	10/10 Cu, Sc	796	7.5	61		
159	3.8.1979	16.47-17.47	8/10 Cu, Sc	797	6.6	70		
160	3.8.1979	17.47-18.47	7/10 Cu, Ci	797	7.0	64		
161	4.8.1979	13.43-14.43	8/10 Cu, Sc	799	8.0	57		
162	4.8.1979	14.43-15.43	8/10 Cu	799	7.0	62		
163	4.8.1979	15.43-16.43	8/10 Cu	799	7.5	65		
164	4.8.1979	16.43-17.43	8/10 Cu	798	8.0	69	10.0	-0.1
165	4.8.1979	17.43-18.43	5/10 Cu	797	8.6	54		
166	4.8.1979	18.43-19.43	6/10 Cu	797	8.5	52		
167	4.8.1979	22.49-23.49	4/10 Cu	797	-	-		
168	4.8.1979	23.49-24.49	4/10 Cu	797	-	-		

## APPENDIX D (continued)

## TYPE (a) CYCLONIC PACIFIC

PROFILE NO.	DATE	TIME (M.D.S.T.)	CLOUD COVER	PRESS. mb	MEAN DRY BULB TEMP. °C	MEAN REL. HUM. %	DAILY MAX. TEMP. °C	DAILY MIN. TEMP. °C
169	5.8.1979	00.49-	-	-	-	-	-	-
170	5.8.1979	01.49-	-	-	-	-	-	-
176	5.8.1979	02.49	4/10 Cu, Ac	796	7.2	81	-	-
177	5.8.1979	08.17-	4/10 Cu, Ci	796	9.1	57	12.4	3.3
178	5.8.1979	09.17-	5/10 Cu, Ci	796	9.8	57	-	-
179	5.8.1979	10.17-	6/10 Cu, Ci	796	8.9	53	-	-
180	5.8.1979	13.43-	8/10 Cu, Thunder	797	11.9	46	-	-
181	5.8.1979	14.43-	8/10 Cu	797	12.1	41	-	-
182	5.8.1979	15.43-	8/10 Rain	797	12.2	41	-	-
183	5.8.1979	16.43-	8/10 Cu, Hall	797	-	-	-	-
184	5.8.1979	17.43-	8/10 Cu	798	10.2	44	-	-
185	5.8.1979	22.13-	4/10 Cu	799	8.0	48	-	-
186	5.8.1979	23.13-	-	-	-	-	-	-
		01.13	-	-	-	-	-	-

## TYPE (2) 'LOCAL' CYCLONIC

PROFILE NO.	DATE	TIME (M.D.S.T.)	CLOUD COVER	PRESS. mb	MEAN DRY BULB TEMP. °C	MEAN REL. HUM. %	DAILY MAX. TEMP. °C	DAILY MIN. TEMP. °C
14	10.7.1979	06.26-07.26	10/10 <sup>As</sup> <sub>Cu</sub>	795	9.4	64		
15	10.7.1979	07.26-08.26	10/10 <sup>As</sup> <sub>Cu</sub>	795	8.1	60	12.7	2.1
16	10.7.1979	08.26-09.26	10/10 <sup>Cu</sup> <sub>St</sub>	795	5.6	94		
20	11.7.1979	16.54-17.38	9/10 <sup>CH</sup> <sub>St</sub>	797	6.0	73		
21	11.7.1979	17.38-18.38	10/10 <sup>Cu</sup> <sub>St</sub>	797	4.8	80		
23	11.7.1979	19.38-20.38	10/10 <sup>Low</sup> <sub>Cu</sub>	797	5.7	73	6.7	3.3
24	11.7.1979	20.38-21.38	9/10 <sup>Cu,Ac</sup> <sub>Cl</sub>	797	5.2	70		
25	11.7.1979	21.38-22.38	10/10 <sup>Cu</sup>	797	5.0	72		
26	11.7.1979	22.38-23.38	9/10 <sup>Cu</sup>	797	4.3	73		

## TYPE (2) 'LOCAL' CYCLONIC (continued)

PROFILE NO.	DATE	TIME (M.D.S.T.)	CLOUD COVER	PRESS. mb.	MEAN DRY BULB TEMP. °C	MEAN REL. HUM. %	DAILY MAX. TEMP. °C	DAILY MIN. TEMP. °C
27	12.7.1979	13.30-14.30	6/10 Cu, Hail	797	6.0	67		
28	12.7.1979	14.30-15.30	8/10 Cu	797	5.1	78		
29	12.7.1979	15.30-16.30	8/10 Cu	797	3.2	72	6.7	2.1
30	12.7.1979	16.30-17.30	10/10 Low Cu	798	2.5	75		
31	12.7.1979	17.30-18.30	10/10 Snow Cu	799	2.5	75		
32	12.7.1979	18.30-19.30	10/10 Snow Cu					
33	13.7.1979	07.54-08.54	10/10 Cu, Sc	800	2.2	72		
34	13.7.1979	08.54-09.54	9/10 Sc Cu	800	2.9	68		
36	13.7.1979	10.54-11.54	8/10 Sc Cu	800	3.3	64	7.1	1.8
37	13.7.1979	11.54-12.54	7/10 Sc Cu	800	5.1	60		
38	13.7.1979	12.54-13.54	9/10 Sc Cu	800	5.0	57		

## TYPE (2) 'LOCAL' CYCLONIC (continued)

PROFILE NO.	DATE	TIME (M.D.S.T)	CLOUD COVER	PRESS. mb	MEAN DRY BULB TEMP. °C	MEAN REL. HUM. %	DAILY MAX. TEMP. °C	DAILY MIN. TEMP. °C
39	14.7.1979	07.16-08.16	9/10 Cu, Sc	801	4.0	66		
40	14.7.1979	08.16-09.16	10/10 Cu, Sc	802	3.9	74	8.8	2.9
41	14.7.1979	09.16-10.16	9/10 Cu, Sc	803	2.8	81		
43	14.7.1979	11.16-12.16	9/10 Cu, Sc	803	5.7	64		
44	14.7.1979	12.16-13.16	9/10 Cu, Sc	803	6.2	64		
171	5.8.1979	02.49-03.49	-	-	-	-		
172	5.8.1979	03.49-04.49	-	-	-	-		
173	5.8.1979	04.49-05.49	7/10 Cu, Ac, Cl	-	-	-	10.0	-0.1
174	5.8.1979	05.49-06.08	7/10 Cu, Ac, Cl	-	-	-		
175	5.8.1979	06.17-07.17	7/10 Cu, Ac, Cl	796	7.2	81		

## TYPE (3) PRONOUNCED ANTICYCLONIC

PROFILE NO.	DATE	TIME (M.D.S.T.)	CLOUD COVER	PRESS. mb	MEAN DRY BULB TEMP. °C	REL. HUM. %	DAILY	
							MAX. °C	MIN. °C
7	9.7.1979	17.47- 18.22	2/10 Cu, Ci	800	9.3	62		
8	9.7.1979	18.22- 19.22	2/10 Cu, Ci	799	9.0	60		
9	9.7.1979	19.22- 20.22	1/10 Cu, Ci, Ag	799	7.4	62	11.6	4.0
10	9.7.1979	20.22- 21.22	1/10 Cu, Ci, Ag	799	7.0	63		
11	9.7.1979	21.22- 22.22	2/10 Ci	798	9.1	60		
12	9.7.1979	22.22- 23.22	5/10 Ci	798	9.5	60		
51	15.7.1979	11.05- 12.05	2/10 Cu	808	7.8	58	11.3	2.3
54	17.7.1979	11.28- 12.28	1/10 Ci	809	13.2	47		
55	17.7.1979	12.28- 13.28	1/10 Ci	809	12.4	48	16.4	7.3
56	17.7.1979	13.28- 14.28	0/10	809	11.8	49		

PROLONGED ANTICLIMATIC (continued)

DATE	TIME (M.D.S. TO COVER)	SKY COVER	PRES. IN.	MEAN TEMP. °C	MEAN REL. HUM. %	DAILY MAX. TEMP. °C	DAILY MIN. TEMP. °C
18-7-1979	10:02- 10:08	0/10	809	10.5	54		
18-7-1979	10:08- 11:08	0/10	809	11.4	53		
18-7-1979	11:08- 12:08	3/10 Cn	809	12.3	51		
17-1979	12:08- 13:08	1/10 Cn	809	13.9	46	19.8	7.8
18-7-1979	13:08- 14:08	1/10 Cn	809	15.8	44		
18-7-1979	14:08- 15:08	1/10 Cn	809	15.9	44		
18-7-1979	15:08- 16:08	1/10 Cn	809	14.5	42		
20-7-1979	08:42- 08:48	1/10 C1	803	10.2	56		
20-7-1979	08:48- 09:48	1/10 C1	803	11.0	54		
20-7-1979	09:48- 10:48	2/10 C1	803	13.0	49	17.5	9.8

## TYPE (3) PROMOUNCED ANTICYCLONIC (continued)

PROFILE NO.	DATE	TIME (M.D.S.T.)	CLOUD COVER	PRESS. mb	MEAN DRY BULB TEMP. °C	MEAN REL. HUM. %	DAILY MAX. TEMP. °C	DAILY MIN. TEMP. °C
74	20.7.1979	10.48-11.48	2/10 Cu, Ci	803	15.1	44		
75	20.7.1979	11.48-12.48	3/10 Cu	803	14.6	43		
76	20.7.1979	12.48-13.48	3/10 Cu	803	12.1	50		
77	21.7.1979	10.55-11.55	3/10 Ci, Cu	798	17.8	42		
78	21.7.1979	11.55-12.55	5/10 Cu, Ci, Ag, Ci	798	17.7	43	18.3	1.4
79	21.7.1979	12.55-13.55	7/10 Cu, Ci, Ag, Ci	797	15.9	47		
80	21.7.1979	13.55-14.55	8/10 Cu, Ag	797				



## TYPE (4) WEAK ANEMIC/CYCLONIC

STATION NO.	MOBILE DATE	TIME (M.D.S.T.)	CLOUD COVER	PRES. MB	MEAN WINDS TEMP. °C	MEAN HUM. %	DAILY TEMP. °C	DAILY TEMP. °C
53	9.7.1979	23:25 24:24	8/10Ag	797	10.0	61	11.6	4.0
52	16.7.1979	18:15 20:56	2/10Cl	808	12.2	54	13.2	5.3
53	16.7.1979	20:56 21:56	2/10Cl	808	8.5	56		
64	19.7.1979	15:16 15:23	1/100u	-	14.0	45		
65	19.7.1979	15:23 16:16	2/10Cl	-	18.1	37		
66	19.7.1979	16:16 17:36	3/10Cu	-	18.0	35	18.2	8.2
67	19.7.1979	17:16 18:16	2/10Cl	-	13.0	44		

## (4) MEAN ANTI-CYCLONIC (continued)

PROFILE NO.	DATE	TIME (G.M.T.)	CLOUD COVER	PRESS. mb	MEAN DRY BULB TEMP. °C	MEAN REL. HUM. %	DAILY MAX. TEMP. °C	DAILY MIN. TEMP. °C
68	19.7.1979	16.16- 19.16	3/10Cu	-	13.8	45	-	-
69	19.7.1979	19.16- 20.16	5/10Cu	-	11.8	47	-	-
70	19.7.1979	20.16- 21.16	7/10Ci, Ac	-	11.8	47	-	-
99	28.7.1979	00.45- 01.39	2/10Sc, Cu	798	6.8	64	-	-
100	28.7.1979	01.39- 02.39	2/10Sc, Cu	798	-	-	-	-
101	28.7.1979	02.39- 03.39	2/10Sc, Cu	798	-	-	14.6	6.7
102	28.7.1979	03.39- 04.39	3/10Cu	798	-	-	-	-
103	28.7.1979	04.39- 05.39	4/10Sc, Cu	798	-	-	-	-
104	28.7.1979	05.39- 06.39	5/10Sc, Cu	797	8.0	68	-	-
105	28.7.1979	06.39- 07.39	6/10Sc, Cu	797	-	-	-	-

## TYPE (4) WEAK ANTICYCLONIC (continued)

PROFILE NO.	DATE	TIME (M.D.S.T.)	CLOUD COVER	PRESS. mb	MEAN		DAILY	
					TEMP. °C	REL. HUM. %	MAX. TEMP. °C	MIN. TEMP. °C
111	29.7.1979	14.21- 15.21	7/10Cu, C1	800	11.3	51		
112	29.7.1979	15.21- 16.21	6/10Cu, C1	800	11.5	48		
113	29.7.1979	16.21- 17.21	3/10Cu, C1	800	13.0	38		
114	29.7.1979	17.21- 18.21	8/10Cb	800	13.0	37	13.9	5.3
115	29.7.1979	18.21- 19.21	3/10Cu	800	13.0	36		
116	29.7.1979	19.21- 20.21	3/10Cu, Sc	800	13.0	36		
117	29.7.1979	22.11- 23.11	8/10Sc	801	9.1	56		
118	29.7.1979	23.11- 00.11	9/10Sc	801	-	-		
45	15.7.1979	05.05- 06.05	1/10C1	807	3.0	81		
46	15.7.1979	06.05- 07.05	1/10 Haze	807	3.0	81		

## TYPE (a) WEAK ANTICYCLONIC (continued)

PROFILE NO.	DATE (M.D.S.T.)	TIME	CLOUD COVER	PRESS. mb	MEAN TEMP. °C	MEAN DRY BULB TEMP. °C	MEAN REL. HUM. %	DAILY MAX. TEMP. °C	DAILY MIN. TEMP. °C
47	15.7.1979	07.05- 08.05	1/10 Haze	807	3.1	3.1	79	11.3	2.3
48	15.7.1979	08.05- 09.05	1/10 Haze	807	3.5	3.5	77		
49	15.7.1979	09.05- 10.05	1/10 Cu	808	6.1	6.1	70		
50	15.7.1979	10.05- 11.05	2/10 Cu	808	7.0	7.0	65		
51	15.7.1979	11.05- 12.05	2/10 Cu	808	7.8	7.8	59		

## TYPE (5) WESTERLY ZONAL

PROFILE NO.	DATE	TIME (M.D.S.T.)	CLOUD COVER	PRESS. mb	MEAN DRY BULB TEMP. °C	MEAN REL. HUM. %	DAILY MAX. TEMP. °C	DAILY MIN. TEMP. °C
107	28.7.1979	08.39-09.02	Cu, Ci Ac, Sc	797	17.7	65		
108	28.7.1979	09.13-09.39	Cu, Ci Ac, Sc	797	9.6	52	14.6	6.7
109	28.7.1979	09.39-10.39	Cu, Ci Ac, Sc	797	-	-		
110	28.7.1979	10.39-11.39	Cu, Ci Ac, Sc	797	-	-		
152	2.8.1979	22.11-23.11	6/10 Rain Hail	797	4.4	84	12.6	2.2
154	3.8.1979	00.11-01.11	-	796	3.3	91	10.8	1.6
187	6.8.1979	01.13-02.13	-	799	-	-		
188	6.8.1979	02.13-03.13	-	-	-	-	12.4	3.3
189	6.8.1979	03.13-04.13	-	-	-	-		
190	6.8.1979	04.13-05.13	-	-	-	-		

## APPENDIX E. PROFILE DATA

PROFILE NO.	DATE	TIME (G.D.S.T.)	1 m VEL. ms-1	2 m VEL. ms-1	3 m VEL. ms-1	4 m VEL. ms-1	5 m VEL. ms-1	6 m VEL. ms-1	7 m VEL. ms-1	MEAN TEMP. DIFF. 1.3 m °C	ST. DEVN. OP TEMP. DIFF. °C	MEAN 2 m WIND DIRM. °	ST. DEVN. OP WIND DIRM. °	RH <sub>1</sub>	RH <sub>2</sub>
1	7-7-1979	12:41- 13:09	5.87	5.98	6.15	5.18	6.39	0.81	0.79	0.81	0.79	250	10	0.18	-
2	7-7-1979	13:09- 14:10	4.62	5.16	5.23	7.69	6.12	1.06	0.93	1.06	0.93	250	14	0.30	0.11
3	7-7-1979	14:10- 15:10	5.35	5.81	5.98	5.11	6.22	0.84	0.90	0.84	0.90	260	12	0.22	-
4	7-7-1979	15:10- 16:10	6.12	6.68	7.20	8.11	7.18	1.00	0.60	1.00	0.60	255	22	0.09	0.08
5	7-7-1979	16:10- 17:10	4.58	4.72	4.77	4.47	5.33	1.31	0.60	1.31	0.60	215	37	1.90	-
6	7-7-1979	17:10- 18:10	4.60	4.84	7.16	8.21	9.12	1.25	1.21	1.25	1.21	255	30	0.02	-
7	8-7-1979	13:47- 16:22	2.97	3.44	3.84	3.37	3.32	2.5	1.14	2.5	1.14	230	6	1.15	0.89
8	9-7-1979	18:22- 19:22	5.06	5.76	5.67	5.38	5.33	3.13	3.02	3.13	3.02	285	4	0.88	0.34
9	9-7-1979	19:22- 20:22	5.30	6.10	6.03	5.64	5.76	2.06	1.41	2.06	1.41	225	7	0.41	0.22
10	9-7-1979	20:22- 21:22	4.65	5.10	5.30	5.16	5.23	2.06	0.51	2.06	0.51	225	8	0.51	0.41



## APPENDIX E PROFILE DATA (continued)

PROFILE NO.	DATE	TIME (M.D.S.T.)	MEAN WIND VELOCITY										MEAN TEMP. DIFF. °C	ST. DEVN. OF WIND DIFF. °C	MEAN WIND DIR. °	ST. DEVN. OF WIND DIR. °	R <sub>1</sub>	R <sub>2</sub>
			1 m ms-1	2 m ms-1	3 m ms-1	4 m ms-1	5 m ms-1	6 m ms-1	7 m ms-1	10 m ms-1	15 m ms-1	20 m ms-1						
21	11-7-1979	16:38-18:38	4.16	-	4.04	3.91	-	4.82	5.11	0.89	0.17	230	15	0.81	-	-	-	-
22	11-7-1979	18:38-19:38	-	-	4.38	3.91	-	3.98	-	0.49	0.19	205	12	-	-	-	-	-
23	11-7-1979	19:38-20:38	1.79	-	2.62	2.47	-	4.20	-	0.45	0.17	240	10	0.11	-	-	-	-
24	11-7-1979	20:38-21:38	4.74	-	5.43	5.57	-	5.71	4.92	0.45	0.07	235	15	0.07	0.16	-	-	-
25	11-7-1979	21:38-22:38	5.21	-	5.98	6.35	-	5.71	5.55	0.41	0.08	235	15	0.05	0.09	-	-	-
26	11-7-1979	22:38-23:38	4.79	-	5.76	5.57	-	5.59	4.50	0.38	0.11	235	15	0.06	0.08	-	-	-
27	11-7-1979	11:30-14:30	4.06	-	4.65	4.78	-	4.74	4.13	0.25	0.48	235	20	0.06	0.11	-	-	-
28	12-7-1979	14:30-15:30	2.45	-	2.77	2.85	-	2.80	2.95	-0.11	0.65	240	20	-0.07	-	-	-	-
29	12-7-1979	15:30-16:30	3.05	-	3.49	3.57	-	3.32	3.74	-0.16	0.17	240	19	-0.06	-	-	-	-
30	12-7-1979	16:30-17:30	4.43	-	5.09	5.50	-	4.74	5.45	-0.16	0.33	250	13	-0.01	-	-	-	-





## APPENDIX K PROFILE DATA (Continued)

PROFILE NO.	DATE	TIME (W.D.S.T.)	VEL. (MB-1)					7 m VEL. (MB-1)	TEMP. DEPT. 1-3 m (OC)	MEAN ST. DEW. OF TEMP. DEPT. (OC)			MEAN ST. DEW. OF WIND DIR. (MI)		
			1 m	2 m	3 m	4 m	5 m			6 m	ST. DEW. DEPT.	WIND DIR.	ST. DEW. DEPT.	WIND DIR.	MI
41	14.7.1979	09.16-10.16	1.69	-	1.09	1.94	-	1.97	1.97	0.50	0.23	215	29	0.97	1.84
42	14.7.1979	10.16-11.16	-	-	1.82	1.74	-	1.82	1.84	0.55	0.80	215	20	-	-
43	14.7.1979	11.16-12.16	2.95	-	3.40	3.42	-	3.58	3.59	0.40	0.62	230	15	0.23	-
44	14.7.1979	12.16-13.16	3.42	-	4.01	4.11	-	4.25	4.30	0.48	0.22	270	11	0.11	-
45	15.7.1979	05.05-06.05	4.16	-	4.99	5.04	-	4.94	4.92	0.95	0.19	200	6	0.13	0.47
46	15.7.1979	06.05-07.05	4.65	-	4.67	5.04	-	4.06	4.07	0.60	0.58	210	8	0.56	0.31
47	15.7.1979	07.05-08.05	3.74	-	4.55	4.16	-	3.91	3.94	-	-	-	-	-	-
48	15.7.1979	08.05-09.05	2.65	-	3.76	3.62	-	3.10	3.00	-	-	-	-	-	-
49	15.7.1979	09.05-10.05	3.20	-	3.84	3.69	-	3.07	3.40	-	-	-	-	-	-
50	15.7.1979	10.05-11.05	3.81	-	4.50	4.33	-	4.25	3.98	1.43	0.80	210	7	0.58	0.11

## APPENDIX E. PROFILE DATA (continued)

PROFILE NO.	DATE	TIME (M.D.S.T.)	VEL. (ms <sup>-1</sup> )						7 m VEL.	1-4 m DIPP.	ST. DEVS. OF TEMP. DIFF.	MEAN ST. DEVS. OF WIND DIRN.	ST. DEVS. OF WIND DIRN.	R <sub>1</sub>	R <sub>2</sub>
			1 m	2 m	3 m	4 m	5 m	6 m							
51	15.7.1979	11.05- 12.05	3.78	4.57	4.38	4.43	4.23	1.68	0.49	210	2	0.43	0.29		
52	16.7.1979	18.45- 20.56	2.95	3.99	3.64	3.37	3.32	3.90	1.42	200	7	0.22	0.89		
53	16.7.1979	20.56- 21.56	1.74	2.62	2.70	1.72	2.52	2.90	1.93	200	4	0.34	1.84		
54	17.7.1979	11.28- 12.28	4.89	5.71	5.62	5.67	4.89	3.6	0.18	200	6	0.70	0.25		
55	17.7.1979	12.28- 13.28	5.23	6.19	6.22	5.95	5.81	4.05	1.76	210	5	0.42	0.33		
56	17.7.1979	13.28- 14.28	5.28	6.29	6.27	5.93	5.74	3.3	2.23	210	2	0.35	0.21		
57	18.7.1979	10.05- 10.25	5.45	6.39	6.31	5.81	5.59	3.9	1.58	210	5	0.52	0.27		
58	18.7.1979	11.05- 11.08	1.67	2.87	2.82	2.47	2.30	3.9	1.58	220	5	0.30	1.21		
59	18.7.1979	11.08- 12.08	1.94	3.07	3.10	2.85	2.72	4.1	1.58	215	3	0.32	1.37		
60	18.7.1979	12.08- 13.08	1.77	2.82	2.90	2.75	2.70	3.1	1.01	200	11	0.425	1.03		







## APPENDIX E PROFILE DATA (continued)

PROFILE NO.	DATE	TIME (M.D.S.T.)	WIND VELOCITY (M.S.)										MEAN TEMP. DIFF. (°C)		MEAN WIND DIR. DIFF. (°)		M <sub>1</sub>	M <sub>2</sub>	M <sub>3</sub>
			1 m	2 m	3 m	4 m	5 m	6 m	7 m	ST. DEVI.	ST. DEVI.	2 m	ST. DEVI.						
91	27.7.1979	01.50-02.50	3.42	-	4.03	4.01	-	3.69	3.74	1.90	1.32	220	4	0.75	0.72				
92	27.7.1979	02.50-03.50	4.18	-	5.04	5.04	-	4.87	4.89	1.93	0.30	220	6	0.27	0.50				
93	27.7.1979	03.50-04.50	4.32	-	5.35	5.76	-	5.26	5.16	2.00	0.44	220	6	0.14	0.39				
94	27.7.1979	04.50-05.50	4.57	-	5.06	5.45	-	5.28	5.28	2.13	1.31	235	8	0.28	0.47				
95	27.7.1979	05.50-06.50	4.4	-	4.18	4.57	-	4.45	4.45	1.73	1.21	235	5	0.51	0.54				
96	27.7.1979	06.50-07.50	3.67	-	4.33	4.65	-	4.38	4.38	1.76	4.76	235	6	0.16	0.51				
97	27.7.1979	07.50-08.50	3.59	-	4.18	4.18	-	3.96	3.94	2.65	2.58	220	14	0.76	0.73				
98	27.7.1979	08.50-09.50	-	-	4.05	4.16	-	3.22	-	2.70	4.13	210	26	-	-				
99	28.7.1979	00.15-01.39	5.09	-	6.00	6.00	-	5.93	5.98	1.48	1.48	235	13	0.19	0.24				
100	28.7.1979	01.39-02.39	3.74	-	4.25	4.28	-	4.28	3.52	2.18	0.55	235	15	2.35	1.00				

## APPENDIX E. PROFILE DATA (continued)

PROFILE NO.	DATE	TIME (M.D.S.T.)	WIND VELOCITY (msec <sup>-1</sup> )							MEAN WIND VELOCITY (msec <sup>-1</sup> )		ST. DEVIATION OF WIND DIRN.		MEAN WIND DIRN.	
			1 m	2 m	3 m	4 m	5 m	6 m	7 m	1-4 m	DIFF. °C	ST. DEVIATION OF TEMP. DIFF. °C	WIND DIRN. °	ST. DEVIATION OF WIND DIRN. °	MEAN WIND DIRN. °
101	28.7.1979	02.39-03.36	4.67	-	5.64	5.69	-	5.52	5.62	2.51	0.39	235	12	0.28	0.11
102	28.7.1979	03.39-04.35	4.25	-	5.11	5.14	-	5.06	5.09	2.55	0.66	230	10	0.38	0.50
103	28.7.1979	04.39-05.39	4.35	-	5.16	5.21	-	4.97	5.06	2.63	0.67	236	8	0.37	0.49
104	28.7.1979	05.39-06.39	4.16	-	5.26	4.89	-	4.79	4.79	2.44	0.63	235	5	0.48	0.32
105	28.7.1979	06.39-07.39	4.18	-	4.37	4.87	-	4.70	4.72	2.51	0.67	240	5	0.35	0.55
106	28.7.1979	07.39-08.39	-	-	4.29	4.77	-	4.28	-	2.78	0.85	235	5	-	-
107	28.7.1979	08.39-09.02	2.97	-	4.35	4.85	-	3.37	3.35	2.03	1.47	235	6	0.10	0.52
108	28.7.1979	09.13-09.39	3.67	-	4.35	4.43	-	4.59	3.64	2.03	1.47	235	11	0.39	0.62
109	28.7.1979	09.39-10.39	4.38	-	5.26	5.67	-	5.35	5.33	1.58	0.85	235	13	0.10	0.49
110	28.7.1979	10.39-11.39	4.33	-	5.14	5.67	-	4.38	5.06	2.03	1.04	235	7	0.12	0.24



## APPENDIX 2 PROFILE DATA (continued)

PROFILE NO.	DATE	TIME (M.D.S.T.)	1 m - 2 m										MEAN				M <sub>1</sub>	M <sub>2</sub>
			VEL. ms-1	VEL. ms-1	VEL. ms-1	VEL. ms-1	VEL. ms-1	VEL. ms-1	VEL. ms-1	VEL. ms-1	VEL. ms-1	VEL. ms-1	7 m VEL. ms-1	1-4 m DIFF. OC	ST. DEVM. OF TEMP. 1-4 m	ST. DEVM. OF WIND DIRN. OC		
111	29.7.1979	15.21-15.21	3.61	4.60	4.77	4.57	4.60	2.48	0.94	230	21	0.27	0.36					
112	29.7.1979	15.25-16.25	3.32	3.86	4.18	3.84	3.86	2.78	7.08	210	22	0.34	0.43					
113	29.7.1979	16.21-17.21	3.69	4.38	4.60	4.30	4.28	2.74	8.79	210	17	0.35	0.39					
114	29.7.1979	17.21-18.21	3.35	3.81	3.86	4.28	3.54	2.33	2.48	210	17	0.92	0.58					
115	29.7.1979	18.21-19.21	2.92	3.69	3.35	3.71	3.35	2.40	4.18	225	36	1.37	0.79					
116	29.7.1979	19.21-20.21	2.90	3.54	3.44	3.07	3.07	2.93	9.82	225	22	1.05	0.53					
117	29.7.1979	22.11-23.11	4.30	5.18	5.14	4.97	4.92	2.70	1.53	210	5	0.41	0.33					
118	29.7.1979	23.11-00.11	2.85	3.30	3.27	2.72	2.72	1.91	3.32	230	10	1.18	0.64					
119	30.7.1979	00.11-01.11	3.17	3.57	3.59	3.40	2.97	3.04	0.15	220	2	1.88	1.32					
120	30.7.1979	01.11-02.11	3.76	4.38	4.06	3.49	3.42	2.63	0.41	280	3	3.08	0.58					

## APPENDIX E. PROFILE DATA (continued)

PROFILE NO.	DATE	TIME (M.D.S.T.)	MEAN							MEAN		ST. DEVN.		MIND OF WIND DIR.	MIND OF WIND O	M1	M2
			1 m ms-1	2 m ms-1	3 m ms-1	4 m ms-1	5 m ms-1	6 m ms-1	7 m ms-1	TEMP. DIFF. °C	TEMP. DIFF. °F	TEMP. DIFF. °C	TEMP. DIFF. °F				
121	30.7.1979	02.11-03.11	4.25	-	5.01	5.04	-	4.11	4.45	2.14	0.62	220	8	0.36	0.47		
122	30.7.1979	03.11-04.11	2.87	-	2.77	-	-	2.27	2.62	2.74	0.48	235	8	-	-		
123	30.7.1979	05.32-06.32	2.55	-	2.45	2.67	-	1.97	1.89	2.70	2.99	235	8	-	-		
124	30.7.1979	06.32-07.32	2.84	-	3.22	3.20	-	3.07	2.99	2.33	0.65	235	4	1.95	0.83		
125	30.7.1979	07.32-08.32	3.62	-	4.33	4.35	-	4.30	4.25	2.89	1.11	235	4	0.57	0.75		
126	30.7.1979	08.32-09.32	3.91	-	4.77	5.16	-	4.70	4.60	3.04	1.19	220	4	0.17	0.56		
127	30.7.1979	09.32-10.32	4.43	-	5.38	-	-	5.04	4.87	4.32	3.02	215	4	-	-		
128	31.7.1979	14.07-15.07	4.67	-	5.64	5.76	-	6.00	6.07	2.21	1.16	235	23	0.20	-		
129	31.7.1979	15.07-16.07	4.79	-	5.81	6.27	-	6.27	-	2.10	0.58	235	20	0.10	-		
130	31.7.1979	16.07-17.07	4.74	-	5.91	6.03	-	6.27	6.36	2.10	1.43	235	13	0.14	-		

## APPENDIX 5 PROFILE DATA (continued)

PROFILE CNO.	DATE	TIME (M.D.S.T.)	VEL. m/s						7 m VEL. m/s	MEAN TEMP. DIFF. OC	ST. DEVN. OF TEMP. DIFF. OC	MEAN TEMP. DIFF. OC	ST. DEVN. OF WIND DIRN. O	N <sub>5</sub>
			1 m	2 m	3 m	4 m	5 m	6 m						
131	31.7.1979	17.07- 18.07	3.81	-	4.65	4.72	-	4.89	4.94	2.16	2.35	230	23	0.28
132	31.7.1979	18.07- 19.07	3.91	-	4.92	4.67	-	4.84	4.92	1.69	0.69	235	38	0.33
133	31.7.1979	19.07- 20.07	3.79	-	4.43	4.52	-	4.67	4.74	1.54	0.72	240	27	0.30
134	31.7.1979	20.07- 21.07	4.13	-	4.89	4.99	-	5.21	5.10	1.54	0.82	255	30	0.22
135	31.7.1979	21.07- 22.07	5.16	-	6.12	6.24	-	6.87	6.58	1.88	1.59	235	15	0.17
136	31.7.1979	22.07- 23.12	4.52	-	5.30	5.38	-	5.57	5.67	1.50	1.43	220	7	0.22
137	31.7.1979	23.12- 24.12	4.50	-	5.21	5.28	-	5.45	5.55	1.43	1.36	235	8	0.07
138	1.8.1979	00.12- 01.12	4.97	-	5.83	5.95	-	6.12	6.29	1.46	1.16	225	11	0.16
139	1.8.1979	01.12- 02.12	4.97	-	6.22	6.03	-	6.31	6.39	1.43	0.38	225	9	0.14
140	1.8.1979	02.12- 03.12	4.25	-	5.04	5.11	-	5.30	5.38	1.65	0.34	240	14	0.24

## APPENDIX E. PROFILE DATA (continued)

PROFILE NO.	DATE	TIME (M.D.S.T.)	1 m	2 m	3 m	4 m	5 m	6 m	7 m	MEAN TEMP. DIFF. 1-4 m	ST. DEVM. OF TEMP. DIFF. OC	MEAN MIND OF MIND DIFF. O	HT. DEVM. OF MIND DIFF. O	R1	R1 S
			VEL. m/s-1	VEL. m/s-1	VEL. m/s-1	VEL. m/s-1	VEL. m/s-1	VEL. m/s-1	OC						
141	1.8.1979	07.12-08.12	3.52	-	4.52	4.28	-	4.43	4.47	2.10	0.63	225	18	0.41	0.83
142	1.8.1979	04.12-05.12	3.62	-	4.79	-	-	4.57	4.62	2.06	0.56	225	12	-	-
143	1.8.1979	05.12-06.12	4.23	-	5.16	-	-	5.47	5.52	2.03	0.62	220	10	-	-
144	1.8.1979	06.22-07.22	4.23	-	5.06	5.04	-	5.06	5.06	2.21	0.71	220	11	0.37	-
145	1.8.1979	07.22-08.22	3.69	-	4.72	4.38	-	4.40	4.43	2.63	1.93	205	4	0.62	0.30
146	1.8.1979	08.22-09.22	3.74	-	4.52	4.92	-	4.57	4.60	2.48	1.15	210	4	0.19	0.57
147	1.8.1979	09.22-10.22	3.91	-	4.79	4.84	-	4.97	4.99	2.33	1.41	195	10	0.30	-
148	1.8.1979	10.22-11.22	3.69	-	4.45	4.47	-	4.52	4.55	2.18	1.43	195	11	0.37	-
149	1.8.1979	11.22-12.22	3.00	-	3.42	3.40	-	3.22	3.40	2.33	2.42	215	18	1.44	0.84
150	1.8.1979	12.22-13.22	3.37	-	4.35	4.06	-	4.13	4.20	2.33	2.00	215	14	0.55	0.52

## APPENDIX E PROFILE DATA (continued)

PROFILE NO.	DATE	TIME (M.D.S.T.)	1 m	2 m	3 m	4 m	5 m	6 m	7 m	MEAN ST. DEVS. OF TEMP. DIFF. 1-4 m		MEAN ST. DEVS. OF TEMP. DIFF. OF WIND DIRN.			
			VEL. ms-1	VEL. ms-1	VEL. ms-1	VEL. ms-1	VEL. ms-1	VEL. ms-1	OC	OC	R <sub>1</sub>	R <sub>2</sub>	R <sub>1</sub>	R <sub>2</sub>	
151	1-8-1979	13.22-14.22	3.22	-	3.86	3.86	-	3.95	4.01	1.95	1.74	215	13	0.51	-
152	2-8-1979	22.11-23.11	2.87	3.52	2.27	3.52	3.57	-	-	1.39	1.24	205	86	0.39	-
153	2-8-1979	23.11-00.11	2.30	2.47	0.85	2.55	1.67	-	-	1.24	0.39	215	6	2.08	2.49
154	3-8-1979	00.11-01.11	2.75	2.97	1.65	3.07	3.12	-	-	0.60	10.10	210	37	0.71	-
155	3-8-1979	01.11-02.11	2.75	2.15	2.30	2.35	2.35	-	-	0.64	1.72	210	19	0.41	-
156	3-8-1979	02.11-03.11	1.57	1.65	1.77	2.10	1.69	-	-	0.98	0.37	205	22	0.38	2.81
157	3-8-1979	18.47-19.47	2.90	3.22	4.01	4.08	3.76	-	-	0.75	0.57	260	35	0.06	0.21
158	3-8-1979	15.47-16.47	3.10	3.42	3.69	3.76	3.84	-	-	0.90	0.44	235	30	0.21	-
159	3-8-1979	16.47-17.47	3.12	3.57	3.84	3.89	3.94	-	-	1.43	0.61	205	12	0.26	-
160	3-8-1979	17.47-18.47	4.62	4.99	4.20	3.66	4.70	-	-	2.06	1.84	200	117	0.40	0.23

## APPENDIX E PROFILE DATA (continued)

PROFILE NO.	DATE	TIME (A.D.S.T.)	1 m	2 m	3 m	4 m	5 m	6 m	7 m	MEAN TEMP. DIFF. 1-3 m	ST. DEVM. WIND DIRN.	MEAN WIND DIRN.	ST. DEVM. WIND DIRN.	H <sub>1</sub>	H <sub>2</sub>
			VEL. mm-1	VEL. mm-1	VEL. mm-1	VEL. mm-1	VEL. mm-1	VEL. mm-1	°C						
161	4.8.1979	14.43-14.43	3.15	3.42	5.85	4.38	4.11	-	-	1.35	2.91	220	12	0.09	0.17
162	4.8.1979	14.43-15.43	3.35	3.27	4.57	4.33	4.35	-	-	2.51	6.85	230	5	0.28	0.51
165	4.8.1979	15.43-16.43	3.94	4.65	5.16	5.01	5.09	-	-	1.80	0.99	230	10	0.16	0.27
164	4.8.1979	16.43-17.43	4.33	5.67	5.26	5.21	5.16	-	-	2.20	-	225	12	0.56	0.32
165	4.8.1979	17.43-18.43	3.40	4.01	4.28	4.25	4.25	-	-	7.56	4.02	230	5	1.39	1.41
166	4.8.1979	18.43-19.43	4.13	4.72	5.14	5.28	4.97	-	-	5.81	0.31	230	5	0.45	0.96
167	4.8.1979	22.49-23.49	2.70	3.57	3.76	3.74	3.74	-	-	3.81	0.28	230	16	0.37	0.99
168	5.8.1979	23.49-00.49	3.22	3.35	3.94	3.98	4.03	-	-	3.12	1.14	240	10	0.57	-
169	5.8.1979	00.49-01.49	2.47	-	2.95	2.97	3.02	-	-	2.61	0.29	240	22	1.08	-
170	5.8.1979	01.49-02.49	2.02	-	2.42	2.47	2.50	-	-	2.65	0.27	230	16	1.54	-

APPENDIX B. PROFILE DATA (continued)

PROFILE NO.	DATE	TIME (M.D.S.T.)	1 m VEL. ms-1	2 m VEL. ms-1	3 m VEL. ms-1	4 m VEL. ms-1	5 m VEL. ms-1	6 m VEL. ms-1	7 m VEL. ms-1	MEAN DIFF. 1-4 m OC	ST. DEVI. OF DIFF. OC	MEAN WIND DIRN.	ST. DEVI. OF DIRN.	NO. OF WIND DIRN.	R <sub>1</sub>	R <sub>2</sub>
171	5-8-1979	02:48 03:49	2.07	-	2.77	2.82	2.92	-	-	2.68	0.45	180	76	0.49	-	-
172	5-8-1979	03:49 04:49	1.89	-	2.47	2.45	2.50	-	-	2.34	0.20	160	71	0.78	-	-
173	5-8-1979	04:49 05:49	1.06	-	1.57	1.57	1.62	-	-	2.50	0.50	160	35	0.97	-	-
174	5-8-1979	05:49 06:00	2.07	-	6.60	7.64	6.75	-	-	6.44	10.81	160	30	0.02	0.59	-
175	5-8-1979	06:17 07:17	2.60	2.90	3.10	3.44	3.27	-	-	6.38	10.81	160	30	0.93	2.94	-
176	5-8-1979	08:17 08:17	3.96	-	4.74	4.87	4.57	-	-	5.33	2.60	190	4	0.65	1.04	-
177	5-8-1979	08:17 09:17	4.20	4.72	5.11	5.23	4.94	-	-	5.31	0.28	195	11	0.13	0.79	-
178	5-8-1979	09:17 10:17	3.54	4.03	4.33	4.79	4.52	-	-	5.38	0.85	215	18	0.37	0.97	-
179	5-8-1979	10:17 11:17	3.84	3.76	4.97	4.72	4.84	-	-	4.38	0.88	210	11	0.58	0.59	-
180	5-8-1979	13:43 14:43	4.77	5.14	5.81	6.00	6.15	-	-	1.06	0.53	250	9	0.07	-	-





## APPENDIX E PROFILE DATA (continued)

PROFILE NO.	DATE	TIME (M.D.S.T.)	1 m		2 m		3 m		4 m		5 m		6 m		7 m		MEAN DIFF. 1-1 m	ST. DEVS. OF TEMP. DIFF. 1-1 m	MEAN DIFF. OF TEMP. OF WIND	ST. DEVS. OF WIND	RA <sub>1</sub>	RA <sub>2</sub>
			VEL. mm-1	VEL. mm-1	VEL. mm-1	VEL. mm-1	VEL. mm-1	VEL. mm-1	VEL. mm-1	VEL. mm-1	VEL. mm-1	VEL. mm-1	VEL. mm-1	VEL. mm-1	VEL. mm-1	VEL. mm-1						
191	6-8-1979	06.37 07.37	2.12	-	2.47	2.42	2.42	-	-	-	-	-	-	-	-	-	-	-	225	25	-	-
192	6-8-1979	07.37 08.37	2.37	-	2.82	2.95	2.90	-	-	-	-	-	-	-	-	-	-	-	220	14	-	-
193	6-8-1979	08.37 09.37	3.15	-	3.84	3.91	4.03	-	-	-	-	-	-	-	-	-	-	-	225	14	-	-

APPENDIX F SIGNIFICANCE OF DIFFERENCES  
 BETWEEN SYNOPTIC TYPES (10 PAIRINGS)

1. 700 mb TEMPERATURE

Significant at 0.001: The differences between synoptic  
 types 1 and 2, 1 and 3, 1 and 5,  
 2 and 3, 2 and 4, 2 and 5, 3 and 5.

Significant at 0.01: Types 1 and 4.

Not significant: Types 3 and 4, 4 and 5.

2. 700 mb HUMIDITY

Significant at 0.001: Types 1 and 3, 2 and 3, 2 and 4.

Significant at 0.01: Types 1 and 4, 2 and 5, 3 and 5,  
 4 and 5.

Not significant: Types 1 and 2, 1 and 5, 3 and 4.

3. 500 mb TEMPERATURE

Significant at 0.001: Types 1 and 3, 2 and 3, 2 and 5.

Significant at 0.01: Types 1 and 5, 3 and 5.

Significant at 0.05: Types 2 and 4, 3 and 4.

Not significant: Types 1 and 2, 1 and 4, 4 and 5.

4. 500 mb HUMIDITY

Significant at 0.05: Types 1 and 3, 2 and 3.

All other pairs not significant.

5. 700 mb WIND DIRECTION

All pairs not significant.

6. 700 mb WIND SPEED

Significant at 0.01: Types 1 and 2.

Significant at 0.05: Types 2 and 3, 2 and 4.

All other pairs not significant.

7. PEYTO CLOUD COVER

Significant at 0.001: Types 1 and 2, 1 and 3, 1 and 4,  
1 and 5, 2 and 3, 2 and 4, 2 and 5,  
3 and 5.

Significant at 0.01: Types 4 and 5.

Significant at 0.05: Types 3 and 4.

8. 700 - 500 mb TEMPERATURE LAPSE

Significant at 0.001: Types 2 and 5.

Significant at 0.01: Types 2 and 3.

Significant at 0.05: Types 1 and 2, 2 and 4.

All other pairs not significant.

9. PEYTO BASE CAMP MEAN MINIMUM TEMPERATURE

Significant at 0.01: Types 2 and 4.

Significant at 0.05: Types 2 and 3.

All other pairs not significant.

10. PEYTO BASE CAMP MEAN MAXIMUM TEMPERATURE

Significant at 0.01: Types 2 and 3, 2 and 4.

Significant at 0.05: Types 1 and 2, 1 and 3, 2 and 5.

All other pairs not significant.

11. PEYTO BASE CAMP PRESSURE

Significant at 0.001: Types 1 and 2, 1 and 3, 1 and 4,  
2 and 3, 2 and 4.

Significant at 0.01: Types 3 and 5, 4 and 5.

Significant at 0.05: Types 1 and 5.

Not significant: Types 2 and 5, 3 and 4.

